2020

Regulation of Wnt/β-Catenin Signaling in Cardiac Valve Development and Disease

Lilong Guo
Medical University of South Carolina

Regulation of Wnt/β-Catenin Signaling in Cardiac Valve Development and Disease

by

Lilong Guo

A dissertation submitted to the faculty of the Medical University of South Carolina in partial fulfillment of the requirements for the degree of Doctor of Philosophy in the College of Graduate Studies
Department of Regenerative Medicine and Cell Biology

2021

Approved by:

Chairman, Advisory Committee _____
Russell (Chip) Norris

_____
Robin C. Muise-Helmericks

_____
Jeffrey Jones

_____
Antonis Kourtidis

_____
Joshua Lipschutz

Dedication

I would like to dedicate this work to my family: my lovely wife Ying, my cutest sons Molin and Moqi, my parents and in laws. Their support and patience and relentless understanding have been an enormous help in accomplishing this work. To my wife Ying for taking care of most of the housework and share the joy and pain that I have been going through, for accompany when I feel frustrated and encouragement when I feel pessimistic. To my mom and dad for always supporting my every decision and offering unconditional love to me and my family. To my parents in law for looking after our sons and supporting us both mentally and financially. Thanks also to the members of the #norrislab Diana, Tyler, Kate, Kathrine, Amanda, Kelsey, Janiece, Rebecca, Cortney, Natalie, Jorden. Without their daily support, collaboration and funny jokes this would not have been possible. Last but not least I would like to thank the friends that I have met here, Zequn, Fei, Hao and Peiheng, who are always there to offer help when I need a hand and always there to talk when I need a break. They are like my families and the love and support from them make me feel warm and happy.

Acknowledgements

First of all, the accomplishment of this study is attributed to Dr. Russell (Chip) Norris, whose unconditional support and critical guidance during the five years have assisted in leading this project to the right direction. His philosophy in running the lab and doing science have helped build a positive image of a scientist that I want to become. Without his mentorship, nothing would have happened. Furthermore, assistance from my lab mates is playing a key role in finalization of this study. Their enthusiasm in science encourages me to push myself a little further to where I am right now. In addition, I would like to acknowledge my committee, Dr. Kourtidis, Dr. Jones and Dr. Lipschutz who is also my co-mentor, they sincerely provided me experiment tips and suggestions which have helped shape this work. Special thanks to Dr. Muise-Helmericks who pulled me out of swamp when I was enduring bumps during the first two years. Her encouragement and advises enlightened me and cheered me up helping me get through the darkness. Whiteout her intervention, I might have already dropped off the program and would have not completed this work. Also, I would like to acknowledge the members of the department of Regenerative Medicine and Cell Biology for always being there to help. Their industrial working attitude inspires me to become a better scientist. Last but not least I would like to acknowledge our collaborators within the Leducq

Mitral Network and the mitral valve prolapse families who participated in our studies. Their willingness in participation is fundamental to this project.

TABLE OF CONTENTS

LIST OF FIGURES

LIST OF TABLES

LIST OF ABBREVIATIONS

AHI1	Abelson Helper Integration Site 1
AL	Anterior Leaflet
APC	Adenomatous Polyposis Coli
ASD	Atrial Septal Defect
AV	Atrioventricular
AVC	Atrioventricular Canal
AVSD	Atrioventricular Septal Defect
BAT-gal	β-catenin-Activated Transgene driving expression of nuclear β-Galactosidase reporter
BAV	Bicuspid Aortic Valve
BBS1	Bardet-Biedl syndrome 1
BBS4	Bardet-Biedl syndrome 4
BMP	Bone Morphogenic Protein
BSA	Bovine Serum Albumin
CBY1	Chibby Family Member 1
CD31	Cluster of Differentiation 31
CEP164	Centrosomal Protein 164
CHD	Congenital Heart Disease
CHX	Cycloheximide
CJ	Cardiac Jelly
CK1	Casein Kinase 1
CRISPR	Clustered Regularly Interspaced Short Palindromic Repeats
DCHS1	Dachsous Cadherin-Related 1
DKK1	Dickkopf WNT Signaling Pathway Inhibitor 1
DMEM	Dulbecco's Modified Eagle Medium
Dvl	Dishevelled
DYNC2H1	Dynein Cytoplasmic 2 Heavy Chain 1
DYNC2L11	Dynein Cytoplasmic 2 Light Intermediate Chain 1
DZIP1	DAZ Interacting Zinc Finger Protein 1
ECM	Extracellular Matrix
EDS	Ehlers-Danlos Syndromes
EMT	Endothelial-to-Mesenchyme Transformation
FAM	5-Carboxyfluorescein
FBN1	Fibrillin 1

FBS	Fetal Bovine Serum
FLNA	Filamin A
FZD8	Frizzled Class Receptor 8
GPCR	G protein-coupled receptors
Gsk3β	Glycogen Synthase Kinase 3 β
HABP	Hyaluronic Acid Binding Protein
HHn	Hamburger Hamilton Stage n (i.e. HH40)
HRP	Horseradish Peroxidase
IFT	Intraflagellar Transport
IFT20	Intraflagellar Transport 20
IFT52	Intraflagellar Transport 52
IFTA	Intraflagellar Transport A
IFTB	Intraflagellar Transport B
IHC	Immunohistochemistry
IP	Immunoprecipitation
ITS	Insulin Transferrin Selenium
IVS	Interventricular Septum
JNK	c-Jun N-terminal Kinase
KAP3	Kinesin-Associated Protein 3
KIF3A	Kinesin Family Member 3A
KIF3B	Kinesin Family Member 3B
LA	Left Atrium
LEF	Lymphoid Enhancer Binding Factor
LEF1	Lymphoid Enhancer Binding Factor 1
LMCD1	LIM And Cysteine Rich Domains 1
M199	Medium 199
MAC	Mitro-Aortic Continuity
MEF	Mouse Embryonic Fibroblast
MF20	Myosin Heavy Chain
MKKS	McKusick-Kaufman Syndrome
MMP	Matrix Metallopeptidase
MMP2	Matrix Metallopeptidase 2
MR	Mitral Regurgitation
MS	Mitral Stenosis
Msx2	Msh Homeobox 2

Msx1	Msh Homeobox 1
MV	Mitral Valve
MVIC	Mitral Valve Interstitial Cell
MVP	Mitral Valve Prolapse
ODF2	Outer Dense Fiber Of Sperm Tails 2
OFT	Out Flow Tract
PAGE	Polyacrylamide gel electrophoresis
PBS	Phosphate-buffered saline
PCP	Wnt/Planar Cell Polarity
PECAM	Platelet and Endothelial Cell Adhesion Molecule
PKA	Protein Kinase A
PKD	Policystic Kidney Disease
PL	Posterior Leaflet
PPP2R5A	Protein Phosphatase 2 Regulatory Subunit B'Alpha
RHD	Rheumatic Heart Disease
RIPA	Radioimmunoprecipitation Assay
RSPO2	R-Spondin 2
RTK	Receptor Tyrosin Kinase
SDS	Sodium dodecyl sulfate
Sox9	SRY-Box Transcription Factor 9
TAT	Trans-Activator of Transcription
Tbx20	T-Box Transcription Factor 20
TCF	T-Cell-Factor
TCF4	T-Cell-Factor 4
TEM	Transmission electron microscopy
Tet	Tetracycline-Controlled Transcriptional Activation
TGF	Transforming Growth Factor
TIMPS	Tissue Inhibitor of Metalloproteinases
TNS1	Tensin 1
Twist1	Twist Family BHLH Transcription Factor 1
VEC	Valvular Endothelial Cell
VIC	Valvular Interstitial Cell
VSD	Ventricular Septum Defect
WNT	Wingless and Int-1
WNT9A	Wnt Family Member 9A

LILONG GUO. Regulation of Wnt/β-Catenin Signaling in Cardiac Valve Development and Disease. (Under the direction of RUSSELL A. NORRIS)

ABSTRACT

Non-syndromic Mitral Valve Prolapse (MVP) is a common disease with associated morbidities and mortality. Affecting 2-3% of the global population, MVP has become a significant health burden in developed countries.

We recently identified mutations in the cilia gene, *DZIP1* in multiple families with MVP. To initially identify the function of DZIP1 in valve biology, we performed proteomics-based approaches with the goal of identifying unique binding partners for DZIP1. These studies revealed a direct interaction between DZIP1 and the β-catenin antagonist, CBY1. We hypothesized that DZIP1 suppresses the Wnt/ β-catenin pathway during mitral valve development through CBY1. Immunofluorescence staining revealed overlap between DZIP1 and CBY1 protein at the basal body of the primary cilium. Increase of activated β-catenin was observed in the $Dzip1^{S14R/+}$ valves. Co-immunoprecipitation confirmed an interaction between DZIP1, CBY1 and β-catenin. Ensuing immunofluorescence staining suggested overlap between β-catenin and the basal body. DZIP1 truncation mutants identified a minimal CBY1 interaction motif within the C-terminus of DZIP1. A membrane permeant mimetic peptide against this motif was synthesized and confirmed

as being able to interact with CBY1 and β-catenin. Treatment of chicken valve interstitial cells with the mimetic peptide resulted in significant decrease in activated nuclear β-catenin. To test whether this pathway was relevant in the context of the DZIP1 mutation, we assayed nuclear vs. cytoplasmic β-catenin expression in *Dzip1*$^{S14R/+}$ MEFs. Western blot analysis showed a significant increase in nuclear β-catenin from the mutant cells. An additional family was identified with a rare DZIP1 variant within the DZIP1-CBY1 interaction motif. The mutation resulted in reduced DZIP1 and CBY1 protein stability and a peptide synthesized with the mutation resulted in an enhanced interaction between DZIP1 and β-catenin and an inhibitory effect on β-catenin signaling. Through analysis of nuclear β-catenin expression profiles during cardiac valve development, we conclude that Wnt/β-catenin signaling is temporally and spatially regulated. It is down regulated after E13.5 and undetectable in the adult. However, β-catenin signaling is significantly upregulated in human myxomatous valves and thus may be a major contributor to disease phenotype.

In conclusion, DZIP1 suppresses Wnt activity to direct mitral valve development through interacting with and stabilizing CBY1. This study characterizes the β-catenin expression profile during murine cardiac valve development and reveals a molecular mechanism, by which mutations in *DZIP1* alter valve development leading to increased β-catenin signaling.

Altered β-catenin signaling may be an early initiating signal in the pathogenesis of MVP.

Chapter 1: Introduction

1.1. Cardiac Valve Growth and Development

1.1.1. Cardiac Valve Structure and Function

The four-chambered vertebrate heart has two sets of cardiac valves: the atrioventricular (AV) valves and semilunar (SL) valves. The AV valves, which include the mitral and tricuspid valves separate the atria and ventricles. The SL valves, which include the aortic and pulmonic valves separate the ventricles from the great arteries at the arterial pole[1].

The AV valves are made up of two (mitral) or three (tricuspid) valve leaflets, while the three leaflets of SL valves are named as cusps. The other difference between AV and SL valves, except for the leaflet's name, is the supporting apparatus. AV valves are supported by chordae tendineae, which attach the valve leaflets to the ventricular papillary muscles[2]. The asymmetric leaflets are hinged to ring-raped annuli. A comparably unique supporting structure is present in aortic and pulmonic roots forming a fibrous annulus[3, 4]. Distinguished from AV valves annuli, the aortic valve annulus is crown-shaped giving rise to the "semilunar" shape of the individual cusps[5]. The names of the cusps are given by their relationship to the coronary artery ostia which are left, right and noncoronary cusps. Similar to AV valves, complete closure of the three cusps during diastole prevents blood regurgitation. To maintain unidirectional blood flow through the heart, heart

valves open and close approximately 40 million times a year and 3 billion times over an average lifetime[6].

Mature cardiac valves consist of complex stratified connective tissue which includes three different extracellular matrix layers (**Figure 1.1**). The layer termed the atrialis (AV) or ventricularis (SL) is predominantly composed of radially orientated elastic fibers. This layer provides assistance in valve tissue movement by allowing extension and recoil of the valve during the cardiac cycle[7]. The layer adjacent to atrialis (AV) or ventricularis (SL) is the spongiosa, which is primarily composed of proteoglycans, such as versican, decorin and biglycan. Proteoglycans in connective tissues serve for hydration, compliance, viscosity and regulation of collagen fibrillogenesis[8]. Their accumulation in tissues is associated with myxomatous degeneration[9]. Due to the compressible feature of proteoglycans, this layer provides a buffer region to absorb high force and allows for changes in leaflet shape during the cardiac cycle[10]. Adjacent to the spongiosa layer is the fibriosa layer, which is away from blood flow and located on the ventricular side of the AV valve leaflets and atrial side of the SL cusps. This layer is composed of densely packed collagen fibers, which provide strength and stiffness to maintain coaptation during diastole when back pressure stretches the valve leaflet or cusps[11]. Noticeably, these layers actually contain not only one type of ECM.

For example, collagen can be found in both atrialis and fibriosa[12], a network of elastic fibers also are present in spongiosa[13], and certain types of proteoglycan such as versican, decorin ,biglycan, tenascin are also observed in fibrosa and atrialis[13, 14]. The highly organized connective tissue system provides an indispensable biomechanical force for coping with the pressure stretches and compression imposed by the blood flow.

Besides ECM, the cells within the valvular tissue play a fundamental role in maintaining connective tissue homeostasis in the cardiac valvular functions. Similar to all the other blood-contacting cardiovascular system surfaces, the valves are lined by a layer of valvular endothelial cells (VECs) and packed with valvular interstitial cells (VICs).

VECs function in endothelial-to-mesenchymal transition during early valvulogenesis through transducing various signals have been elucidated profoundly while its roles in later stage still remain unclear[15-17]. The transformation of endothelial cells to mesenchymal cells requires the downregulation of intercellular adhesion junctions such as VE-cadherin. Pro-EMT-inducing stimuli such as Tgf-β and Notch secreted from adjacent myocardium coordinate reprogramming of endothelial cells towards a mesenchymal phenotype. Prototypical EMT-inducing transcription factors

such as Snail proteins are activated by Tgf-β and Notch and directly repress VE-cadherin expression by binding to promoters of VE-cadherin[18].

VICs are the most common cells in the valve and are composed of heterogeneous embryonic progenitor endothelial/mesenchymal cells, quiescent VICs (qVICs), activated VICs (aVICs), progenitor VICs and osteoblastic VICs[19]. Studies have shown that the heterogeneous behavior and expression of ECM demonstrated by VICs derived from different regions of valve tissue may be due to their diverse mechanical and extracellular environments *in vivo*[20-22].

The complex and well-defined ECM deposition as well as heterogeneous VICs give rise to the hints that diseased valvular tissues demonstrate altered ECM localization. The disturbed arrangement of connective tissue leads to valvular morphological change. (**Figure 1.2**)

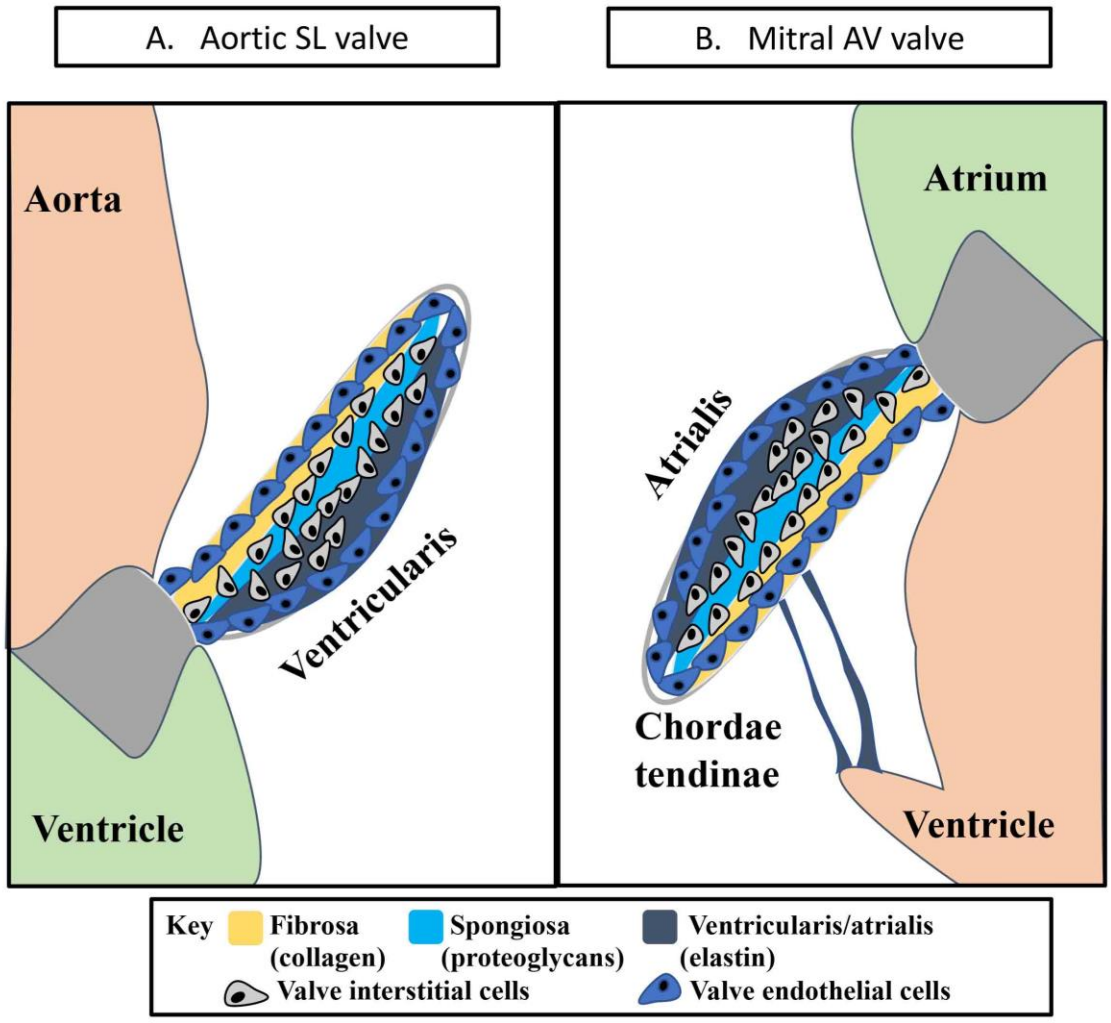

Figure 1. 1 Overview of microarchitecture of adult cardiac valves

Valve leaflets are composed of three layers of stratified extracellular matrix, including an elastin-rich ventricularis layer in SL valves (**A**) or the atrialis layer in the AV valves (**B**) shown as yellow, a proteoglycan-rich spongiosa layer shown as blue and a collagen-rich fibrosa layer shown as black. Valve tissue is sheathed in a monolayer of valve endothelial cells (VECs) and interspersed with valve interstitial cells (VICs). Mitral valve leaflet is supported by chordae tendinae, which attach leaflet to papillary muscles in ventricle. *Adapted from Katherine E. Yutzey, Dvelopment,2020.*

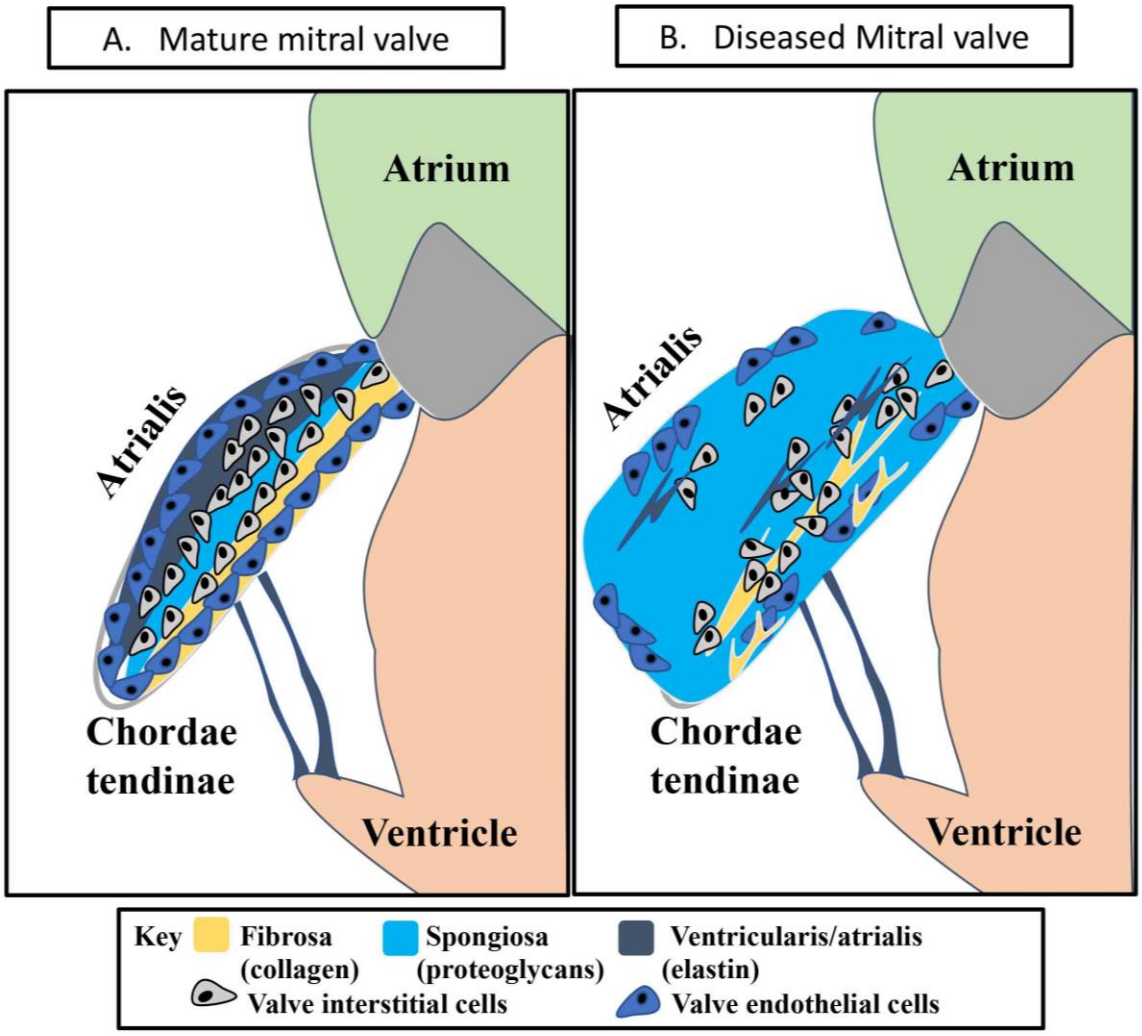

Figure 1. 2 Diseased mitral valve is associated with disorganized ECM, disrupted VECs and altered VICs

A. Well defined monolayer of VECs sheathing valve tissue and organized stratified ECM layers. **B**. Diseased mitral valve showing disrupted interspaces between ECM layers, disorganized VICs and interrupted VECs. *Adapted from Katherine E. Yutzey, Dvelopment,2020.*

1.1.2. Endocardial cushion formation

During early vertebrate embryogenesis, the heart tube consists of an outer layer of myocardial cells and an inner lining of endocardial cells[23-27]. Specialized ECM composed of proteoglycans and glycosaminoglycans separates the myocardial and endocardial cell layers which is referred as cardiac jelly (CJ)[28]. Soon after rightward looping of the heart, the myocardium localized within specific regions of the primary heart tube, the atrioventricular canal (AVC) and outflow tract (OFT) increase ECM secretion, of which hyaluronan and chondroitin sulfates are the major components. This process gives rise to "swellings" of CJ into the lumen of the heart tube. Thus, the structure termed "endocardial cushion" is formed[1, 28-31]. The AVC or inlet connects atria and ventricles, and the OFT connects the ventricular outlets to the great arteries. Paracrine signals stimulate a subset of AVC and OFT endocardial cells to lose cell-cell contact, leading to their transformation into migratory mesenchyme. As a result, newly transformed mesenchymal cells seed the CJ separating endocardium and myocardium and proliferate to populate endocardial cushions. The process whereby subsets of AVC and OFT endocardial cells transform into a mesenchyme is called endothelial-to-mesenchymal transformation (**Figure 1.3**)[32, 33].

Due to the EMT, the CJ between AVC and OFT becomes mesenchymalized and grows progressively into the lumen of the AVC and OFT as the primordium of future valve leaflets of the atrioventricular inlet (mitral and tricuspid valves) and the ventricular outlet (aortic and pulmonary semilunar valves). The fused atrioventricular cushions (AV cushions) lead to the eventual formation of the posteroinferior and septal leaflets of the tricuspid valve and the aortic leaflet of the mitral valve (anterior leaflet). During superior and inferior cushion fusion, the lateral cushions formed at the right and left AV junctions accounts for the development of anterior and posterior leaflets of tricuspid valve and the mural leaflet of the mitral valve[34, 35]. This radical event is dependent on myocardium derived soluble factors to signal the endocardium[36].

Formation of semilunar valves originates from cushion mesenchyme in the outflow tract. At 4-5 weeks of gestation, two big swellings in the truncal region (truncal cushion) and two small swellings in the conal region (conal cushion) develop in the outflow tract. The exact borderline between the truncal and conal cushion is almost unassessable in mammals. So, they are collectively termed conotruncal cushions. The mesenchyme of truncal cushions is mainly from neural crest cells, where the truncal mesenchyme then fuses and differentiates to form aortopulmonary septum that divides the aorta

and pulmonary trunk. The mesenchymal conal cushions then merge to form a conal septum, separating the proximal OFT into the right and left ventricular outlets. The mesenchyme of conal cushions is derived from EMT of the endocardium, they give rise to the posterior right and left pulmonary valve cusps and to the anterior right coronary and left coronary aortic valve cusps. Adjacent to the conotruncal cushions are two other distinct cushions- the right-posterior and the left-anterior intercalated cushions. They develop respectively into the posterior noncoronary aortic valve cusps and anterior pulmonic valve cusps[37] (**Figure 1.4**).

The endocardial cushions not only give rise to valve structures but also contribute to the septation of the cardiac chambers. After endocardial cushions fuse across the midline of the AVC and proximal OFT, the junctional segments are divided anatomically into right and left or dorsal-ventral channels or outlets by septal partitions originated from the cushion fusion[38-40].

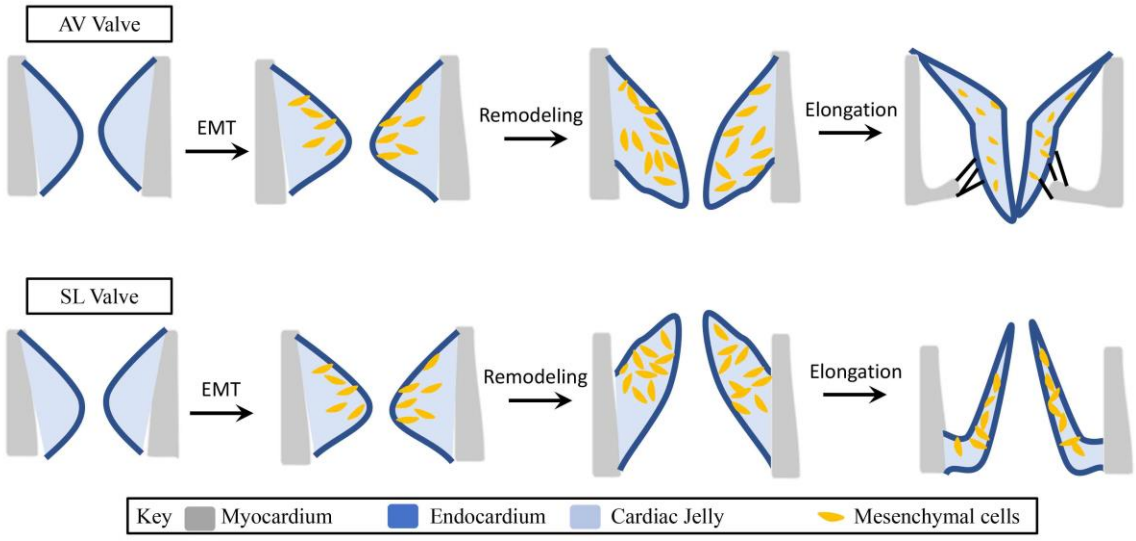

Figure 1. 3 Epithelial-to-mesenchymal transformation and valve elongation

Endocardial cells in the AV cushions and conal cushions undergo endothelial-to-mesenchymal transformation (EMT) and generate mesenchymal cells that populate the cushions. The mesenchymal cushions then remodel and elongate themselves to from primitive valves that mature into thin valve leaflets (shown here for the atrioventricular valves and the semilunar valves). *Adapted from Ching-Pin Chang, Development,2012.*

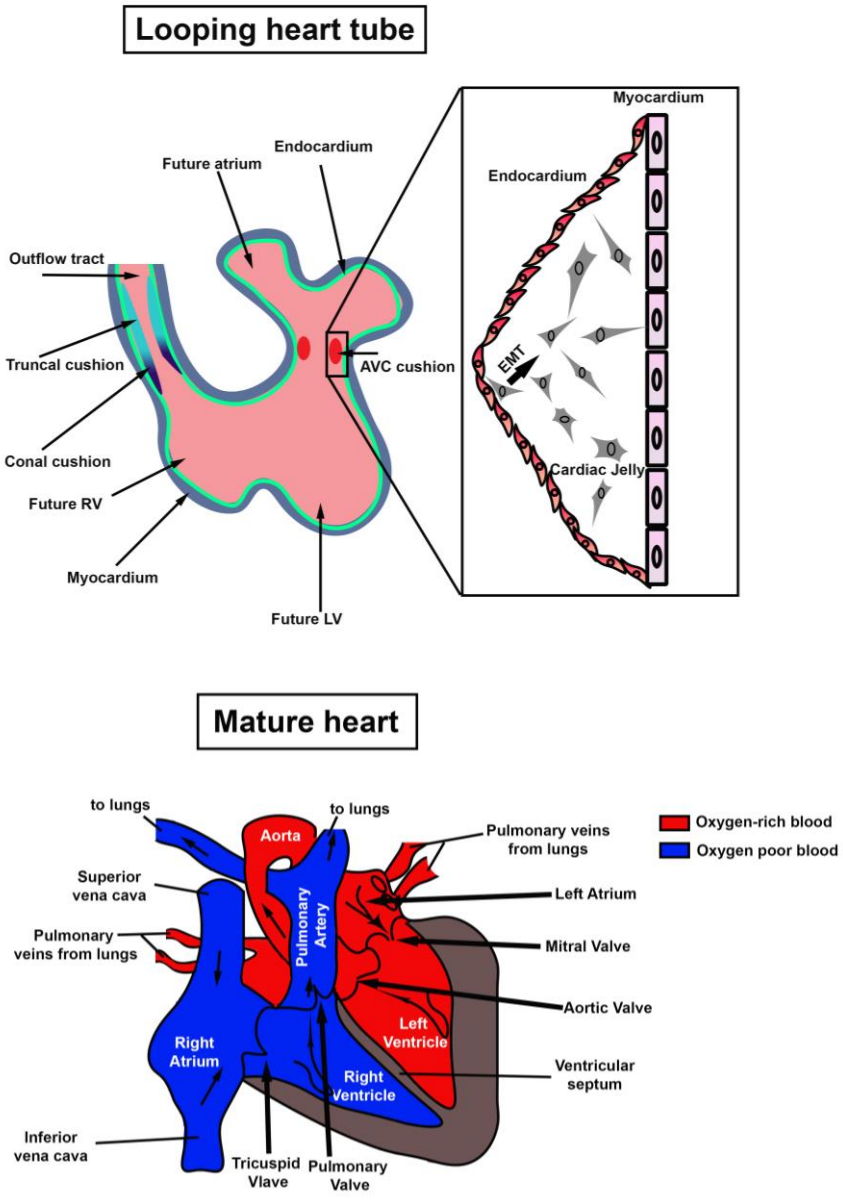

Figure 1. 4 Cardiac valves development

Looping heart tube: During embryogenesis the cardiac valves develop through EMT of the endocardial cells. AVC cushion become AV leaflets and conotruncal cushion and intercalated cushions (not shown) become SL cusps. Mature heart: separated four chambers and AV/SL structure. Arrows illustrate the blood flow directions in circulation. *Adapted from Peter ten Dijke, Springer,2013.*

1.1.3. Wnt signaling in cardiac EMT and valve morphogenesis

The initiation of endocardial cushion EMT has been marked by activation of valvular endothelial cells (VECs) in response to a variety of signals derived from the adjacent networking myocardium[36]. Most of the signaling pathways crucial for early embryogenesis have been demonstrated to have an effect on endocardial cushion EMT, including transforming growth factor beta (TGF-β), WNT, and bone morphogenetic protein (BMP) ligands[1, 41-44]. This section is mainly focusing on Wnt/β-catenin signaling.

It has been asserted that Wnt signaling is used by cells to influence the fate or behavior of neighboring cells during development[45-48]. Wnt molecules are implicated in maintaining stem-cell-like fates in the interstitial epithelium[49], skin[50], hemopoietic cells[51] and promoting proliferation in AV cardiac cushion cells[52]. They are considered to signal through canonical and non-canonical pathways.

Canonical Wnt signaling has been investigated in a large number of developmental and disease processes. Simply speaking, a Wnt ligand is secreted and binds to and activates the Frizzled (FZD) class of receptors with low-density-lipoprotein receptor-related protein (LRP) on the cellular membrane, through complicated regulatory components, leading to the

stabilization and nuclear localization of β-catenin and subsequently activates Wnt target genes in working with TCF/LEF1 family transcription factors[53]. In the absence of Wnt ligands, β-catenin is sequestered and phosphorylated by a degradation complex consisting of Adenomatosis polyposis coli (APC), AXIN, Glycogen synthase 3 β (GSK3β), and Casein kinase 1 (CK1). Phosphorylated β-catenin is targeted for degradation by the proteasome (**Figure 1.5**).

Upon Wnt stimulation, this GSK3β/AXIN/APC destruction complex is inactivated through phosphorylation and subsequently stabilizes β-catenin and releases it for entry into the nucleus. This pathway is critical for both endocardial cushion mesenchyme formation and later valve remodeling[18]. Studies in zebrafish revealed the contributions of Wnt/β-catenin signaling in determining endocardial cell fate. The *apc* mutant zebrafish hearts which had constitutive activation of the pathway failed to loop and form excessive endocardial cushions. Conversely, overexpression of Apc or Dickkopf 1 (Dkk1), a secreted Wnt inhibitor, resulted in the block of cushion formation[42]. Studies in mice reinforce the observations in zebrafish that endothelial deficiency of β-catenin demonstrated a lack of heart cushion

formation. The impairment of the β-catenin null cells to transform upon TGF-β 2 stimulation implied a cross-talk between Tgf-β and Wnt-signaling pathways during EMT[54]. However, this study did not clarify whether the loss of AV cushion mesenchyme in endothelial β-catenin (*Ctnnb1*)-null mice results from disrupted Wnt signaling or the distinct adherens junction role of β-catenin[55]. A recent study using inducible Tet-On transgenic system that provides spatiotemporal Wnt inhibition through *Dkk1* expression suggested that canonical Wnt signaling is required for proximal outflow tract but not AVC cushion EMT. The loss of AVC cushions in endothelial β-catenin null mice is due to loss of adherens junctions. The Wnt signaling actually supports AVC cushion expansion as being required for AVC mesenchyme proliferation during EMT and enables mitral valve cushion mesenchyme to respond to subsequent ECM patterning cues[56].

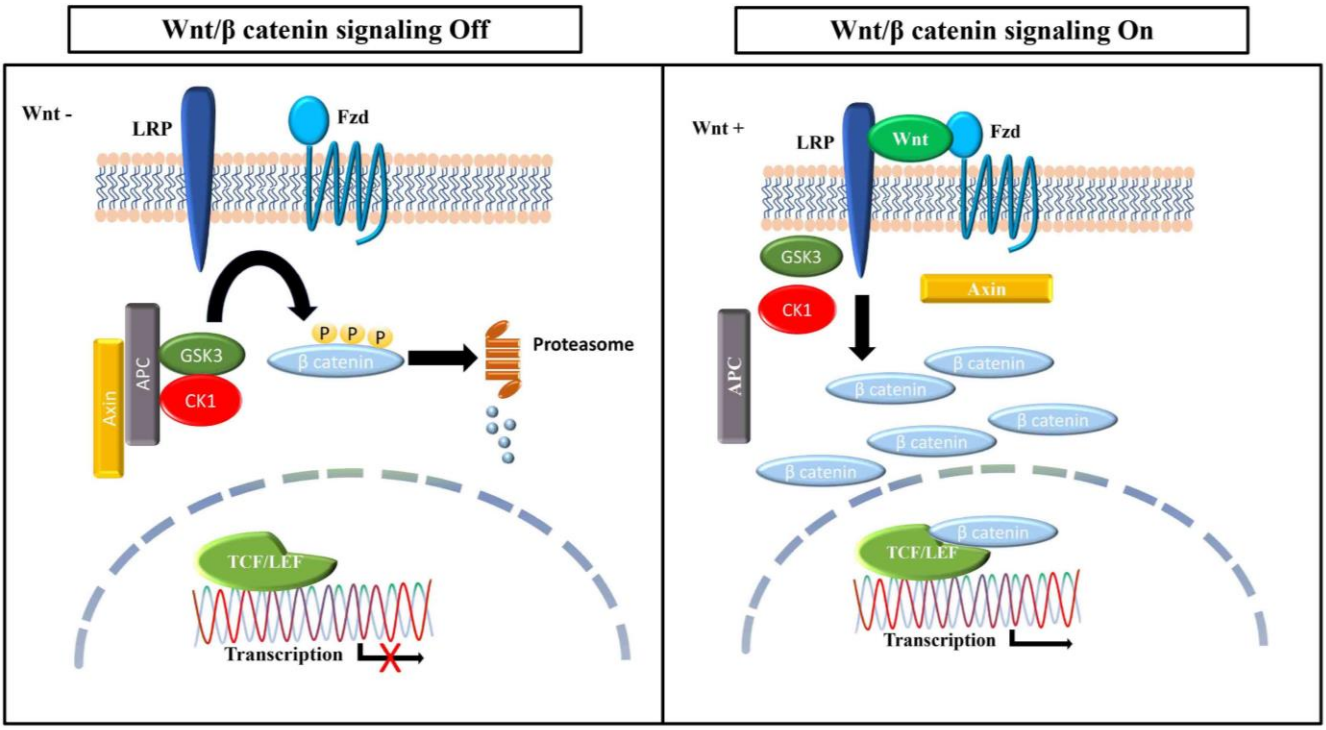

Figure 1. 5 Overview of Wnt/β catenin signaling

In the off-state, or absence of Wnt, cytoplasmic β-catenin forms a complex with APC, Axin, CKI, and GSK-3 and then is targeted for proteasomal degradation while Wnt target genes are repressed by TCF/LEFs. In the on-state, or presence of Wnt, a receptor complex forms between Frizzled and lipoprotein receptor-related protein families, which leads to accumulation of β-catenin in the cytoplasm and nucleus, where it serves as a coactivator for T CF/LEFs to activate Wnt-responsive genes. CK1, Casein kinase 1; GSK-3, glycogen synthase kinase 3; TCF/LEF, T cell-factor proteins/ Lymphoid enhancer-binding factor; LRP, low-density-lipoprotein receptor-related protein; APC, adenomatous polyposis coli. *Adapted from Evangelisti C, Int. J. Mol. Sci. 2020.*

Another study by Hulin *et al*[57] using *Axin2* knockout (*Axin2*$^{LacZ/LacZ}$ *or* *Axin2*$^{-/-}$) mice offers significant advantage to study the role of canonical Wnt/β-catenin signaling in valve homeostasis. Axin2 is an inhibitor of canonical Wnt/β-catenin signaling, the study showed hyperactivated Wnt/β-catenin signaling due to loss of *Axin2* leads to progressive myxomatous ECM in mitral valves and aortic valve calcification.

Genetic studies from human myxomatous mitral valves suggested increases of multiple canonical Wnt/β-catenin signaling components including Wnt ligand (WNT9A), and receptor (FZD8), transcription factors (TCF4), and extracellular positive modulators of Wnt signaling (RSPO2), which is an Wnt/β-catenin signaling agonist through attenuation of DKK1-dependent inhibition of Wnt ligands[58-60]. TGF-β2-treated human mitral valve interstitial cells (MVICs) demonstrated increased nuclear translocation of β-catenin while total protein levels stay unchanged in keeping with the prior study showing the cross talk between TGF-β and Wnt/β catenin signaling[54, 60, 61].

The other branch of Wnt signaling is the planar cell polarity (PCP) pathway, which is regulating the cells' orientation relative to an axis along the plane of the tissue. Due to its independence of β-catenin, this is also called

non-canonical Wnt pathway. The core components of the pathway include transmembrane protein Frizzled, Vangl, Celsr and cytoplasmic proteins Prickle and Dvl[62]. Noncanonical Wnt ligands (Wnt5a and Wnt11) bind Fzd receptor and activate the recruitment of cytoplasmic Dvl to the plasma membrane to initiate downstream diverse pathways regulating different aspects of cytoskeleton reorganization in cell movements and polarity including RhoA, JNK, Profilin[62].

Normal cardiac development is dependent on PCP signaling, and the disrupted expression of proteins in PCP pathway contributes to heart defects. Loop-tail (Lp) mutations in *Vangl2* abrogated its interaction with *Dvl* and results in outflow tract errors during development. Lp homozygotes mice manifested double-outlet right ventricle defects and double-sided aortic arch defects[63]. Mutations in *Dvl2* gene show the similar OFT defects seen in Lp mice including double-outlet right ventricle and ventricular septal defects and the mechanism is thought to influence neural crest cell migration in PCP signaling[64]. More other studies have demonstrated that the rest PCP components are interfering the heart development, however, it is interesting to notice that no genes within the PCP pathway that cause cardiovascular defects in humans have been described thus far. This is largely due to the

fundamental role of PCP during very early gastrulation, and individuals with the mutations might be embryonical lethal[65].

1.1.4. Maturation of valve development

After formation of endocardial cushion is finished, EMT is stopped and VECs regain cell-cell contacts and get back an uninterrupted endothelium. At the same time, the connective tissue within the developing valve structures goes through extensive remodeling and cells continues to proliferate. The mature valve structure is made up of highly organized ECM that is sectionalized into three layers: the fibrosa, spongiosa, and atrialis (AV) or ventricularis (SL) as described in the first section.

The ECM of endocardial cushions before EMT is rich in hyaluronan, and the mesenchymal cells in the cushions start to produce collagens and matrix metalloproteinases (MMPs) 1, 2, 13, which promote cell migration[66-69]. The ECM composition of the mature valves is dependent of the synthetic activity of the VICs. Genes that encode fibrillar collagens, chondroitin sulfate proteoglycans and elastin are associated with the stratified ECM of the valve leaflets during the valve remodeling[3, 70]. At the molecular level during mid-stages of valvulogenesis, loss of expression of mesenchymal-specific genes, including *Twist1*, *Tbx20*, *Msx1*, and *Msx2*, were observed in VICs. *in vitro* experiment showed that VICs isolated from pre-fused endocardial cushions

appear to have decreased differentiation potential as development progresses. Differentiation markers including *Sox9* for chondrocyte and *Scleraxi*s for tendon cells start to express in the VICs concurrently[71-74]. The complexity of ECM protein expression and stratification are the structural basis for valve function throughout life[10, 75]. Loss of the proteoglycan versican results in endocardial cushion maturation defects. Expressions of MMPs and their inhibitors, tissue matrix metalloproteinases (TIMPS) have been validated in the remodeling valves, and increased expression of several of these genes have been associated with human myxomatous valve disease as being observed with ECM disorganization[76-78].

1.2. Primary Cilia

1.2.1. structure and function

The primary cilium is a microtubule-based organelle that projects from the surface of the vertebrate cells[79]. Since as early as 1898 when primary cilium was first discovered, the primary cilium had long been ignored and was considered to be a vestigial remnant of evolution[80]. As intensive studies recently brought primary cilia into the spotlight, biologists have gained more insights of its structure and functions in development, human disease and cancer[81].

Sharing similar structure components with other types of cilia (motile cilia, nodal cilia), primary cilia demonstrate unique constructions which are closely tied to its function. Structurally, a primary cilium is composed of an axoneme and basal body. Generally speaking, most cells posse one cilium, an exception being olfactory sensory neurons where each cell possess about 10 primary cilia[82]. The axoneme of a primary cilium contains a ring of nine outer microtubule doublets (known as 9+0 axoneme) which differs from motile cilium containing additional two central microtubule singlets surrounded by a ring of nine outer microtubule doublets (known as 9+2 axoneme). Besides the central microtubule singlets, motile cilia possess dynein arms (outer and inner dynein arms) and radial spokes, the structures essential for and regulate cilium motility[83, 84]. The extension and maintaining of the axoneme are mediated by IFT (intraflagellar transport) machinery which transports various of particles along the axoneme. There are two trafficking systems defined by different compositions and trafficking directions. The anterograde IFT, moving from base toward cilium tip, is composed of kinesin-2 motor (contains KIF3A, KIF3B and KAP3) and IFTB proteins. While the retrograde IFT, moving from cilium tip toward the base, consists of dynein motor (DYNC2H1 and DYNC2L11) and IFTA proteins[85]. The two reversed trafficking complexes functions uniquely

during ciliogenesis. Perturbation of the anterograde IFT blocks cilia formation, however, disruption of the retrograde IFT leads to shortened cilia[85-89].

The basal body, a barrel structure of nine triplet microtubules, is derived from the mother centriole (**Figure 1.6**). During G1 phase, the centriole moves to the cell surface where it acts as a basal body to initiate ciliogenesis. Then, the cilia are resorbed during mitosis, and the basal body moves to the spindle pole and revert to centriole[90]. Basal bodies are absolutely required for ciliogenesis. One of the crucial functions is that basal bodies provide the template for the formation of the array of nine microtubule doublets of the axoneme. Studies showed that basal bodies that lost ninefold symmetry failed to propagate symmetry information to the axoneme, which had an effect on the doublets number in axoneme[91, 92]. It is also indicated by the electron micrographs that the outer doublet microtubules of the axoneme are contiguous with the triplet microtubules in the basal body[93]. In addition to acting as a template for microtubules, basal bodies also play a key role in membrane docking during ciliogenesis through ultrastructural features called transitional fibers by contacting the cell surface[90]. By forming centriole-associated vesicles prior to the fusion with plasma membrane, the docking process is a specialized type of exocytosis[94]. Finally, basal bodies provide docking stations for proteins during primary cilia biogenesis through the

specialized structures at its distal end. Elongation of a growing cilium requires IFT cargo to transport ciliary proteins. Basal body contains recognition sites to recruit these assembly factors as evidenced by IFT accumulation around the basal body[95].

Between axoneme and basal body is the transition zone, and transition fibers, collectively known as "ciliary gate" (**Figure 1.6**). Structurally, the transition zone includes Y-shaped links, ciliary necklace, and terminal plate (often visualized as an electron-dense aggregate on TEM). Y-shaped links act as connectors between microtubule doublets and primary cilia membrane microtubule doublets and primary cilia membrane. Ciliary necklace consists of several parallel strands of intramembrane particles separating terminal plate from plasma/cilia[96]. In motile cilia, the boundary between the axoneme and transition zone is referred to basal plate which is considered to participate in the nucleation of the central microtubules[97]. Because the lack of the central microtubules, primary cilia do not have this structure. It is proposed that the transition zone is to regulate ciliary protein composition in *Chlamydomonas*, *C. elegans* and mammalian cells through regulating the trafficking during ciliogenesis. However, the details of how the proteins are sorted have been undecided[98-100]. Transition fibers derive from basal body triplet microtubules forming a "pinwheel-like" structure on TEM cross-sections.

They are thought to anchor microtubules to the plasm membrane through CEP164[101, 102] and ODF2. Also, transition fibers may play a role in docking the IFT and motor proteins required for ciliogenesis as evidenced by studies showing the localization of IFT52 on transition fibers[95].

Being distinguished from architecture of axonemal microtubules, both motile and non-motile cilia are prevalently present in multiple tissues and organs throughout the body regulating key events during development and in the adult. Motile cilia are mainly used to move extracellular fluid and gametes. The motility is required to determine embryonic left-right asymmetry though a generation of extraembryonic fluid flow[103]. Motile cilia present on respiratory epithelial cells are contributing to mucus clearance[104]. Furthermore, the ependymal flow is also mediated by motile cilia[105]. On the other hand, primary cilia, lack of dynein arms and radial spokes, are fundamentally involved in chemo- and mechanosensory process that coordinate a variety of signaling pathways, such as the pathways mediated by Hedgehog (HH), G-protein-coupled receptors (GPCR), WNT, receptor-tyrosine kinases (RTKs) and TGF-β/BMP receptors[79, 106-123].

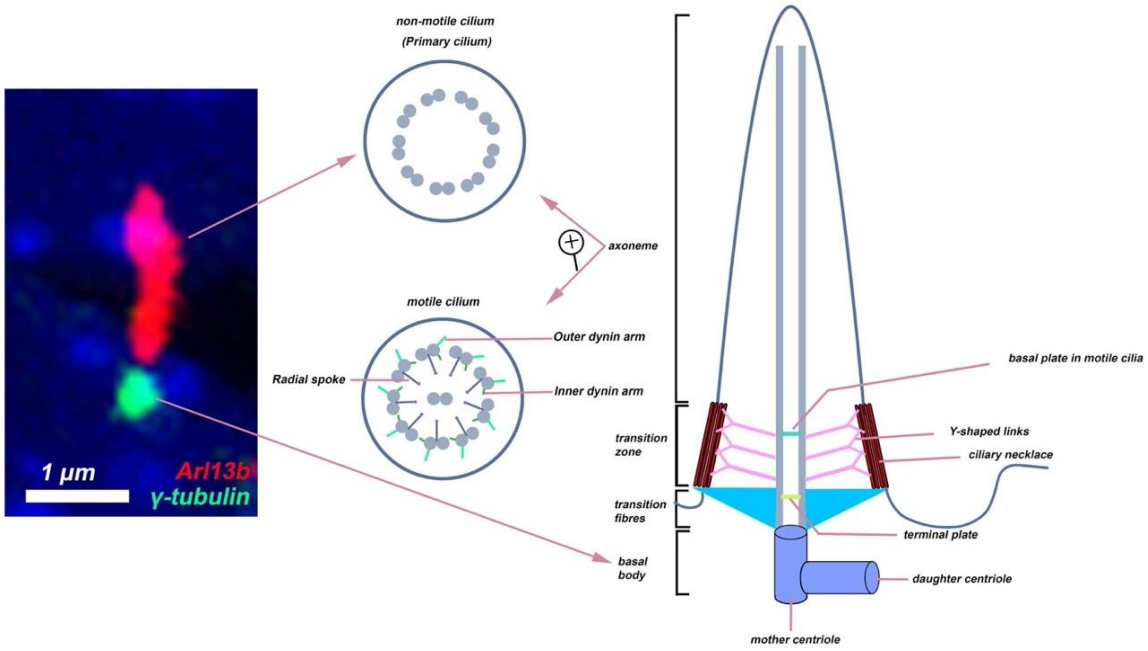

Figure 1. 6 Schematic representation of cilia ultrastructure

Cilium is microtubule-based organelle structurally including axoneme, transition zone, transition fibers and basal body. On the middle part, is cross-sections at axoneme in non-motile (Aka. Primary cilium) and motile cilium. Non-motile cilium has a 9+0 microtubule composition whereas motile cilium has a 9+2 microtubule composition possessing dynein arms, radial spokes. Ciliary motility of motile cilium is regulated by outer and inner dynein arms. On the left-hand side, is an enlarged immunofluorescence micrograph of a single primary cilium on an neonatal mouse mitral valve tissue for the cilia marker Arl 13b (red), the basal body marker γ-tubulin (green). Scale bar = 1 µm. *Adapted from Szymanska and Johnson, Cilia, 2012.*

1.2.2. Primary cilia in cardiac development

Expression of primary cilia in cardiac tissue during development is conserved across species[124]. Human embryonic and adult heart were also found to have primary cilia first by R Myklebust, et al in 1977[125]. Later on the spatiotemporal distribution of primary cilia during heart development have been described by showing the presence of primary throughout the E9.5 embryonic mouse heart, lining the endothelium of both atrial primordia and persistence of primary cilia in the atrium and the ventricular trabeculation and epicardium at E12.5[126], yet no motile cilia were found in the embryonic heart through transmission electron microscopy (TEM)[127].

The expression pattern of primary cilia during the mitral valves and aortic valves development have been demonstrated by our previous studies. Primary cilia were ubiquitously present in e11.5 mouse endothelial cushions. As AV cushions develop and stratify into valves, the number of primary cilia decreases and almost are absent on adult tissue (3 months). Whereas the primary cilia length increases and reaches its peak at P0[128]. During aortic valve development, primary cilia were present on the OFT cushions at E11.5. As development proceeds into fetal life, the number of primary cilia decreases, and length increases reaching its peak at e17.5. They are largely undetectable

postnatally, similar to what have been observed in mitral valve tissue[129]. Interestingly, these studies about primary cilia spatiotemporal patterns have indicated that primary cilia were rarely seen on valve endocardium. The re-absorption of cilia in the endothelium of the endocardial cushions is probably due to the fluid sheer stress as the biomechanical forces exerted by blood flow are sensed by the endothelium[130-134].

The cilia length is a predictor of proper cilia function due to the findings of cilia function and several ciliopathies have been associated with defects in cilia length[135-137]. A number of ciliary genes affecting the elongation of primary cilia have been linked to congenital heart disease (CHD). *Ift88*, a component of the IFT system, is required for the formation and maintenance of primary cilia axonemes and has been studied extensively. Mice with *Ift88* mutations have defects in chamber maturation including atrial septal defects (ASD), ventricular septal defect (VSD), atrioventricular septal defect (AVSD), and OFT septal defects[126, 127, 138]. Furthermore, global loss of *Kif3a*, a component of kinesin-2 motor (refer to 1.2.1), results in complete lack of endocardial cushions[126] . In addition, targeted deletion of *Ift88* demonstrated a hypoplasia of endocardial cushions[138]. All these studies suggest that primary cilia are involved in formation and development of endocardial cushions.

Studies from our group demonstrated that conditional ablation of *Ift88* with *NfatC1 Cre* which knocked out *Ift88* exclusively from endocardial and endocardial derived cells results in myxomatous mitral valve disease and bicuspid aortic valves (BAV). The mechanism is still not quite clear, but the RNA-seq analysis confirmed that loss of primary cilia results in robust activation of ECM gene pathways. Subsequent IHC showed altered ECM expansion and deposition in *Ift88* deficient valve tissue. These observations highly suggest that primary cilia are likely to impact valvulogenesis through restraining ECM production[128, 129].

1.2.3. Wnt signaling and primary cilia

The Wnt signaling network is critical to valve development. As discussed above, either up or down-regulated Wnt/β-catenin signaling leads to morphological change during valvulogenesis. With more and more ciliary proteins being identified to paly roles in Wnt/β-catenin signaling, there has been a controversial argument about the link between Wnt signaling and the primary cilium.

Among them, Dvl regulates activation of the canonical pathway through inhibiting GSK3β/Axin/APC complex. In this way, Dvl protects β-catenin from being degraded by proteasome. Early studies showing Inv localized to cilia and physically interacted with Dvl first connects cilia and the canonical

Wnt pathway[139-141]. Following research using Wnt-responsive reporter construct suggested that Inv abrogated the ability of Dvl to activate Wnt signaling. These studies indicate that canonical Wnt signaling is actually constrained rather than promoted by events at cilia[140]. Disruption of primary cilia in mice containing mutations in *Kif3a, Ift88 or Ofd1* (an X-linked gene encoding a basal body protein required for ciliogenesis[142]) resulted in a remarkable increase in cellular response to canonical Wnt signaling in both cultured mouse embryonic fibroblasts (MEFs) and embryonic stem cells[143]. However, confounding results were observed in *Ahi1* mutant mice, which showed a loss of basal canonical Wnt signaling activity resulting in cystic kidney disease[144]. *AHI1* in humans encodes Jouberin, a cilia protein, mutation of which causes a severe multi-organ ciliopathy including polycystic kidneys[145]. This study might seem to indicate a positive, rather than negative role for cilia in Wnt signaling.

Some studies argue that there is in fact no role at all for cilia in Wnt signaling. The study in *ift88* mutant zebrafish did not show apparent defects in Wnt-dependent developmental processes or in expression of known Wnt target genes while did display the absence of primary cilia[146]. The *Ift88, Ift172, Kif3a* and *Dync2h1* mutant mice embryos did not show distinguishable *Axin2*, a downstream target of canonical Wnt signaling. Using BAT-gal

transgenic mouse embryo to report canonical Wnt signaling in those mutants did not show β-galactosidase expression patterns alterations, either[147]. The Wnt reporter quantification in MEFs generated from wildtype and cilia-defective mice did not find any difference in the response to Wnt ligand, as well[147]. From the confounding studies, it is very much clear that regulatory role of canonical Wnt signaling from primary cilia is cell type specific. It is drastically more subtle than the role of cilia in other signaling pathways, such as Hh signaling[148].

Additional researches about roles of cilia upon non-canonical Wnt signaling (PCP) add a further layer of complexity to relationship between cilia and Wnt signaling. Multiple PCP components are localized to basal body such as *Vangl2* and *Dvl2,* of which defections result in OFT and ventricular defects as discussed previously[63, 64, 149]. In support of the idea that non-canonical Wnt signaling is associated with cardiac primary cilia, ciliary genes such as *Gmap210* was deleted in mice embryos. GMAP210 functions with IFT20 in the trafficking of ciliary proteins for ciliogenesis. The model demonstrated cardiac phenotypes resembling those observed in multiple PCP mutants[150]. But this is not direct evidence that the cardiac phenotypes observed in the *Gmap210*$^{-/-}$ mouse are associated with defective non-canonical Wnt signaling. In recent years, the PCP pathway has been considered to be required for the

orientation of basal bodies involved in the establishment of left-right asymmetry during embryogenesis[151-153]. However, as PCP components are also required for basal body assembly/docking, a key question that remains to be determined is what is required first: intact PCP signaling for ciliogenesis/basal body positioning, or intact cilium for subsequent PCP events? Another question that needs to be elucidated is whether the cilium is responsible for the phenotypes observed in some PCP mutants. Since many of the ciliary proteins have now been identified in other cellular locations. These ciliary proteins could be necessary for some other cellular functions. For example, the basal body protein CBY1 has been reported to directly regulate β-catenin signaling[154].

1.3. Mitral valve Disease

1.3.1. Anatomy

As discussed in the first section that mitral valve (MV) apparatus is a complex structure composed of the annulus, leaflets, chordae tendineae, and papillary muscles[155-158]. Detailed anatomical features of MV will be illustrated here.

The MV annulus is a support compartment in continuity with the aortic valve through the fibrous aortic-mitral curtain. The two mitral leaflets meet at lateral and medial commissures and each leaflet is divided into three scallops

from lateral to medial—in the human. There are two dominant papillary muscles attached to MV leaflets via chordae tendineae, one anterolateral and the other posteromedial. Anterolateral papillary muscles engaging in dual blood supply while posteromedial only has single blood supply which are more prone to injury from myocardial infarction. The fibrous chordae tendineae are divided into three types based on their insertion level: primary chordae insert on the leaflet tips functioning to maintain coaptation of leaflets, the secondary chordae insert on mid-body of the leaflets providing support length to leaflets, and the tertiary chordae insert only on the basal part of the posterior leaflet functioning as structural support. Any pathological alterations at any level of the MV apparatus can lead to MV dysfunction.

1.3.2. Mitral valve pathology

1.3.2.1. Mitral valve stenosis

MV dysfunction contains mainly two types: MV stenosis (MS) and MV regurgitation. The most common cause of mitral valve stenosis world-wide is rheumatic heart disease (RHD). It is considered to be associated with an exaggerated immune response initiated by cross-reactivity between a streptococcal antigen and the valve tissue[159]. Although it is less common in western countries, it remains a major public health issue in developing countries[160]. Other rare etiologies of MS includes systemic inflammatory

disorders such as lupus erythematous and rheumatoid arthritis, congenital causes such as parachute mitral valve, double-orifice mitral valve, or supravalvular mitral ring[161].

1.3.2.2. Mitral valve regurgitation

The most common cause of mitral valve regurgitation (MR) requiring surgical intervention in developed countries is MV prolapse (MVP)[161]. MVP can be classified into syndromic and none-syndromic MVP. Syndromic MVP affect the connective tissue, such as Marfan syndrome, Ehler-Danlos syndrome, osteogenesis imperfecta and pseudoxanthoma elasticum, which result from genetic mutations associated with ECM homeostasis. MVP is one of the manifestations among multiple system impacted symptoms[161]. Non-syndromic MVP, which primarily affects mitral valve, results from myxomatous degeneration characterized by abnormal accumulation of proteoglycan, collagen fragmentation and hyperactivated fibroblast[162]. Over time, leaflets become thickened and floppy which may billow into left atrium during cardiac systolic cycle. On echocardiography, MV prolapse is defined as an abnormal leaflet systolic displacement of $\geqslant 2$ mm above the mitral annulus plane in a long-axis view[163]. The bulging leaflet gives rise to back flow of the blood into left atrium during cardiac systolic cycle

resulting in mitral regurgitation which causes left atrial and left ventricular volume overload.

Based on the time course of the development of the regurgitation, MR is divided into acute MR and chronic MR. Acute MR may culminate in cardiogenic shock due to significantly declines of forward output since much of the flow is directed to the left atrium. Also, the sudden marked increase in preload results in a significant increase in LV filling pressures which are transmitted to the pulmonary circulation leading to pulmonary edema. Chronic MR has a longer progression from early compensated stage to a decompensated stage marked by the development of symptoms. Long-term regurgitation leads to the enlargement of LA, which forms the nidus for the development of atrial arrhythmias[164].

1.4. Genetic Discoveries in MVP

MVP is a common cardiac valvular disorder that affects about 2%-3% of the general population and predisposes the affected individual to a greater risk for MR, arrhythmia and sudden cardiac death as discussed in previous section[165-167]. Increased understanding of valvular development, in combination with current advances in genome-wide association studies, has led to uncovering of a number of genetic contributors to MVP.

The first discovery of genetic basis of MVP in humans has occurred through investigation of Marfan syndrome which gives rise to syndromic MVP[168]. Mutations in Fibrillin 1 (*FBN1*), a crucial content of ECM microfibrils, have been discovered to cause Marfan syndrome[169-171]. Subsequent studies elucidated the molecular mechanism that FBN1 limits the activation of TGF-β signaling, excessive activation of which leads to ECM remodeling in the embryonic development of valves[172]. Mouse model carrying a C1039G mutation in *Fbn1* exhibit thickened valves phenocopied the myxomatous valves in human which was rescued by Tgf-β antagonism supporting the role for Tgf-β signaling in MVP[173].

Not only in Marfan's syndrome, MVP appears in other connective tissue dysplasia such as Ehlers-Danlos (EDS), Stickler, and osteogenesis imperfecta suggesting the association between genetic mutation of collagen genes and etiology of MVP. The family of collagen genes found in human valvular disease to date includes *Collagen types I-III, V and XI[174]*.

By studying families with inherited non-syndromic MVP, three genes that are associated with MVP have been identified. The first gene linked to non-syndromic myxomatous valve disease in humans is *Filamin A (FLNA)[175]*. This mutation was mapped to Xq28 in 1998 and the causal

relation of *FLNA* to X linked MVP was documented by additional four families[176-179]. *FLNA* is a structural cytoplasmic protein in the cytoskeleton and interacts with cell-surface integrins[175]. Expression of *FLNA* in the endocardium, epicardium and interstitial cells of the valves have been characterized, and mouse study with *Tie2-Cre* confirmed that loss of endothelial *FLNA* results in myxomatous mitral valves[180]. In 2015, a loss-of-function mutation in the *DCHS1*, which encodes a member of the cadherin superfamily and critical for PCP, was identified. This mutation reduces protein stability and *Dchs1*$^{+/-}$ mice develop thickened and prolapse mitral leaflets[181]. The third gene mutation was identified in *DZIP1,* which is both essential for ciliogenesis and for Hh signaling[128, 182]. Knock-in mice manifested myxomatous mitral leaflets which phenocopied human MVP and ciliopathy indicating that primary cilia contribute to the MVP disease pathogenesis[128].

In 2015, Dina *et al* identified the first 3 risk loci for MVP by performing a meta-analysis of 2 genome-wide association studies in 1412 MVP cases and 2439 controls[183]. Among the genes located within the associated haplotypes, they identified *LMCD1* (Lim and cysteine-rich domains 1), knockdown of which in zebrafish resulted in increased AC regurgitation and *TNS1* (Tensin 1), a focal adhesion protein involving cytoskeleton organization,

knockout of which in mice caused enlarged posterior mitral leaflets. This study suggests new mechanisms involved in MVP regurgitation development.

1.5. Summary

Cardiac valve development is a complex process involving multiple signaling pathways. This thesis work is mainly focusing on the canonical Wnt/β-catenin signaling. As discussed in 1.2.3, Wnt/β-catenin signaling pathway is indispensable for AVC cushions mesenchymal proliferation and for OFT EMT. A variety of Wnt signaling components are increased in myxomatous valve degeneration. Hyperactivation of Wnt/β-signaling during cardiac valve give rise to myxomatous degeneration. All these evidences suggest the importance of well-controlled Wnt/β-catenin during cardiac valve development. But the regulation of the signaling during valvulogenesis has not been profoundly investigated. The basic question that how β-catenin distributes during valve development is still not clear. The Chapter 2 of this thesis work is to clarify the expression profile of β-catenin during murine valve development. Since membrane bound β-catenin accounts for cell-cell adhesion, yet nuclear bound β-catenin is responsible for gene transcription, it is crucial to separate them when considering the roles of β-catenin during valvulogenesis. This characterization provides a platform where future studies of β-catenin signaling regulation in valve biology could be conducted.

Genetic analysis within non-syndromic MVP give rise to valuable clues in etiology of MVP. One of the genetic mutations that has been validated to cause myxomatous valve degeneration so far is *DZIP1*. Immunohistochemistry study on myxomatous valve in Chapter 2 revealed overexpression of β-catenin. To explore how Dzip1 involves in the β-catenin signaling regulation is the focus in Chapter 3.

Chapter 2: Dynamic Expression Profiles of β-Catenin during Murine Cardiac Valve Development

2.1. Introduction

β-catenin is a multifaceted protein with various functions based on its subcellular localization[184-188]. Expression studies have demonstrated its presence on the cell membrane, free within the cytoplasm and in the nucleus[189-193]. Its subcellular functions are likely driven by conserved structural motifs within the protein, which confer unique protein-protein interactions[194-196]. The basic protein organization of β-catenin consists of an amino terminal domain, a central region consisting of 12 Armadillo repeats and a carboxyl-terminal region[197, 198]. Through the Armadillo repeats, β-catenin serves as both a structural scaffold and signaling protein for a multitude of interaction partners in adherens junctions, the cytoplasm as well as the nucleus[199-203].

At the level of the membrane, β-catenin was initially discovered as being associated with E-cadherin, a critical protein essential for Ca^{2+}-dependent cell-cell adhesions[204-206]. Through these cadherin-catenin interactions the adherens junctions become stabilized[207-209]. Upon receiving a Wnt signaling and/or phosphorylation of β-catenin at specific residues, this interaction is disrupted, and β-catenin is released from its junctional components[210-212]. The fate of β-catenin following this release is complex but likely results in either its cytoplasmic destruction or its nuclear import[213,

214]. Although β-catenin does not contain an import or export signal, its nuclear presence can be driven by either protein chaperones or its binding to nuclear pore complexes[215-217]. Within the nucleus, β-catenin has been shown to regulate many aspects of nuclear biology. Most routinely analyzed are its ability to interact with co-transcription factors in the TCF/LEF1 gene family[218-220]. It is, however, becoming clear that β-catenin can have unique TCF/LEF1 independent functions in the nucleus including the regulation of chromatin remodeling as well as inducing or repressing gene transcription through association with other co-factors[221-225]. Through the complexities of the structural and signaling roles of β-catenin, it is no surprise that perturbation of its expression can impact many different tissues in various ways. For example, gain and loss of function studies in the heart have revealed a critical role for β-catenin in cardiac development, especially related to valve morphogenesis[56, 226].

Although heavily studied, a more thorough characterization of the expression and localization of either nuclear or membrane β-catenin throughout cardiac development has yet to be reported. Additionally, scant data have been shown that clarify the correlation of Lef1 and nuclear β-catenin at different gestation stages. This information is needed to inform various cardiovascular phenotypes due to its genetic perturbation. Our detailed

analysis of β-catenin's temporal, cell-specific subcellular protein expression pattern is the focus of this chapter. Herein we report a detailed β-catenin expression map within the heart, which will facilitate proper interpretation of gain and loss of function data as well as provide new insight into fundamental biological processes that are regulated by this important protein.

2.2. Results

β-catenin expression during embryonic cardiac development

IHC staining for both activated (β-catenin^{pS552}) and membranous β-catenin revealed dynamic staining patterns that are spatially and temporally regulated during embryonic gestation. At E11.5, activated β-catenin is ubiquitously expressed in the nuclei of virtually all cardiac cells including myocardium, epicardium, endothelium and aortic and atrioventricular valve progenitor cells (**Figure 2.1A-D**). A slight, yet consistently lower IHC intensity of activated nuclear β-catenin expression was observed where the superior and inferior AV cushions fuse (**Figure 2.1D**-arrows). In the outflow segment, activated β-catenin is observed throughout the myocardium and outflow tract cushions (**Figure 2.2E-H**). Within the myocardial sleave of the outflow tract, the cell membrane of myocytes also stained positive for activated β-catenin (**Figure 2.2G, H**-arrowheads). This staining seemed specific for the conotruncal myocardium as no other myocardial regions within the heart showed membrane staining for activated β-catenin.

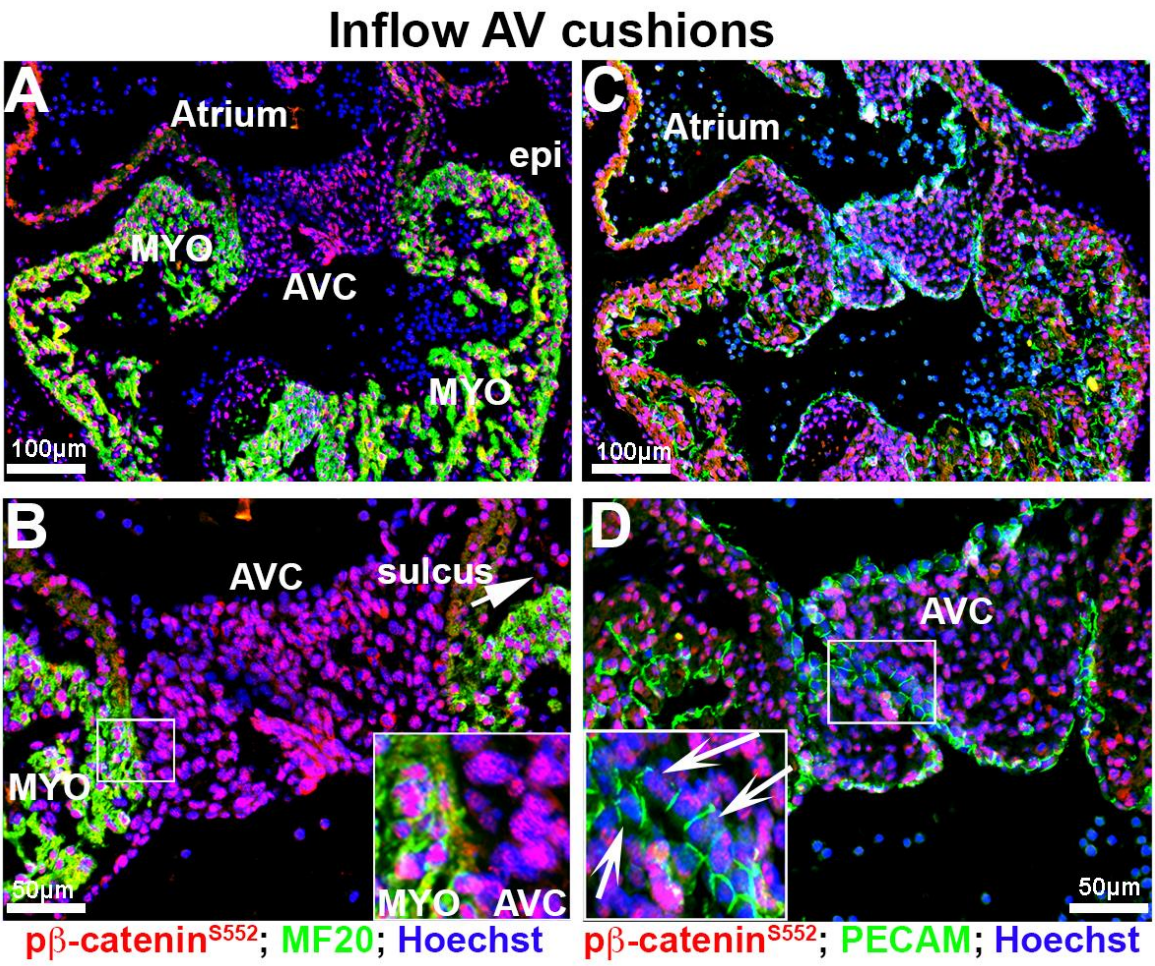

Figure 2. 1 Activated β-catenin expression at E11.5 inflow AV cushions.

Representative images of E11.5 inflow AV cushions immunostained for activated β -catenin (red), MF20 (green), PECAM (green) and nuclei counterstained with hoechst (blue). Myo=Myocardium, AVC=atrioventricular cushions, epi=epicardium, arrows=endocardium.

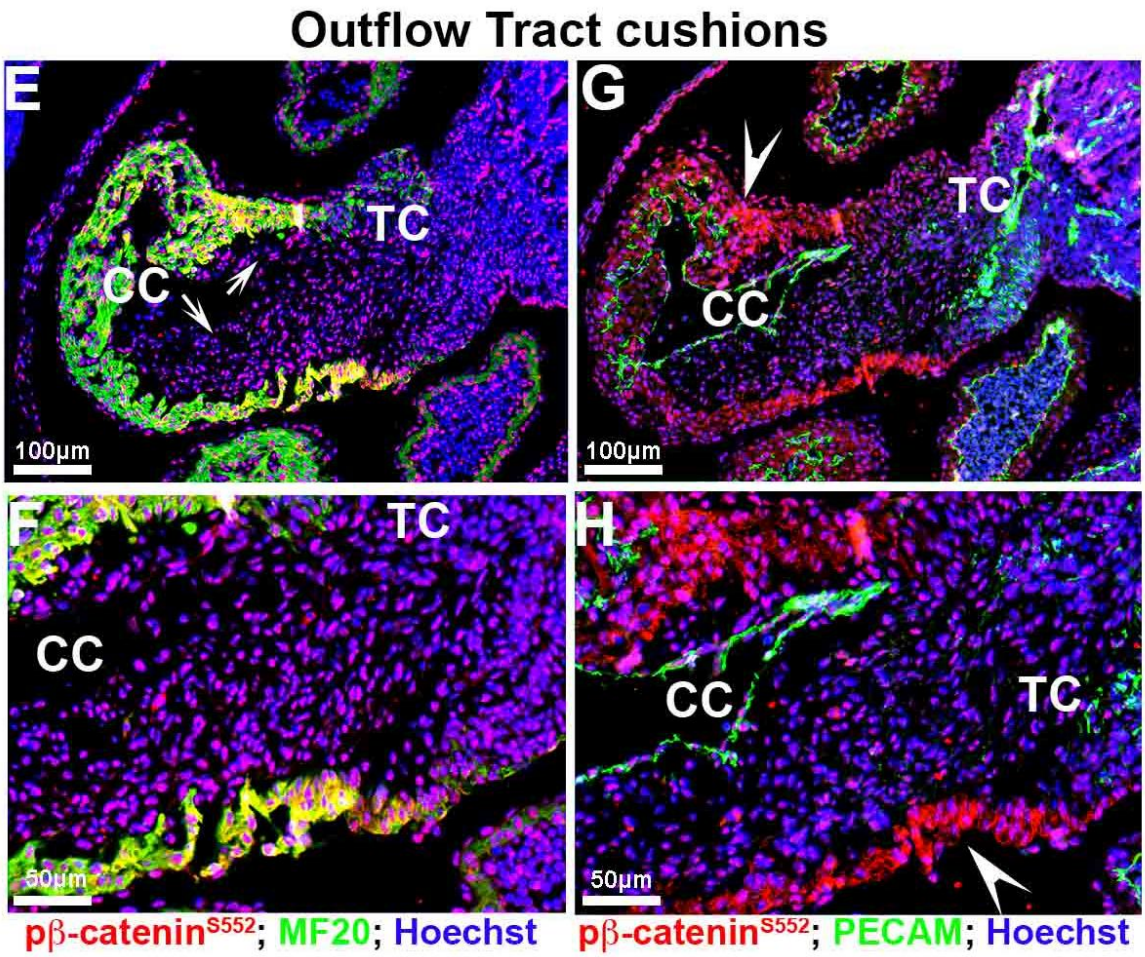

Figure 2. 2 Activated β-catenin expression at E11.5 outflow tract cushions.

Representative images of E11.5 outflow tract cushions immunostained for activated β-catenin (red), MF20 (green), PECAM (green) and nuclei counterstained for hoechst (blue). CC=conal cushions, TC=truncal cushions, arrows=endocardium within outflow tract, arrowheads=myocardium within conaltruncal myocardial sleeve.

Much like activated nuclear β-catenin expression, non-phosphorylated membrane β-catenin was also extensively observed throughout the heart at E11.5 (**Figure 2.3 & Figure 2.4**). Within the developing atrioventricular and outflow tract cushions, membrane β-catenin was observed in the endocardial and interstitial mesenchyme. Within these structures, the highest degree of intensity was observed nearest the cushion endocardium. However, in areas where the major cushions fuse, both PECAM, the adherens junctions marker, and β-catenin expression appeared dysregulated and with reduced staining intensity (**Figure 2.3D-**arrowheads). This was similar to the pattern of membrane β-catenin in the conal cushions in which the endocardial epithelium displayed lower staining intensity (**Figures 2.4E, F, and G-**arrowheads). Membrane expression of β-catenin was prominent in all cardiomyocytes as well as ventricular endocardium and epicardium at this time point.

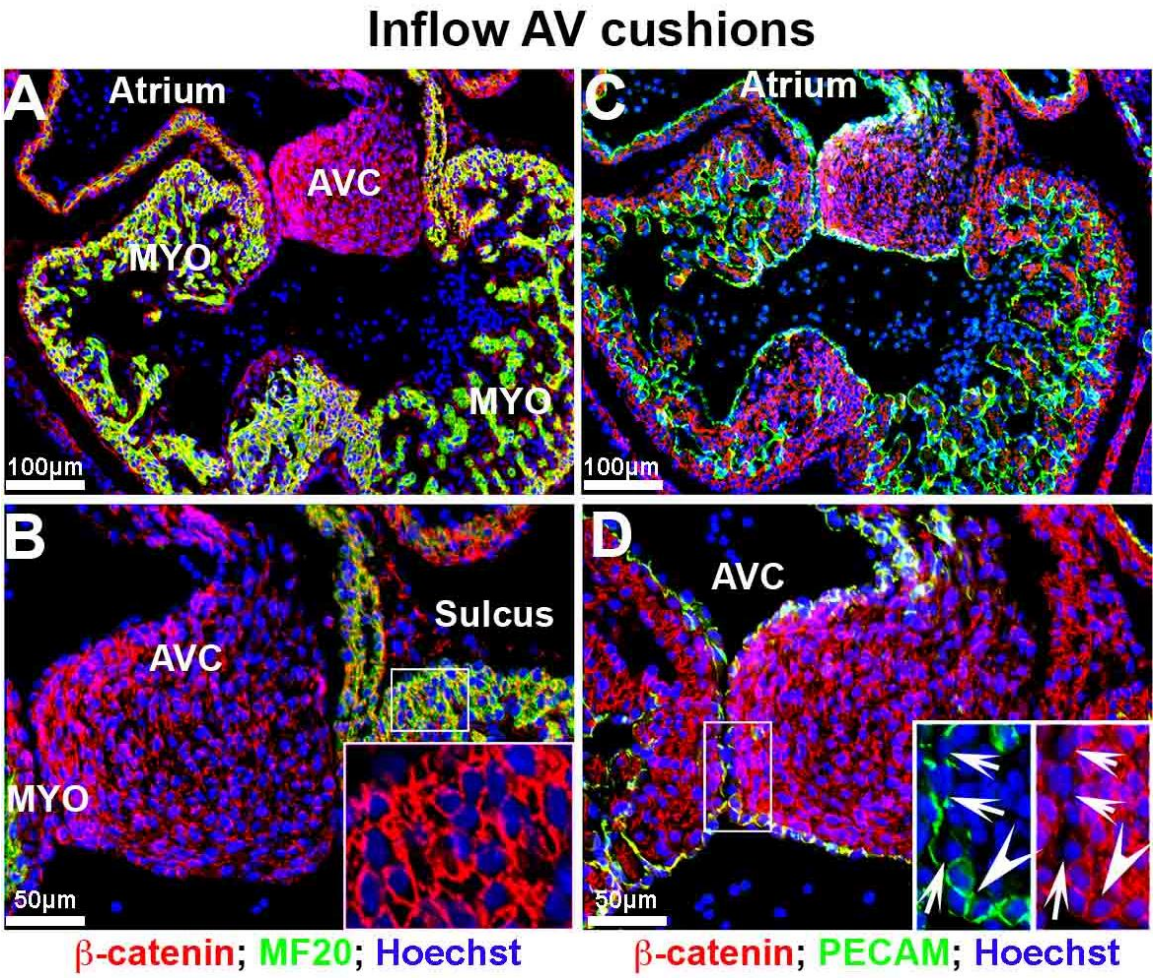

Figure 2. 3 Non-phosphorylated β-catenin expression at E11.5 inflow AV cushions.

Representative images of E11.5 inflow AV cushions immunostained for non-phosphorylated β-catenin (red), MF20 (green), PECAM (green) and nuclei counterstained with hoechst (blue). MYO=myocardium, AVC=atrioventricular cushions, arrows=endocardial cells with less IHC intensity, arrowheads=endocardial cells with no IHC intensity.

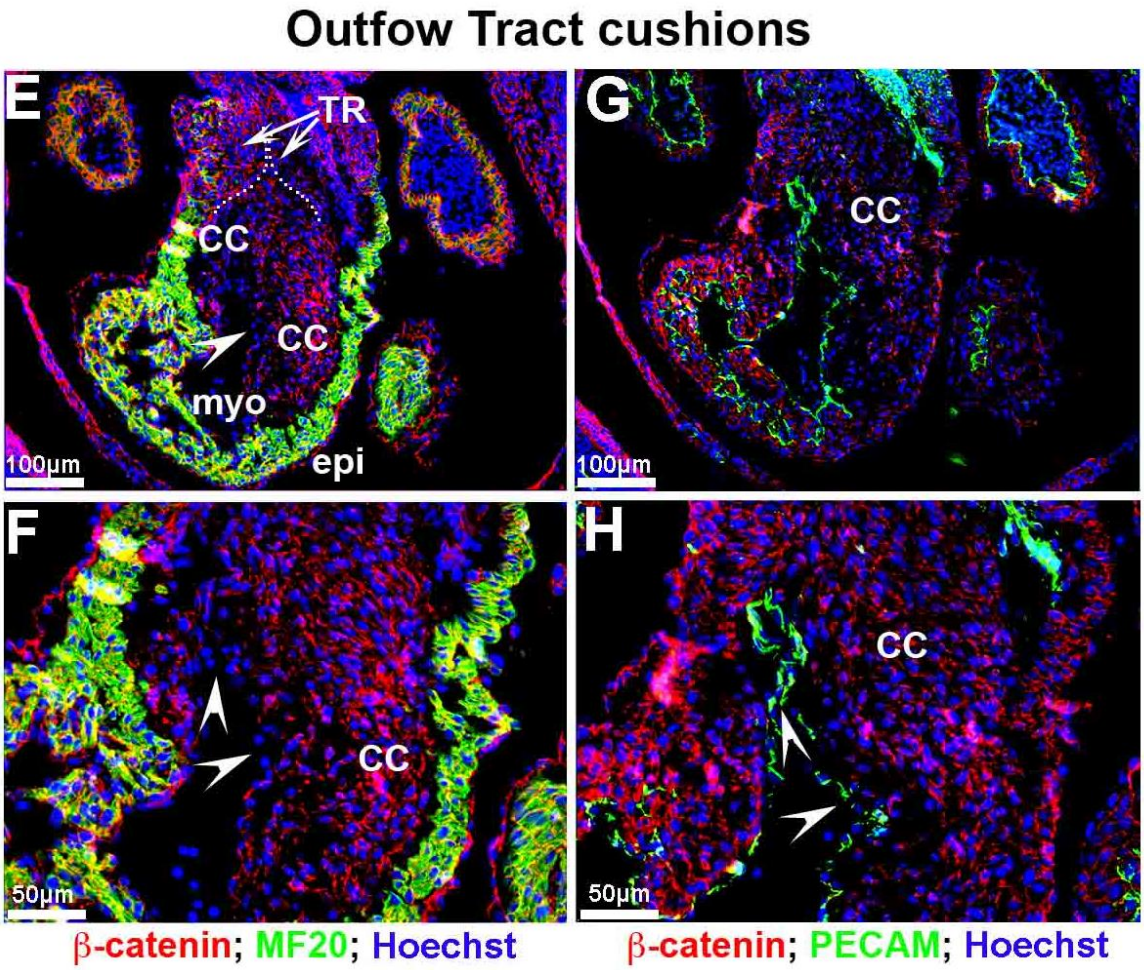

Figure 2. 4 Non-phosphorylated β-catenin expression at E11.5 outflow tract cushions.

Representative images of E11.5 outflow tract cushions immunostained for non-phosphorylated β-catenin (red), MF (green), PECAM (green) and nuclei counterstained with Hoechst (blue). CC=conal cushions, epi=epicardium, myo=myocardium, TR=truncal ridges, arrowheads=endocardium.

By E13.5, although expression within the mesenchymal cells of the AV valves is still evident, expression of activated nuclear β-catenin appears reduced with evidence of perinuclear or membrane expression, especially within the AV valve endocardium (**Figure 2.5B, D- arrowheads**). Additionally, many interstitial cells within the AV valves failed to exhibit detectable activated β-catenin (**Figure 2.5B, D- arrows**). Valve interstitial cells closest to the AV valve endocardium appear to have lost or greatly downregulated expression of activated β-catenin as nuclear expression is primarily restricted to a core group of cells within the valve (**Figure 2.5 B, D- dotted line**). Downregulation of activated nuclear β-catenin was not specific to the AV valves as we also observed this expression change in the developing semilunar valves of the outflow tract (**Figure 2.6E-H**). However, within the outflow tract valves, expression of activated β-catenin was almost completely confined to the valve endocardium with only a few interstitial cells staining positive. Within valve endocardial cells, punctate, nuclear expression was evident as well as its presence on the cell membrane (**Figure 2.6F – boxed region**). Within the E13.5 myocardium activated β-catenin was evident within the nuclei as well as on the cell membrane. Thus, within the heart at E13.5, a change in subcellular localization of activated β-catenin is evident as compared to the E11.5 timepoint, whereby a nuclear to membrane shift of

protein is observed. In addition, our stainings reveal a profound downregulation of the phosphorylated, activated form of β-catenin within the developing mitral and aortic valves.

As our data showed reduced nuclear β-catenin activation at E13.5, we tested whether expression of non-phosphorylated β-catenin showed a concurrent up-regulation and/or prominence at the cell membrane. As shown in **Figure 2.7 &Figure 2.8**, membrane β-catenin was robust in all areas of the heart analyzed. The endocardium and subendocardial mesenchyme within the E13.5 atrioventricular (AV) valves displayed prominent membrane β-catenin staining. (**Figure 2.7A-D**). The graded staining pattern within the AV valves appeared similar to that observed at E11.5, albeit more pronounced at E13.5. The dotted lines in **Figures 2.7A-D** demarcate this unique spatial boundary between two apparent different cell phenotypes based on membrane stainings for β-catenin. Within the central mass of the valves there appears to be a core of interstitial cells that display uneven distribution of β-catenin staining. This is converse to the circumferential, staining of the endocardial and subendocardial mesenchyme. Much like at E11.5 (**Figure 2.3**), this pattern of uneven distribution of staining possibly demarcates an interstitial cell type that is more primitive and/or shares a phenotype consistent with a less mature fibroblastic cell. A similar spatial pattern of β-catenin expression on the

membrane is observed within the outflow tract mesenchyme of the semilunar valves. One noticeable difference is that the majority of the interstitial mesenchyme in these valves do not display circumferential β-catenin expression, but rather a punctate pattern (**Figure 2.8F**-boxed region). The outflow tract valve endocardium shows membrane expression of β-catenin along the basal aspect of these cells, consistent with the presence of adherens junctions (**Figure 2.8F, H**-arrows). Within the left coronary cusp, many of the interstitial cells had very low to undetectable expression of β-catenin (**Figure 2.8E-H**-asterisks). Outside of the valves, membrane expression of β-catenin was robust in all areas observed including on cardiomyocytes, the epicardium, aortic wall and ventricular endocardium.

These expression data correlate with a time point of robust growth within the heart, consistent with a previously identified role for β-catenin in proliferation events. It is interesting to note that the endocardium of AV and conal cushion tissue that are destined to fuse at E11.5 show disorganized or reduced expression of both membrane and nuclear β-catenin, suggesting that downregulation of the protein may be required for differentiation of these cell types or may represent a consequence of compressive mechanical forces known to occur at these areas. Consistent with this concept of differentiation is the gradient of membrane expression observed within the AV cushions

observed at E11.5 and E13.5. Alternatively, the difference in staining intensity could simply represent a different ultrastructural phenotype of the cell membrane within the valve interstitium. Previous reports by us and others have shown that subendocardial cushion mesenchyme are denser compared to the more dispersed interstitial cells proximal to the myocardium, thereby likely demarcating at least two different cell types within the AV cushions at this stage of development. The difference of staining pattern and intensity within the core of the inflow and outflow tract valves at E13.5 further support this hypothesis.

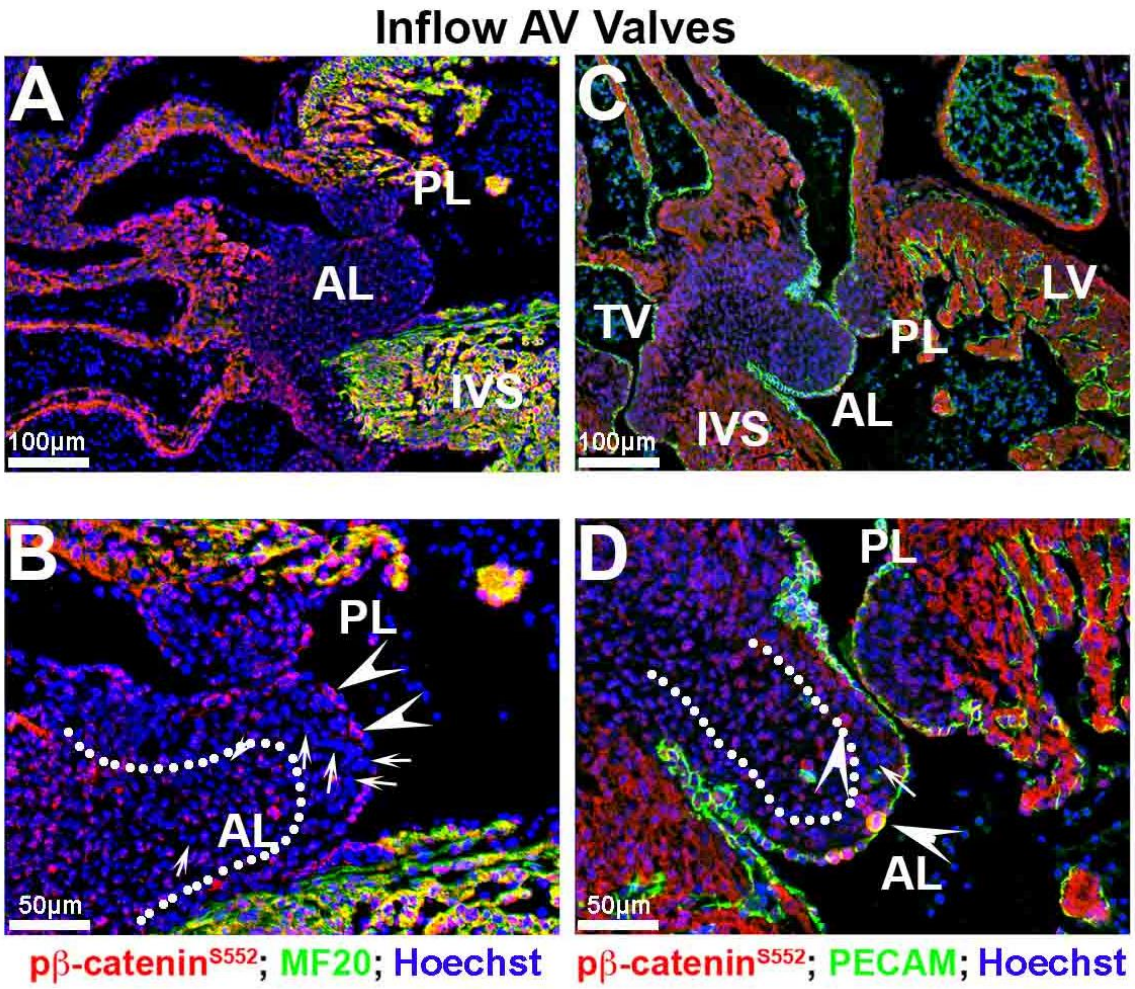

Figure 2. 5 Activated β-catenin expression at E13.5 inflow AV valves.

Representative images of E13.5 inflow AV valves immunostained for activated β-catenin (red), MF20 (green), PECAM (green) and nuclei counterstained with Hoechst (blue). AL=anterior leaflet, PL=posterior leaflet, IVS=intraventricular septum, LV=left ventricle, TV=tricuspid valve.

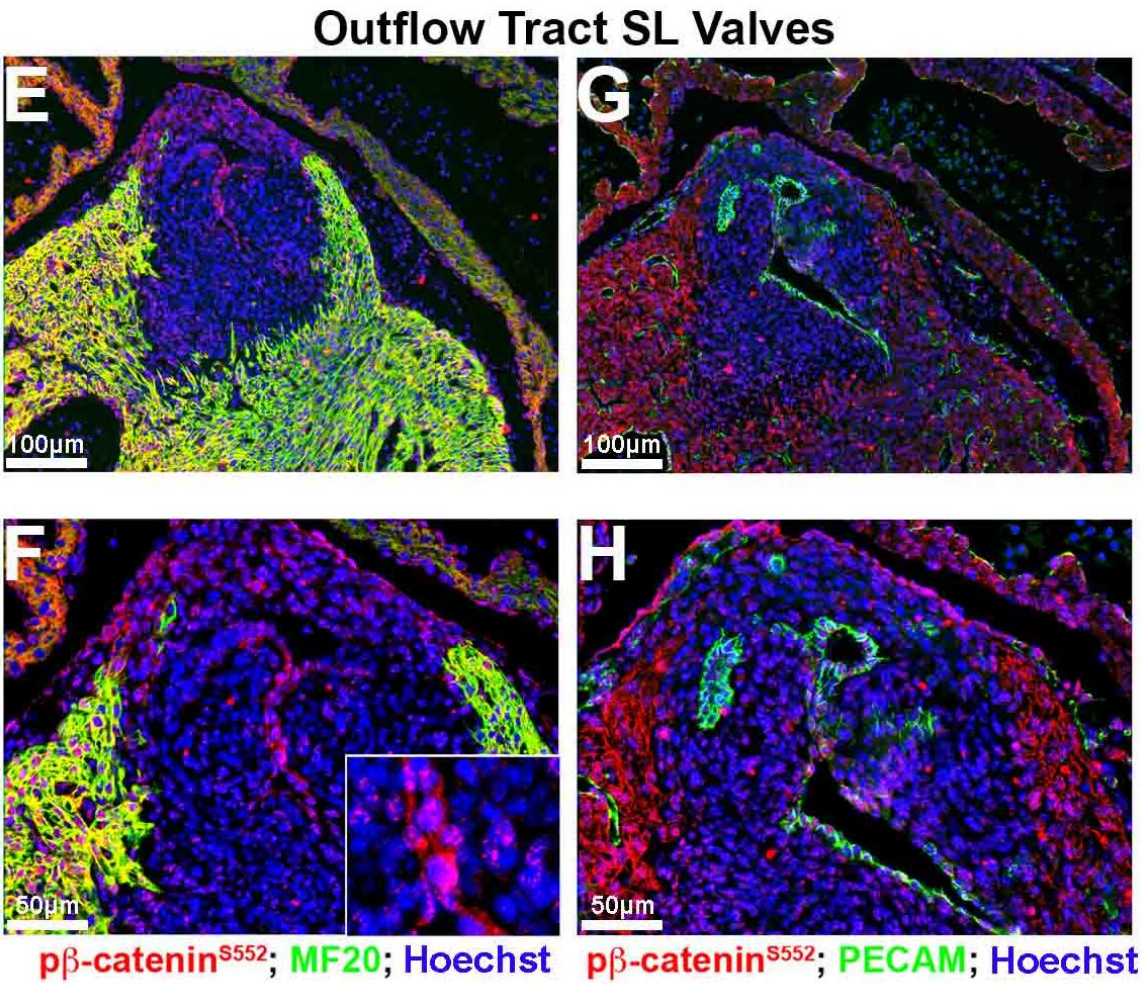

Figure 2. 6 Activated β-catenin expression at E13.5 outflow tract SL valves.

Representative images of E13.5 outflow tract SL valves immunostained for activated β-catenin (red), MF20 (green), PECAM (green) and nuclei counterstained with Hoechst (blue).

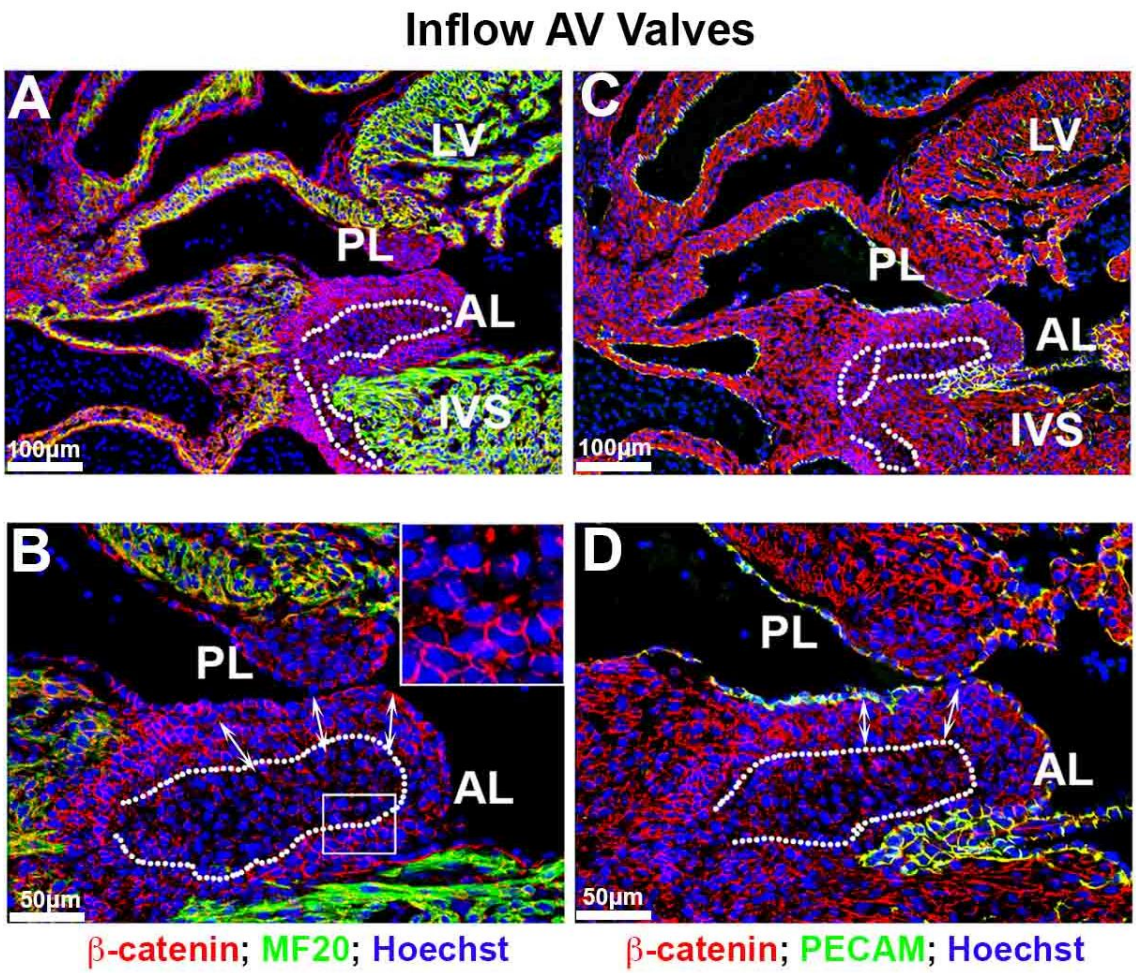

Figure 2. 7 Non-phosphorylated β-catenin expression at E13.5 inflow AV valves.

Representative images of E13.5 inflow AV valves immunostained for non-phosphorylated β-catenin (red), MF20 (green), PECAM (green) and nuclei counterstained with hoechst (blue). AL=anterior leaflet, PL=posterior leaflet, IVS=intraventricular septum, LV=left ventricle.

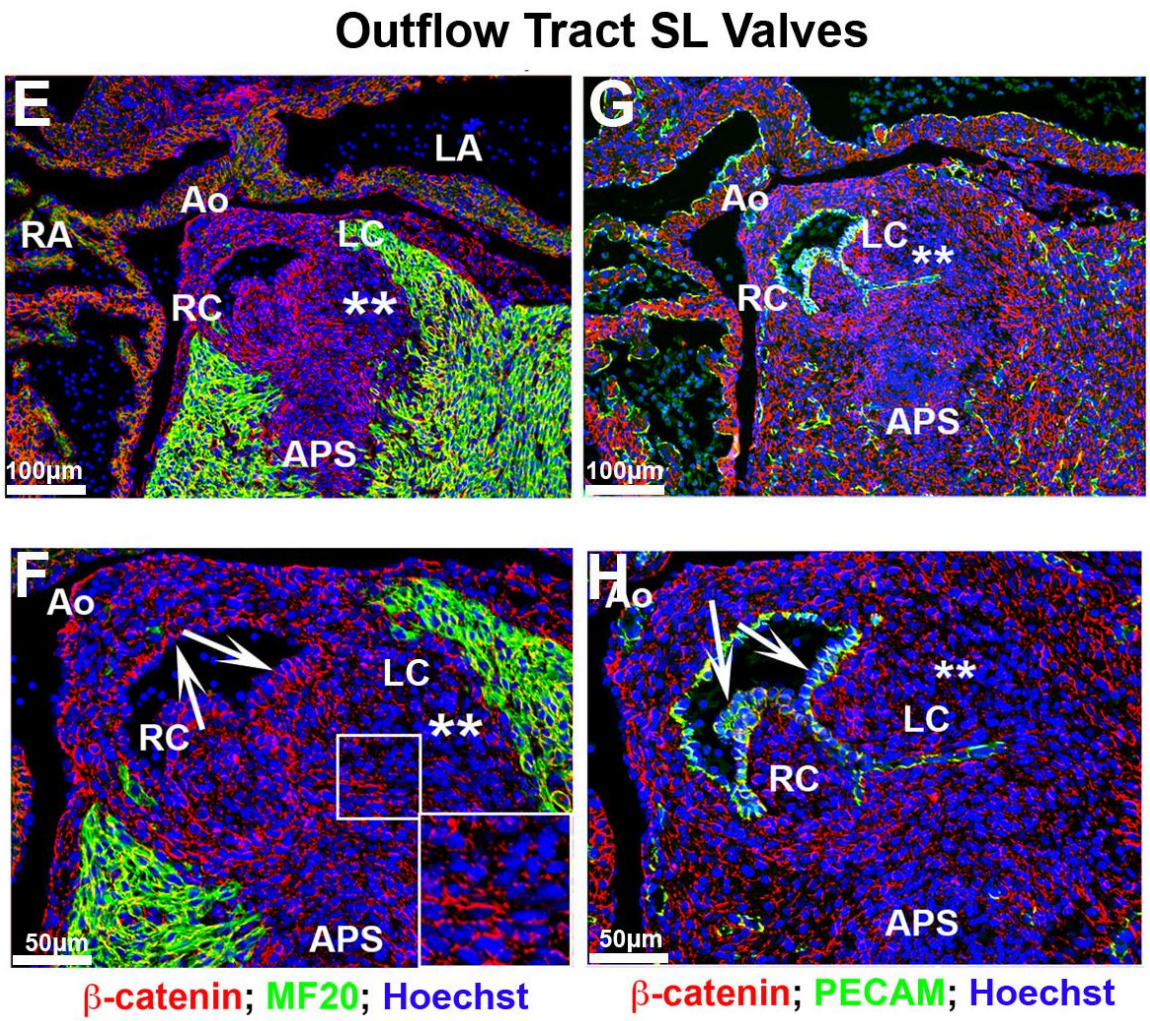

Figure 2. 8 Non-phosphorylated β-catenin expression at E13.5 outflow tract SL valves.

Representative images of E13.5 outflow tract SL valves immunostained for non-phosphorylated β-catenin (red), MF20 (green), PECAM (green) and nuclei counterstained with Hoechst (blue). RA=right atrium, Ao=aorta, LA=left atrium, RC=right coronary, LC=left coronary, APS=aorticopulmonary septum. Arrows=endocardial cells.

β-catenin expression during fetal cardiac development

Immunohistochemical stains were performed for both activated (β-catenin^{pS552}) and non-phosphorylated β-catenin during fetal cardiac morphogenesis at E17.5. Within the mitral valves, activated β-catenin was observed in the nuclei of some cells in a spatial pattern similar to what was observed at E13.5 (**Figures 2.5A-D and 2.7A-D**) with some slight, differences. Within the belly of the mitral leaflets, most interstitial cells exhibited either undetectable or low levels of β-catenin nuclear expression. Some, but not all, mitral valve endocardial and subendocardial interstitial cells displayed weak expression of nuclear β-catenin (**Figure 2.9B, D**). This pattern of expression within the valves is reminiscent of the proteoglycan rich spongiosa region of the mitral valve. Co-immunostains of activated nuclear β-catenin with hyaluronan binding protein confirmed that nuclear β-catenin is primarily restricted to this particular valvular region at both E17.5 and E13.5 (**Figure 2.18**). Within the aortic valves, activated β-catenin was only observed in a few cells within the hinge regions connecting the aortic cusps to the aortic wall (**Figure 2.10F-arrows**). Additionally, a few cells along one side of the right coronary cusp were positive for nuclear β-catenin expression (**Figure 2.10F-arrowhead**). Thus, within the fetal mitral and aortic valves, our data

would support a continual, gradual downregulation of nuclear β-catenin during gestation.

Regions outside of the mitral or aortic valves showed prominent nuclear β-catenin staining including the primary atrial septum, the myocardial rim lining the mitral-aortic continuity and the inter ventricular septum (**Figure 2.9 & Figure 2.10**). The myocardium of the left atrium also appears to be positive, albeit at a much lower staining intensity than the adjacent left ventricular wall (**Figure 2.9C**). Within the left ventricular wall, we noticed that nuclear β-catenin within the distal/posterior basal myocardium showed robust staining, yet in more proximal sections this staining was largely absent (**Figure 2.10G-arrow**). Within the proximal/anterior heart regions, expression is observed within the myocardial reflections adjacent to the aortic wall (**Figure 2.10G-arrowhead**). These data suggest that β-catenin expression within the left ventricular myocardium is non-uniform and may demarcate either different cell populations or spatially dependent functional requirements for these cells.

The staining for membrane-bound, non-phosphorylated β-catenin at E17.5 exhibited a much different pattern than observed for the nuclear form, especially within the aortic valves (**Figure 2.12**). Within the anterior and posterior mitral leaflets, membrane β-catenin was expressed prominently throughout the valve endocardium (**Figure 2.11A-D-arrows**). Cells sub-

adjacent to the atrialis endocardium of the mitral leaflets displayed positive staining with much less, to undetectable expression within the rest of the mitral leaflets (**Figure 2.11D-arrowheads**). Within the aortic valves, widespread membrane β-catenin was evident on all endocardial cells and most interstitial cells (**Figure 2.12E-H**). Unlike the activated form of β-catenin, low to undetectable membrane staining was evident on interstitial cells within the hinge regions (**Figure 2.12H-boxed region**). Unlike the mitral valve, the staining within the aortic valve does not appear to be confined to one particular cell layer within the valve cusps. Outside of the mitral and aortic valves, membrane expression is observed in most cell types including ventricular endocardium and myocardium and on myocytes within the mitro-aortic continuity (MAC) (**Figure 2.12E-G**). Membrane β-catenin was undetectable on epicardial cells within the left ventricle or within the atrioventricular sulcus (**Figure 2.11A, B-asterisk**).

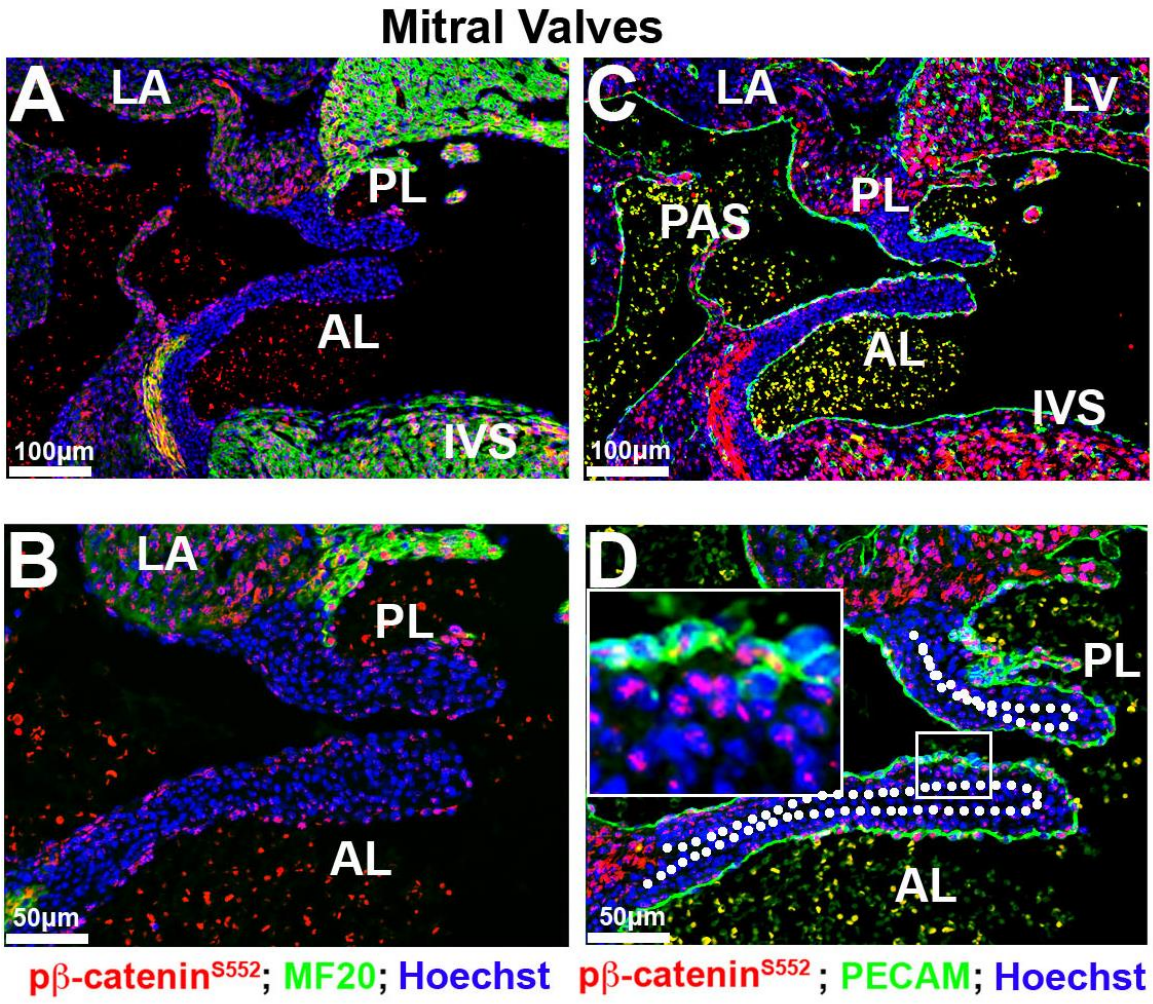

Figure 2. 9 Activated β-catenin expression at E17.5 mitral valves.

Representative images of E17.5 mitral valves immunostained for activated β-catenin (red), MF20 (green), PECAM (green) and nuclei counterstained with hoechst (blue). LA=left atrium, PL=posterior leaflet, AL=anterior leaflet, LV=left ventricle, IVS=intraventricular septum, PAS=primary atrial septum.

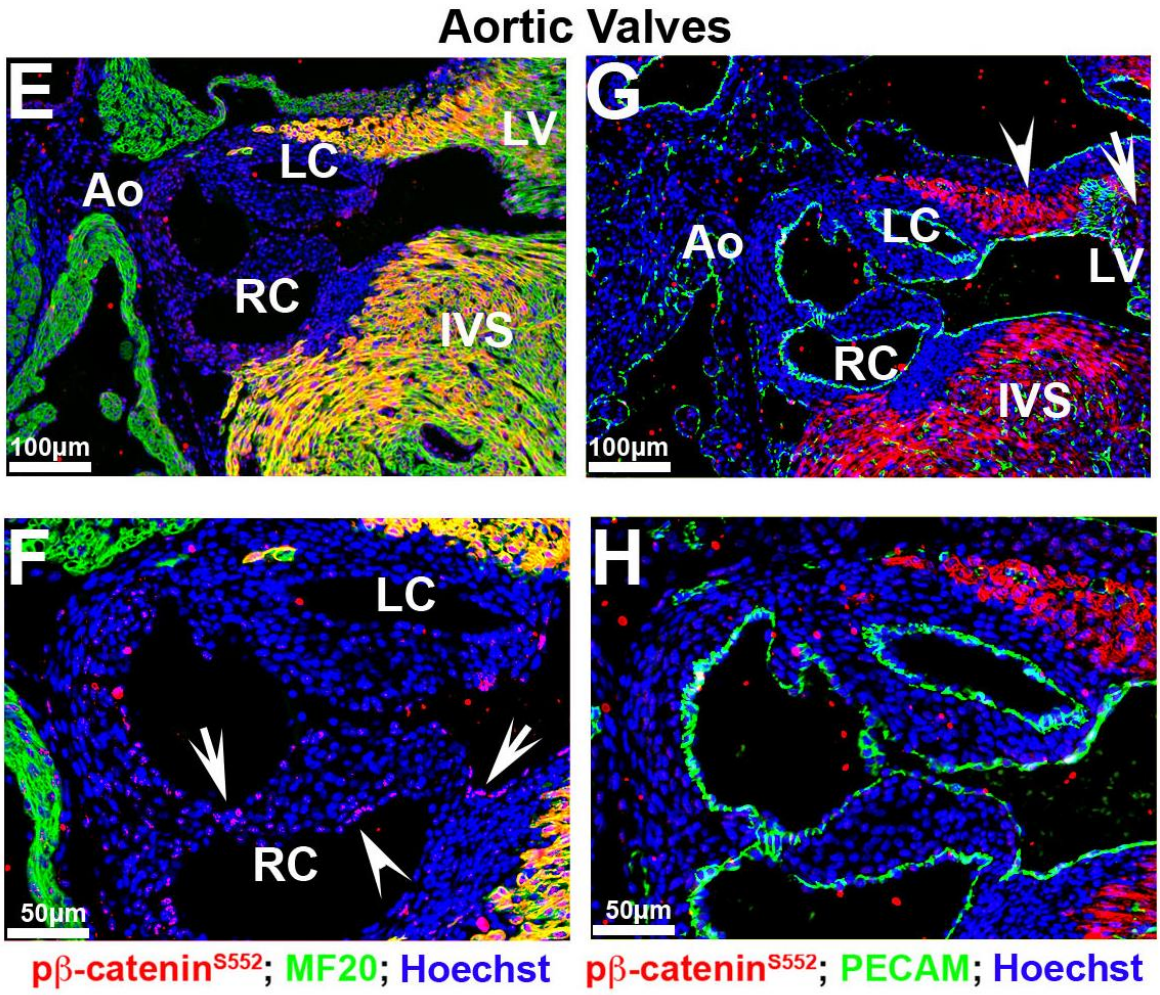

Figure 2. 10 Activated β-catenin expression at E17.5 aortic valves.

Representative images of E17.5 aortic valves immunostained for activated β-catenin (red), MF20 (green), PECAM (green) and nuclei counterstained with hoechst (blue). Ao=aorta, LC=left coronary, RC=right coronary, LV=left ventricle, IVS=intraventricular septum.

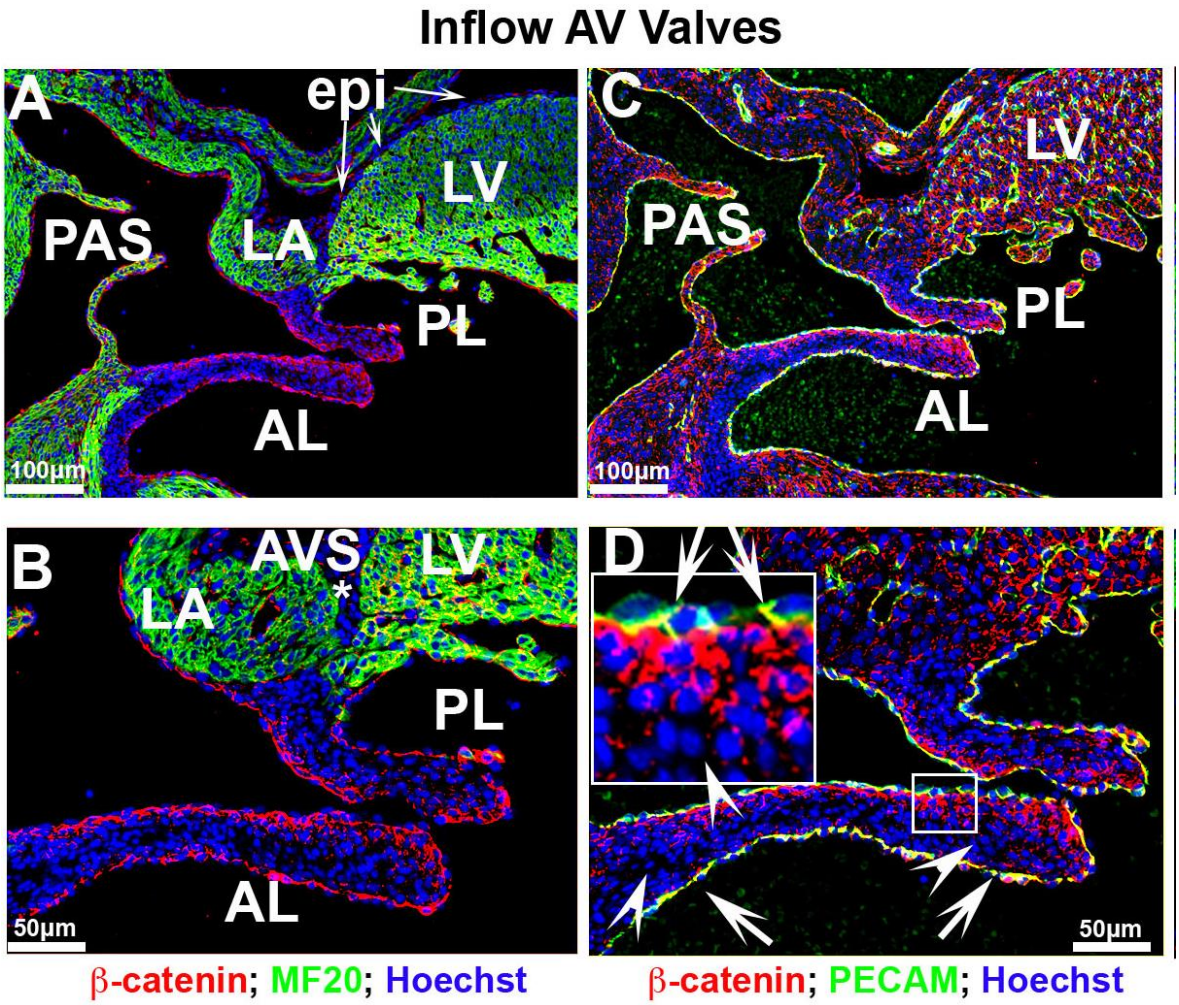

Figure 2. 11 Non-phosphorylated β-catenin expression at E17.5 mitral valves.

Representative images of E17.5 mitral valves immunostained for non-phosphorylated β-catenin (red), MF20 (green), PECAM (green) and nuclei counterstained with hoechst (blue). Epi=epicardium, PAS=primary atrial septum, LA=left atrium, LV=left ventricle, AL=anterior leaflet, PL=posterior leaflet, AVS=atrioventricular sulcus.

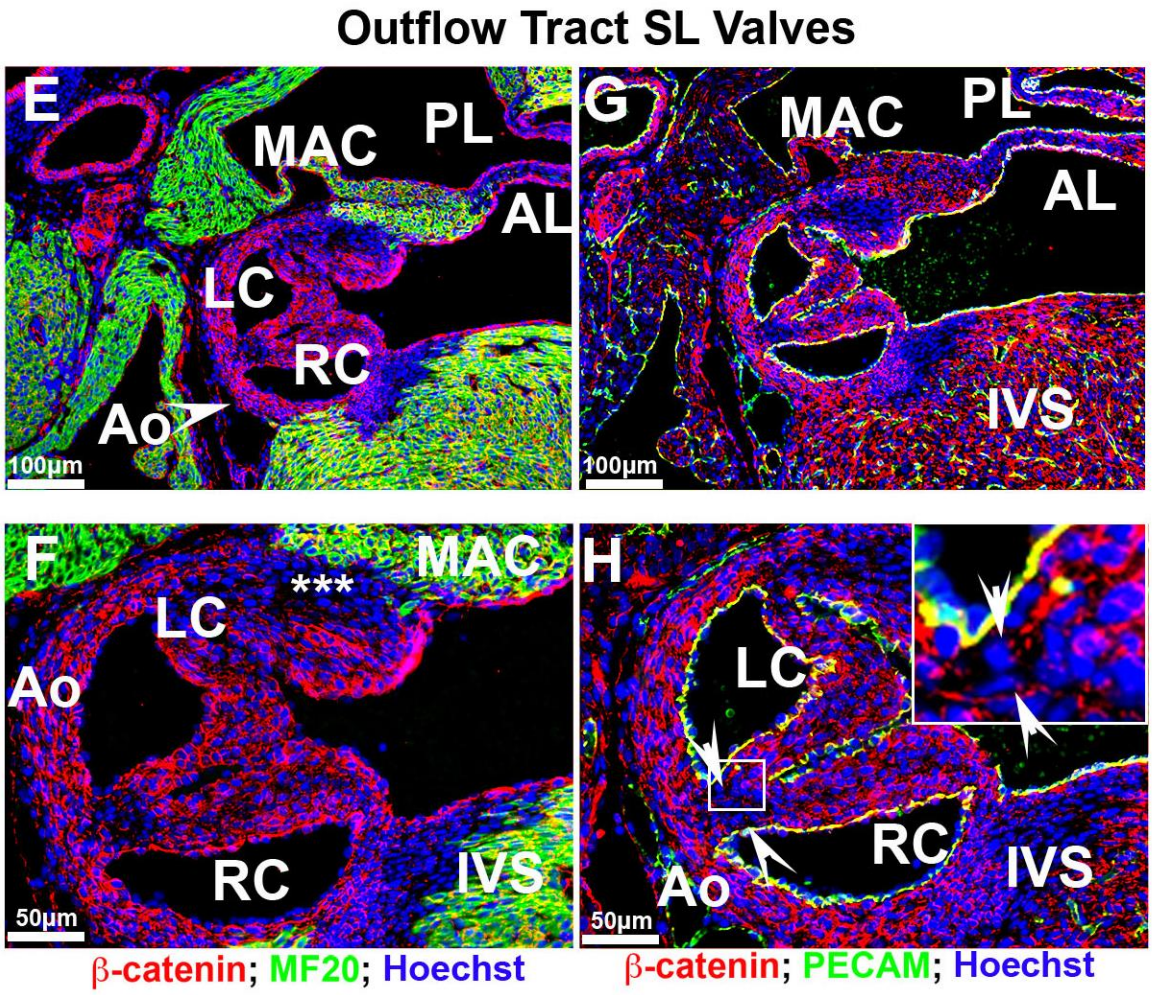

Figure 2. 12 Non-phosphorylated β-catenin expression at E17.5 aortic valves.

Representative images of E17.5 aortic valves immunostained for non-phosphorylated β-catenin (red), MF20 (green), PECAM (green) and nuclei counterstained with Hoechst (blue). Ao=aorta, LC=left coronary, RC=right coronary, AL=anterior leaflet, PL=posterior leaflet, MAC=mitro-aortic continuity, IVS=intraventricular septum.

Postnatal cardiac β-catenin expression

As either loss of or gain of function of β-catenin has been shown to contribute to cardiac valvular diseases and postnatal cardiac regenerative processes, we sought to evaluate expression of β-catenin after birth. As shown in **Figure 2.13**, activated β-catenin is only present within a subset of mitral valve interstitial cells confined to the tips at neonatal timepoints. The mitral valve endocardium is mostly devoid of positive nuclear staining (**Figure 2.13A, B**). On the contrary, membrane staining for β-catenin is robust in the mitral valve endocardium and co-labels with CD31/Pecam at adherens junctions (**Figure 2.13D, E**). In adult mice no detectable nuclear β-catenin is observed within the mitral leaflets whereas the non-phosphorylated β-catenin isoform is present primarily along the valve endocardial lining of the atrialis (**Figure 2.14**). Consistent with previous reports, nuclear β-catenin is undetectable within the IVS myocardium (**Figure 2.14 left**), but the non-phosphorylated isoform is observed within the intercalated discs of cardiomyocytes (**Figure 2.14-boxed region**). The aortic valves show a similar pattern for β-catenin expression compared to the mitral valves, with one exception (**Figure 2.15 & Figure 2.16**). While membrane bound β-catenin co-localizes with CD31/Pecam within the aortic valve endocardium as well as a subpopulation of interstitial cells at the tips of the cusps (**Figure 2.15J, K-**

arrows), we fail to detect the presence of nuclear β-catenin within the aortic valves (**Figure 2.15 G, H**). Similarly, neither form of β-catenin is observed in the adult aortic valve leaflets (**Figure 2.16)**. At the postnatal timepoints we do not observe β-catenin expression within the hinge regions of the aortic cusps but do observe membrane staining within the aortic wall (**Figure 2.15 J, K-asterisks**). These data demonstrate that activated nuclear β-catenin expression is only detectable during a developmental and early neonatal window, whereas membrane bound β-catenin continues throughout life, at least in the atrial aspect of the mitral valve.

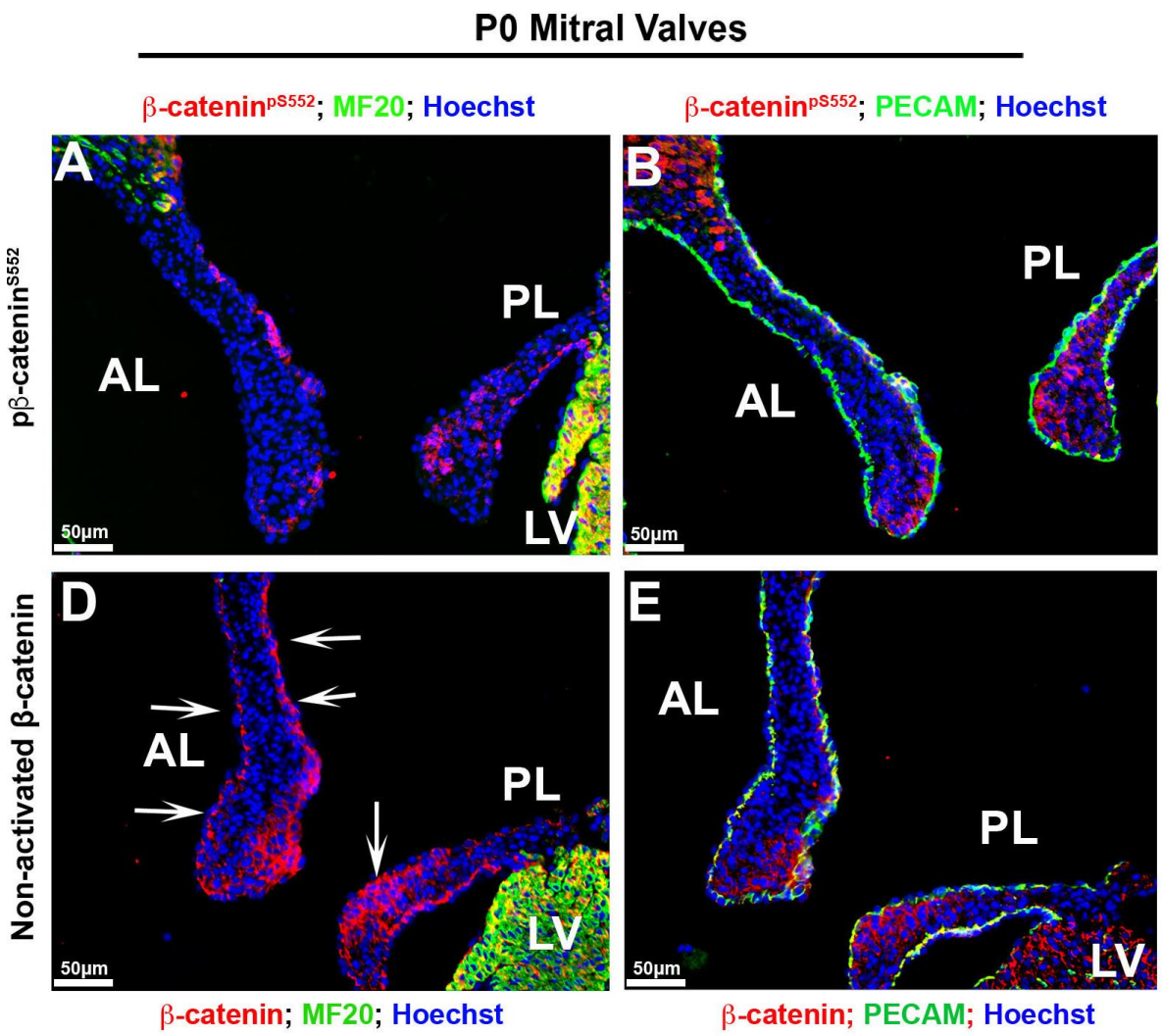

Figure 2. 13 β-catenin expression at neonatal mitral valves.

Representative images of P0 mitral valves immunostained for both forms of β-catenin (red), MF20 (green), PECAM (green) and nuclei counterstained with hoechst (blue). AL=anterior leaflet, PL=posterior leaflet, LV=left ventricle.

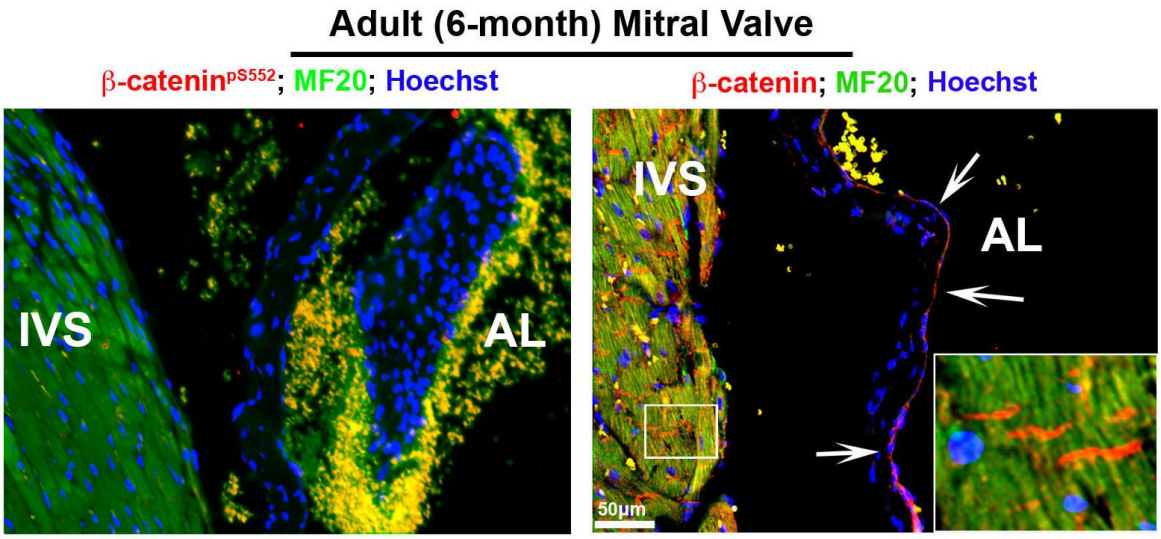

Figure 2. 14 β-catenin expression at adult mitral valves.

Representative images of 6-month mitral valves immunostained for activated β-catenin (red), MF20 (green) and nuclei counterstained with hoechst (blue). IVS=intraventricular septum, AL=anterior leaflet, arrows=endothelium.

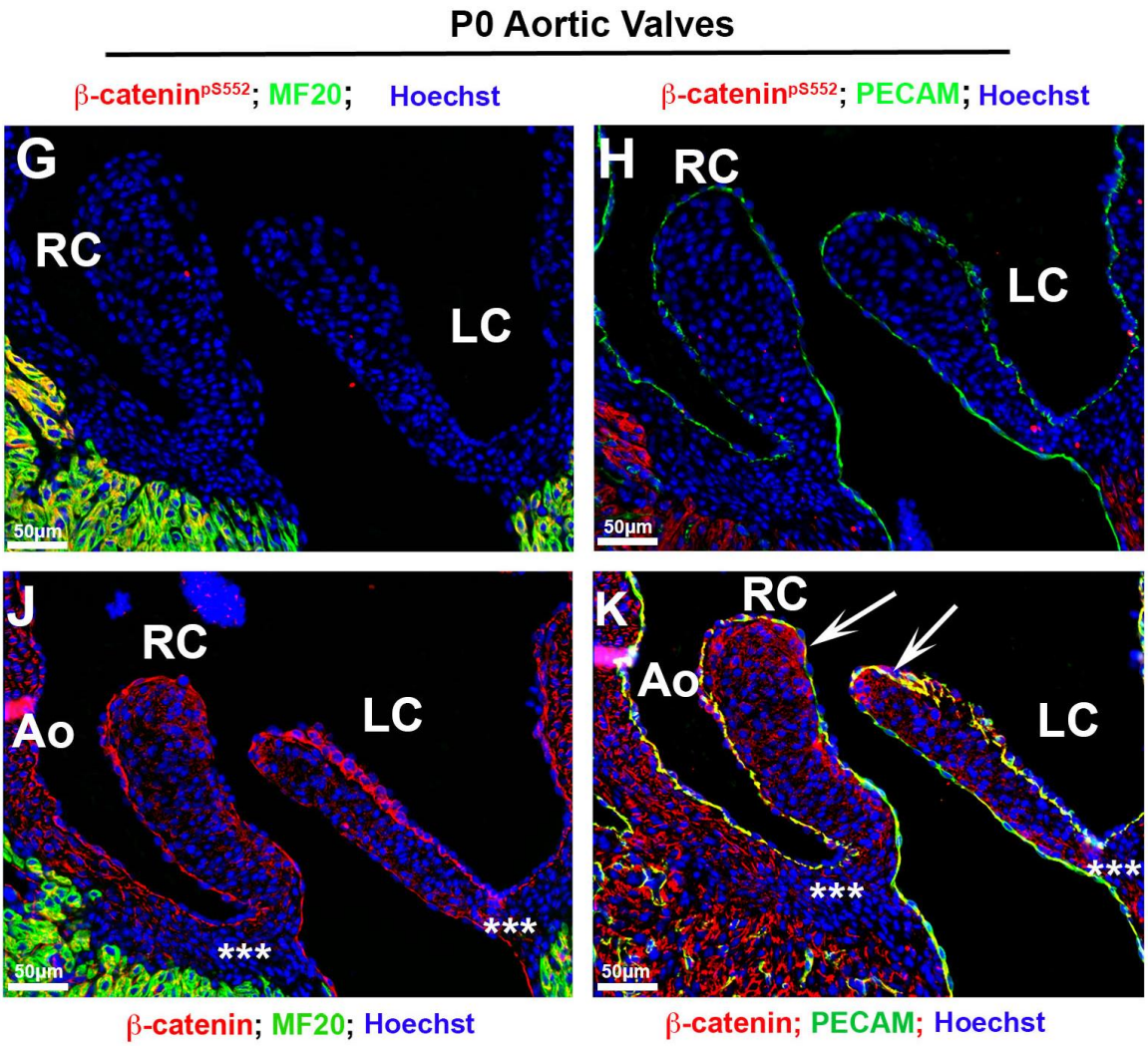

Figure 2. 15 β-catenin expression at neonatal aortic valves.

Representative images of P0 aortic valves immunostained for both forms of β-catenin (red), MF20 (green), PECAM (green) and nuclei counterstained with hoechst (blue). RC=right coronary, LC=left coronary, Ao=aorta, arrows=endocardium, asteroids=hinge regions of the aortic valve.

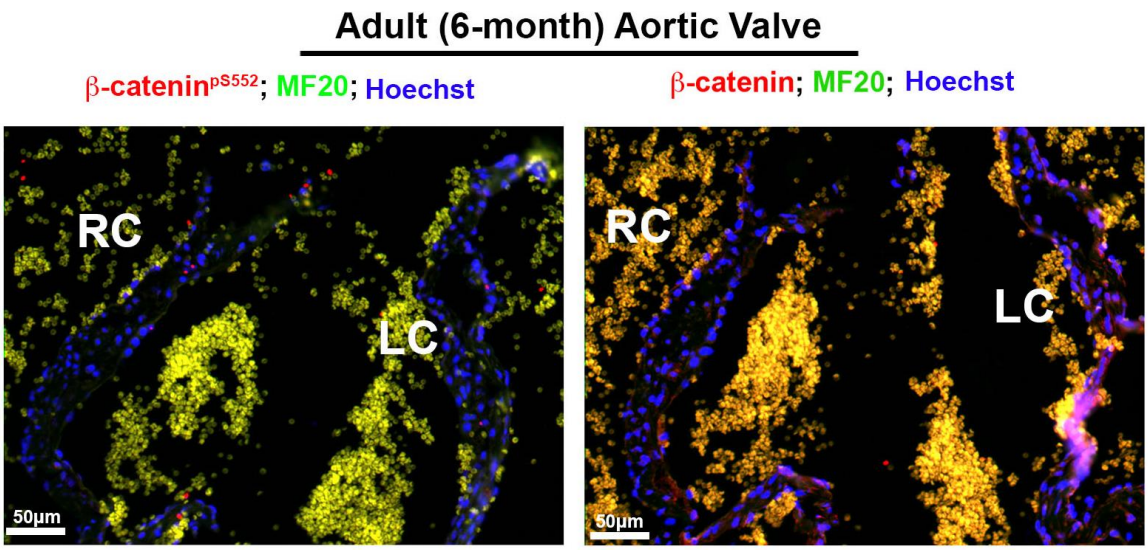

Figure 2. 16 β-catenin expression at adult aortic valves.

Representative images of 6-month aortic valves immunostained for both forms of β-catenin (red), MF20 (green) and nuclei counterstained with hoechst (blue). RC=right coronary, LC=left coronary.

Correlation of β-catenin activities with Lef1

Activated β-catenin can enter the nuclei and bind TCF/LEF transcription factor to activate transcription of downstream target genes[209, 218, 227]. Therefore, Lef1 is commonly used as a readout marker for β-catenin signaling [228-233]. More recently, the existence of β-catenin-independent functions for Lef1 have been documented, bringing into question whether lef1 reporters represent physiologically accurate measures of β-catenin signaling. To test this concept, we co-stained activated β-catenin with Lef1 on mitral valve tissues during embryonic and fetal gestation to determine if they co-localized with each other (**Figure 2.17**). During embryonic timepoints, most of the Lef1 positive stained cells were co-stained with nuclear β-catenin. However, a major discrepancy at this timepoint was that Lef1 was positive only in a subset of cells, indicating a lef1-independent nuclear role for β-catenin. The staining at E17.5 showed an even more striking discrepancy between Lef1 and nuclear β-catenin staining. Lef1 positive cells were observed within nuclei of mitral valve interstitial cells localized to the tip of the leaflets. However, these positively stained Lef1 cells showed little detectable β-catenin staining (**Figure 2.17 I-arrows**). We rarely observed valve endocardial cells that co-stained with both markers (**Figure 2.17 I-arrowhead**). These data support the contention that although there is a small subset of cells that co-express Lef1

and β-catenin, the majority of their activities are not mutually inclusive; likely representing independent roles for these proteins during cardiac valve development.

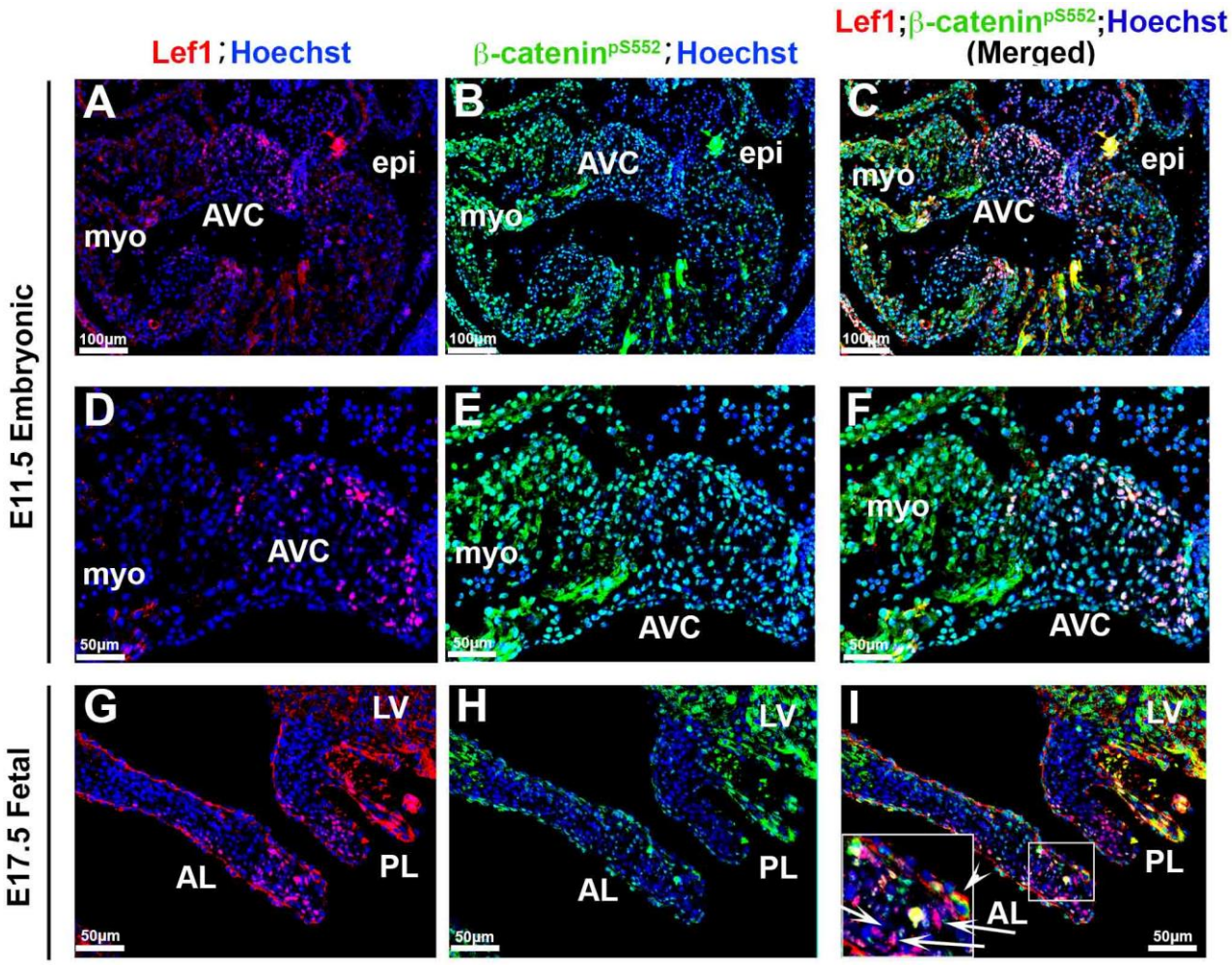

Figure 2. 17 Correlation of β-catenin activities with Lef1.

(A-F). Activated β-catenin (green) and Lef1 (red) were co-stained on E11.5 tissue. Only a subset of activated β-catenin positive cells was co-stained with Lef1. **(G-I)** Co-staining Lef1 with activated β-catenin at E17.5. Lef1 positive cells were localized to the tip of the leaflets showing no appreciable β-catenin staining (**G, I-arrows**) and valve endocardial cells that co-stained with both markers were rarely observed (**I-arrowhead**). AVC= atrioventricular cushions, myo= myocardium, epi= epicardium, AL= anterior leaflet, PL= posterior leaflet, LV= left ventricle.

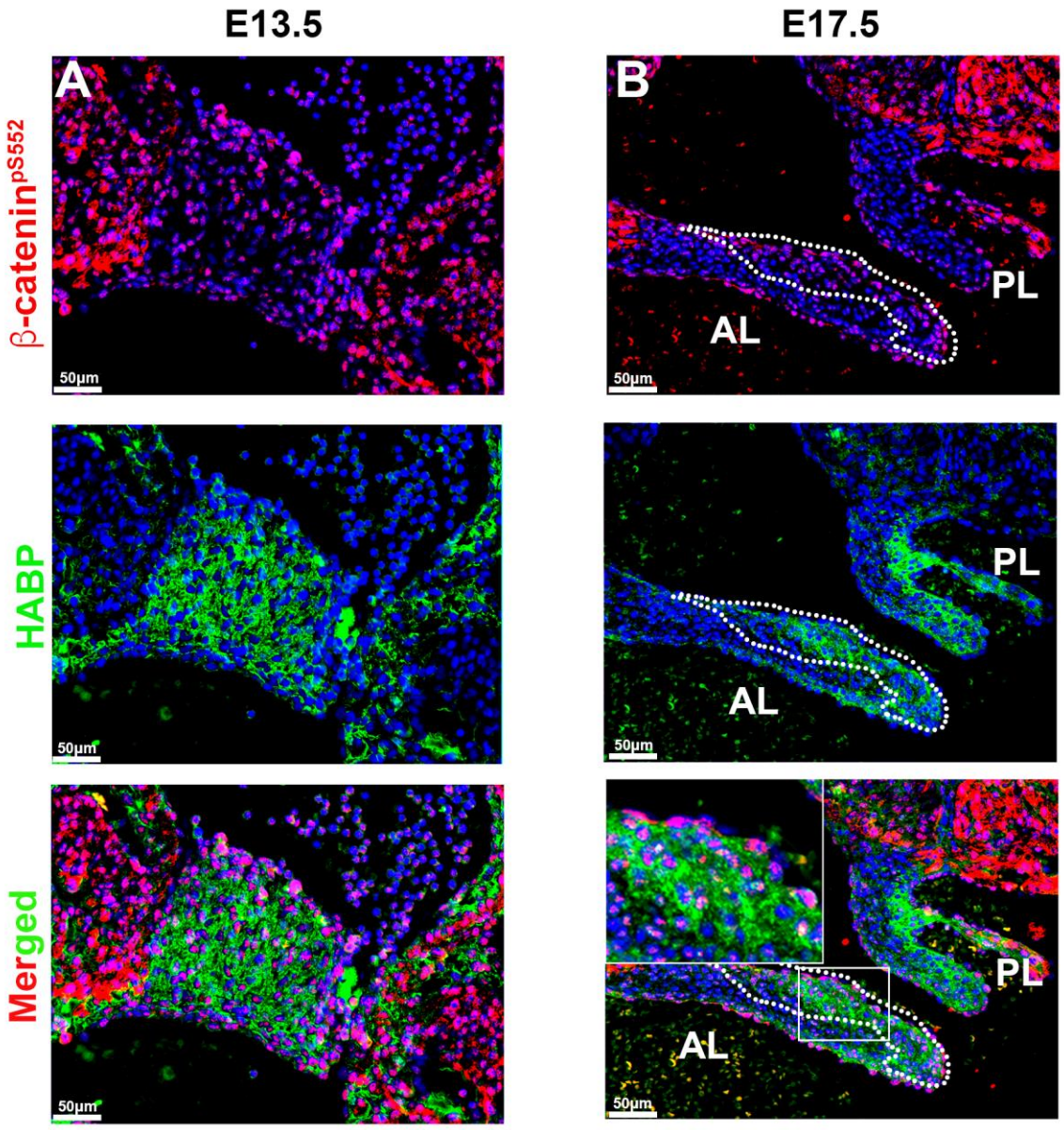

Figure 2. 18 Activated β-catenin is prominent in proteoglycan enriched region.

Representative images of E13.5 AV valves and E17.5 mitral valves immunostained for activated β-catenin (red), HABP (green) and nuclei counterstained with Hoechst (blue). PL=posterior leaflet, AL=anterior leaflet, HABP=hyaluronan acids binding protein.

Human myxomatous mitral valves have increased nuclear β-catenin.

To determine the importance of canonical Wnt/β catenin signaling in human myxomatous valves, activated and membrane bound β-catenin antibodies were used to stain human valve tissues. Similar to what was observed in murine adult tissues (**Figure 2.14**), unaffected human valve tissue had undetectable β-catenin expression. However, the human myxomatous valve had increased expression of both activated and membrane bound β-catenin suggesting a significant increase in its expression (**Figure 2.19**).

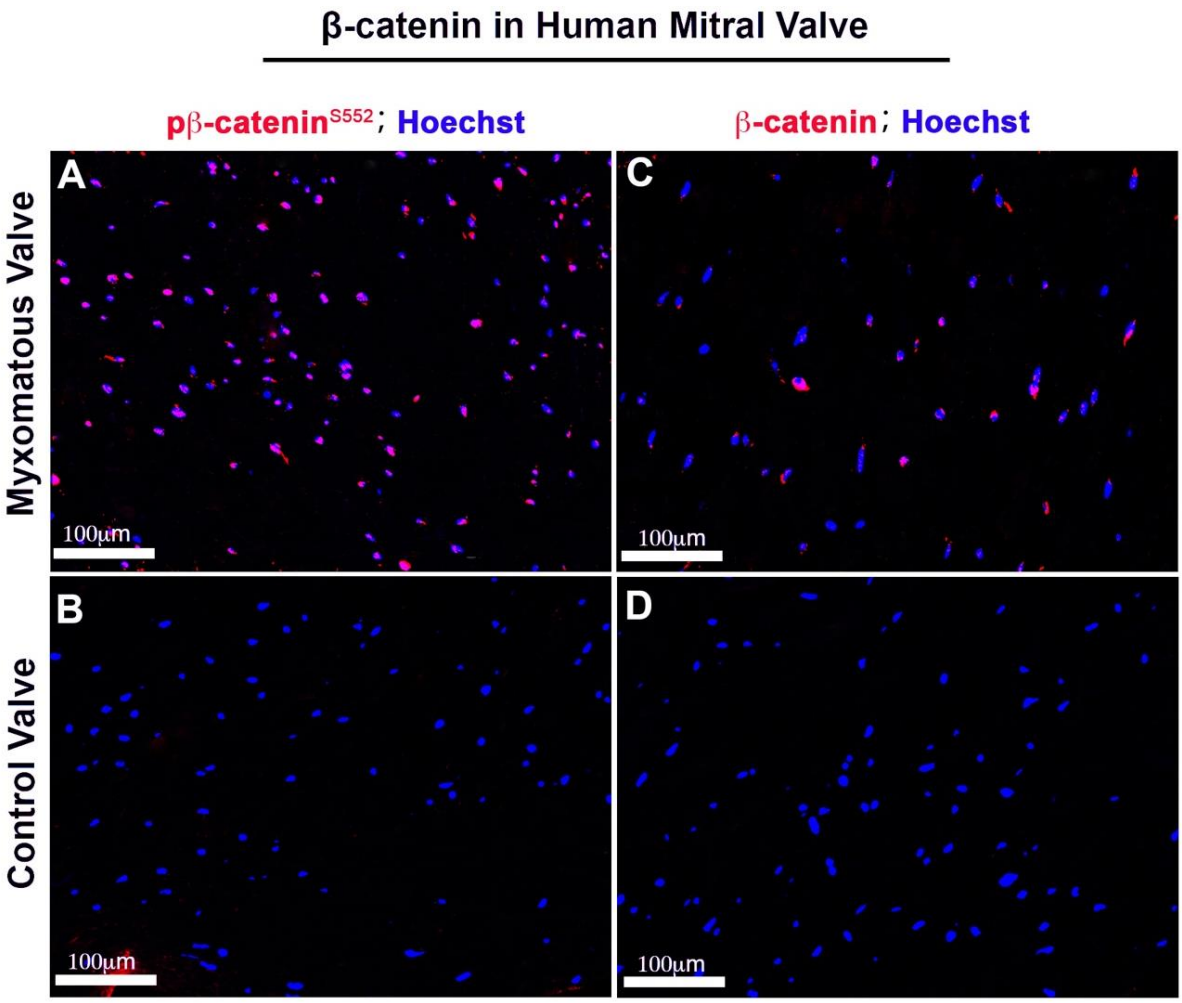

Figure 2. 19 Human myxomatous mitral valves have increased nuclear β-catenin

Representative images of human myxomatous and health control valve tissues immunostained for both forms of β-catenin (red) and nuclei counterstained with hoechst (blue).

2.3. Discussion

β-catenin is a member of the armadillo family proteins which plays a significant role in cadherin-based cell-cell adhesion and is an indispensable co-activator of Wnt-mediated gene expression[218, 234-236]. The dynamic regulation of its subcellular distribution, driven by phosphorylation and/or dephosphorylation events likely dictate its versatile functions[237].

Within the membrane, β-catenin is a critical component of the adherens junction which helps stabilize intercellular interactions[208]. This Ca^{2+} dependent cell-cell adhesion event is fundamental for regulating morphogenetic processes such as endocardial stabilization post-EMT[238, 239]. The function of β-catenin at the membrane is distinct from its unique transcriptional-regulating properties within the nucleus[240]. Of note, we propose that care should be given in interpreting Lef1 data and/or reporter systems that use Lef1 as a readout for β-catenin nuclear activities. Our data demonstrate that co-expression of Lef1 with nuclear β-catenin is minimal within the heart. It remains possible that β-catenin is interacting with other TCF factors within the heart. Future studies should reveal whether these additional factors are co-expressed and interact with β-catenin and are needed to activate or repress target gene transcription. Regardless, our expression studies support a very early embryonic role for nuclear β-catenin, which

correlates with active growth and proliferation of the heart. As the heart matures, we observe a reduction in nuclear expression coincident with known timepoints of reduced proliferation[68]. Previous studies have revealed that loss of β-catenin or the β-catenin antagonist, Axin2, can result in profound valvulopathies in mice[57]. Based on our detailed subcellular expression maps for β-catenin, it seems most likely that the phenotypes have their origins in altered intercellular communications, and not due to altered nuclear presence of β-catenin. If true, this concept would be consistent with other findings in the mitral and aortic valve that have linked disease phenotypes to altered cell-cell interactions, including recent studies on the cadherin proteins DCHS1 and CAD-11 [241-243]. Thus, we posit that understanding how cadherin biology and intercellular interactions drive valve morphogenesis at the level of the membrane may reveal new mechanisms of development that are likely to be relevant to human disease phenotypes.

Chapter 3 DZIP1 regulates mammalian cardiac valve development through a Cby1-β-catenin mechanism

3.1. Introduction

Mitral valve prolapse (MVP) affects 2-3% of the general population and is associated with secondary co-morbidities such as arrhythmias, heart failure and sudden cardiac death[166, 244-246]. MVP is characterized as the billowing of one or both leaflets above the level of the mitral annulus during cardiac systole. Structural changes of the valve result in an inability for the valve to be mechanically proficient during the cardiac cycle. These changes are characterized by alterations in the amount and types of extracellular matrix (ECM) present within the valves[247]. For example, increased proteoglycan and collagen deposition are evident with fragmented collagen and elastin being present. The loss of normal zonal boundaries is evident with expansion of proteoglycans throughout the valve layers. Valve interstitial cells (VICs) are thought to contribute to valve degeneration by becoming activated into myofibroblasts which undergo hyperplasia and produce excess ECM and growth factor ligands. Over time, the valve becomes thickened and floppy which results in incompetence, prolapse and mitral regurgitation. Surgery is the only curative option for patients with severe MVP[247-249].

To date, the molecular and cellular causes of MVP are poorly understood[247]. Recent genetic studies have revealed a role for primary cilia during valvulogenesis[250-253], indicating a potential unifying pathway for

disease initiation. Recently, mutations in the cilia gene DZIP1 were reported in multiple families with inherited, autosomal dominant non-syndromic MVP[128]. DZIP1 is a zinc finger protein localized to the basal body and nucleus and can regulate various downstream pathways involved in hedgehog and Wnt/β-catenin signaling[254-256]. However, how Dzip1 mutations result in MVP is unknown.

To investigate the mechanism of DZIP1 in MVP, we identified Chibby-1 (CBY1) a binding partner of DZIP1 thorough proteomics analyses. CBY1 is not only a ciliary gene essential for both motile and primary cilia assembly[257-261], but has also been shown to be a weak β-catenin antagonist by directly interacting with β-catenin to affect nuclear vs cytoplasmic shuttling of β-catenin[262-264]. In this chapter we report that a protein complex consisting of DZIP1-CBY1 and β-catenin are required for valve morphogenesis and disruption of their interactions cause valve defects and alterations in ECM production that progress to myxomatous degeneration. Additionally, identification of a multigenerational family with a rare, potentially damaging mutation within the DZIP1-CBY1 interaction domain further support this pathway as causative in patients with MVP.

3.2. Results

CBY1 Interacts and colocalizes with DZIP1 in developing mitral valves

To identify direct binding partners for DZIP1 in the heart, yeast two-hybrid screens were performed where full length DZIP1 was used as the bait. We screened 113 million clones from a human embryonic and adult heart library. **Table 1.1** highlights the prevalent DZIP1 interactors in the heart. PPP2R5A and vimentin had previously been identified as directly interacting with DZIP1, thus serving as positive controls for the experiment. CBY1, was the next highest prioritized interactor from our study and was further analyzed. Co-immunoprecipitations (Co-IPs) confirmed an interaction between DZIP1 and CBY1 in HEK293T cells (**Figure 3.1A**). Co-expression of CBY1 and DZIP1 was analyzed by immunohistochemistry (IHC) at E13.5. As shown in **Figure 3.1B and C**, Dzip1 and Cby1 show overlap at the basal body of primary cilia in valve mesenchyme. Whereas Dzip1 is observed both at the basal body and in the nucleus as we previously reported[128], Cby1 appears enriched at the basal body. Within the basal body, the pattern of both Dzip1 and Cby1 appear similar and stain only a small fraction of this subcellular structure, suggesting a function within a discrete portion of the basal body. We did observe areas in which the two proteins did not co-localize, possibly

representing unique subcellular expression domains or various snapshots of expression within shuttling complexes.

Table 1.1 DZIP1 Interactors

Yeast two-hybrid screening showing previously identified DZI1 interactors (yellow) and DZIP1-CBY1 interaction (green) with very high confidence levels (based on # of clones, see Chapter 6 materials and methods).

Gene ID	Confidence	Clones	Unique Clones
PPP2R5A	Very high	14	6
VIM	Very High	11	8
CBY1	Very High	11	2
PCNT	High	1	1

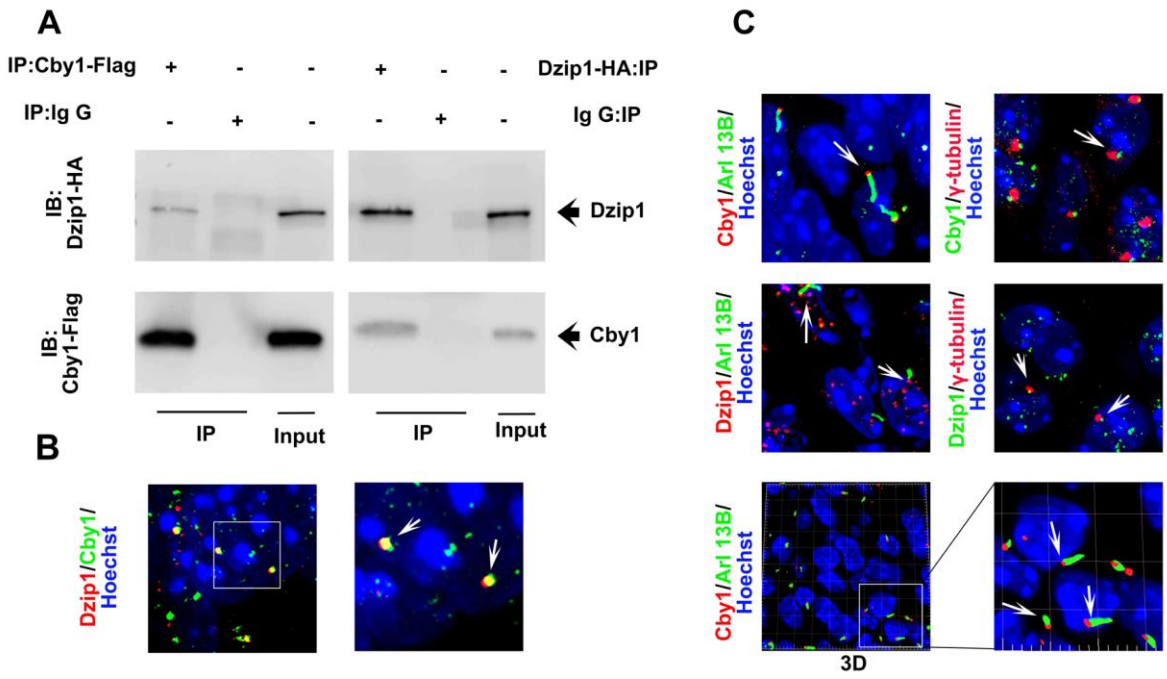

Figure 3. 1 Cby1, Identified as Dzip1's binding partner, localizes to primary cilia basal body in developing mitral valves

A, Co-Immunoprecipitation (IP) and immunoblotting (IB) analysis of DZIP1 with CBY1 in HEK293T whole-cell lysis. Co-IP was performed using FLAG or HA antibodies reciprocally. **B,** Representative images of E13.5 murine atrioventricular canal cushions (AVC) immunostained for Dzip1 (red), Cby1 (green) and nuclei counterstained with hoechst (blue). Arrows, Dzip1/Cby1. **C,** Representative images of E13.5 murine AVC immunostained for Arl13b, γ-tubulin, Cby1, Dzip1 and nuclei counterstained with hoechst (blue). Left panel: Arl13b (green), Dzip1/Cby1 (red); Right panel: γ-tubulin (red), Dzip1/Cby1 (green). Bottom panel: 3D reconstruction of Cby1 (red) and Arl13b (green) staining on E13.5 murine embryos. Arrows, Cby1/Dzip1.

Mapping of the DZIP1-CBY1 interaction domain

Various amino and carboxyl-termini deletion constructs for DZIP1 were generated and expressed in HEK293T cells followed by Co-IP in order to identify CBY1-interaction motifs. Constructs expressing just the N-terminal 356 amino acids (1-356) failed to interact with CBY1. Likewise, constructs only expressing the amino acids 613-to the C-terminus (613-867) were unable to interact with CBY1. However, amino acids 357-612 revealed a positive interaction between DZIP1 and CBY1 (**Figure 3.2A**). This region was further dissected into two polypeptide stretches and tested by Co-IP. As shown in **Figure 3.2B**, only region 485-612 harbors the DZIP1-CBY1 interaction motif. Fine mapping of this region was performed by generating biotinylated 30-35 amino acids overlapping peptides and tested by Co-IP (**Figure 3.2C**). Within this region we identified a bipartite interaction motif whereby 2 unique peptides (amino acids 531-560 and 564-593) were capable of interacting with CBY1 (P2: 531-560 and P5:564-593). Scrambled and reverse peptides for P5 served as negative controls and failed to show an interaction as expected. Computational modeling of the peptides revealed similarities between these 2 peptides in conformation indicating a potential likelihood of interacting with overlapping/similar residues on CBY1 (**Figure 3.3A, B**). Heatmap analyses showed that the P2 and P5 peptides are predicted to interact within similar

regions of the CBY1 protein indicating that structurally, these two regions of DZIP1 are similarly oriented in 3D space (**Figure 3.3C**).

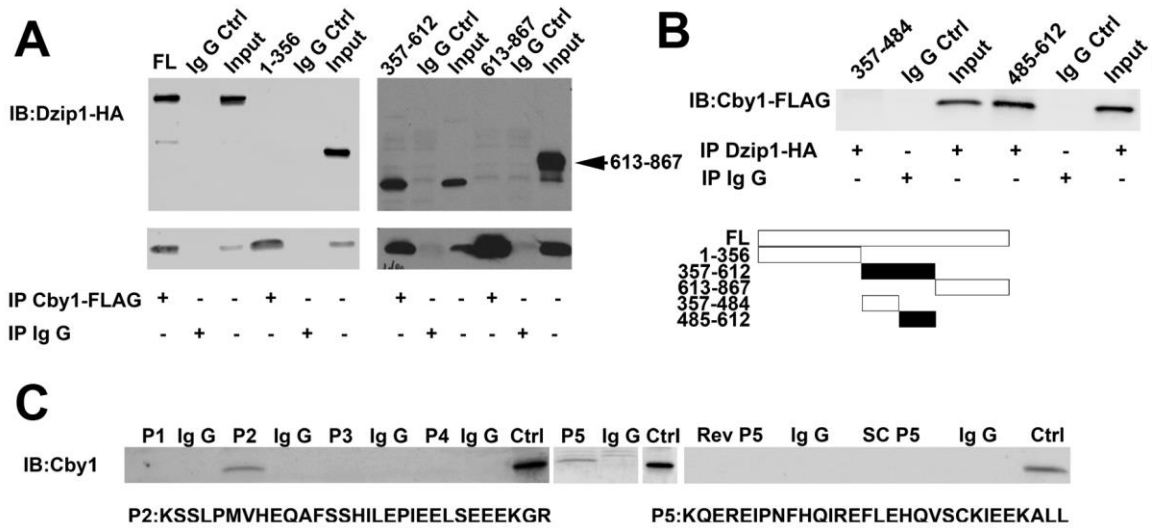

Figure 3. 2 Refined DZIP1-CBY1 interaction domain on DZIP1

A, Co- IP and IB analysis of CBY1 with varies DZIP1 truncated constructs in HEK293T whole-cell lysis. **B**, Co-IP and IB analysis of CBY1 with DZIP1-(357-484)/DZIP1-(485-612) in HEK293T whole-cell lysis. **C,** Co-IP and IB analysis of CBY1 with peptides in HEK293T whole-cell lysis.
Scrambled (SC P5) and Reverse (Rev P5) peptides for P5 served as negative controls. HEK293T cell lysates served as positive control.

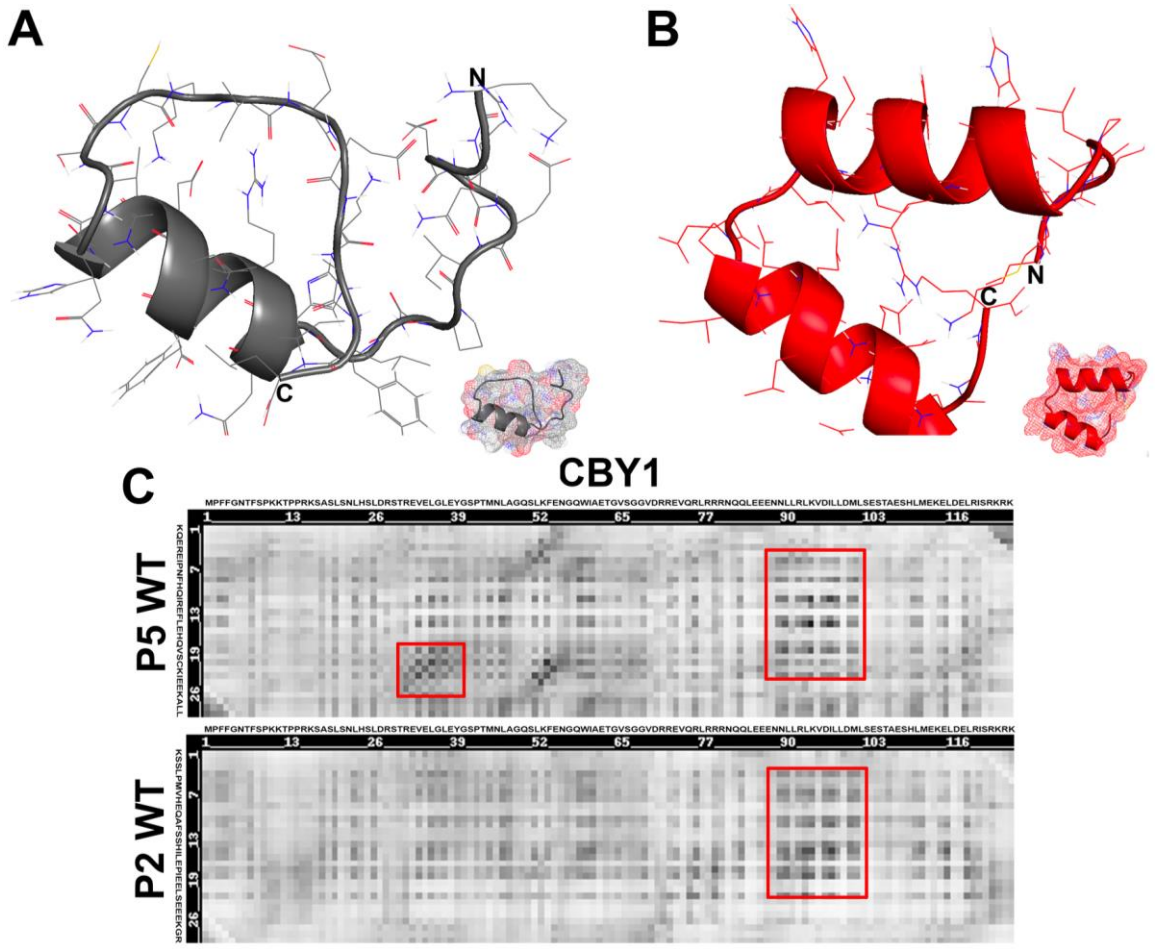

Figure 3. 3 3D structural predictions for peptides.

A, B, Computational modeling of the two peptides: P2 (A) and P5 (B). Modeling was generated through RaptorX. **C**, Heatmap analysis of predicted peptide binding residues within CBY1 across P2 and P5. Red box, similar binding residues within CBY1 between P2 and P5.

DZIP1 peptide interacts with CBY1 and β-catenin.

As Cby1 was previously shown to directly interact with β-catenin[154], we used Co-IP experiments to test whether Dzip1 was capable of a β-catenin interaction through a CBY1 linker moiety. As shown in **Figure 3.4A**, full length (FL) Dzip1 was able to interact with both CBY1 and β-catenin. When we tested the amino end (1-356) DZIP1 expression construct, no interaction with CBY1 or β-catenin was observed, as expected. When the C-terminal 357-867 amino acids of DZIP1 were tested, a CBY1 interaction was detected, but β-catenin was not evident in the IP reaction. This paradoxical observation indicated that upon CBY1 binding to DZIP1, the amino end of DZIP1 may be important in stabilizing the β-catenin interaction. It also remains possible that in the absence of the amino end of DZIP1, the 357-867 DZIP1 polypeptide folds around CBY1, encasing the protein, hindering interaction with other proteins. To test this hypothesis, we assayed whether the minimal DZIP1-CBY1 interaction motif (peptide 5), was sufficient to pull down the entire complex. As shown in **Figure 3.4B**, peptide 5 (P5) was able to co-immunoprecipitate both CBY1 and β-catenin in cultured human valve interstitial cells. Subsequent immunohistochemistry confirmed that β-catenin is found at the basal body in developing murine mitral valves at E13.5,

coincident with the temporal-spatial presence of both Dzip1 and Cby1 (**Figure 3.5A, B**).

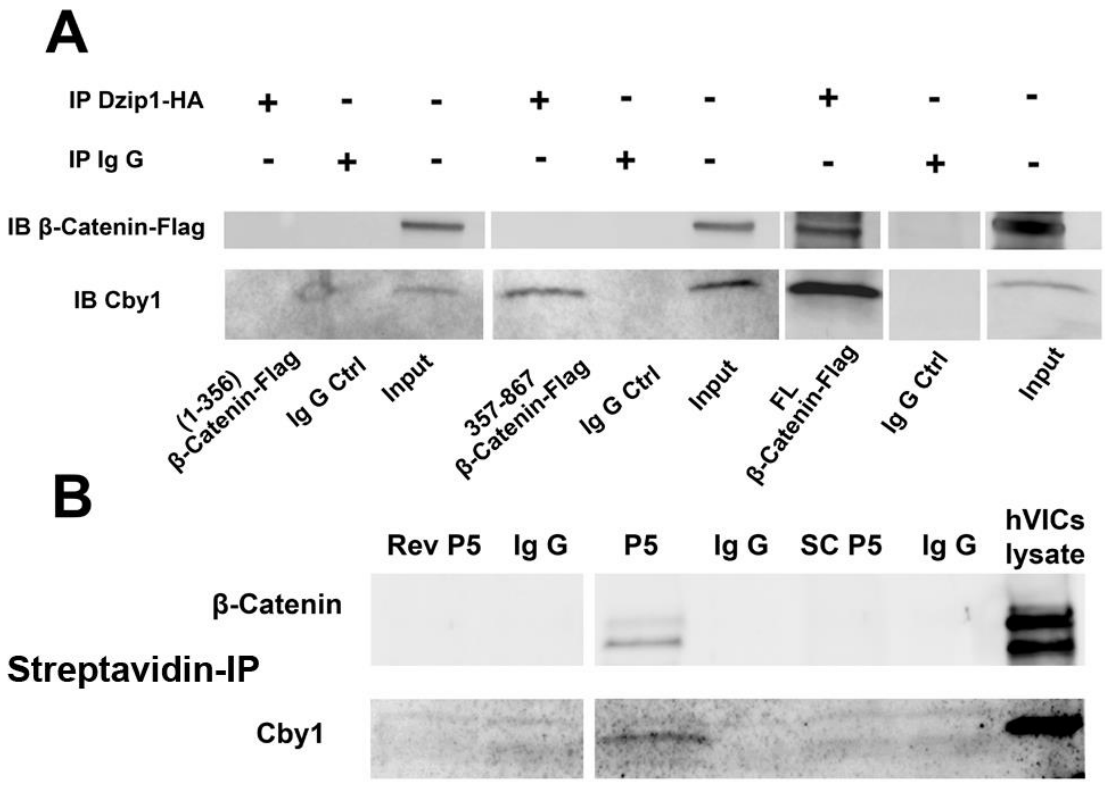

Figure 3. 4 DZIP1 interacts with β-catenin through CBY1

A, Co-IP and IB analysis of β-catenin with DZIP1 in HEK293T whole-cell lysis. (1-356), amino acids 1-356 within DZIP1; (357-867), amino acids 357-867 within DZIP1; FL, full length DZIP1. HEK293T cells were co-transfected with full length DZIP1-HA / (1-356) DZIP1-HA/ (357-867) DZIP1-HA and β catenin-FLAG constructs. Co-IP was performed by pulling down HA tag. (1-356) DZIP1-HA served as negative control. **B,** Co-IP and IB analysis of β-catenin with P5 in cultured human valvular interstitial cells (hVICs) whole-cell lysis. Biotinylated P5 was incubated with hVICs lysate at 4 ℃ overnight and was pulled down by streptavidin beads.

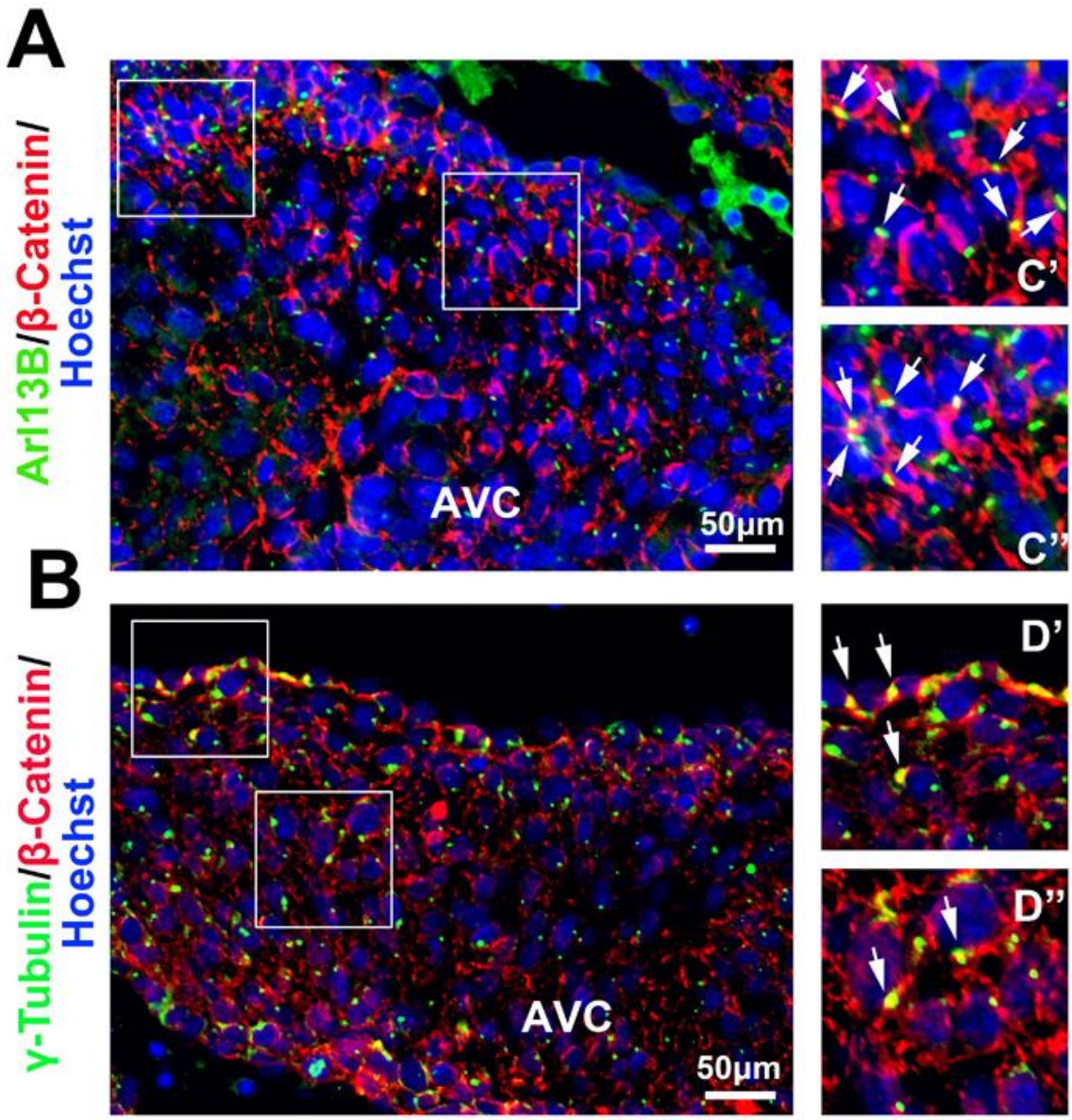

Figure 3. 5 β-catenin locates to primary cilia in developing murine mitral valves at E13.5

A, Representative images of E13.5 murine AVC immunostained for β-catenin (red), Arl13b (green) and nuclei counterstained with hoechst (blue). **C'**&**C''**, arrows, β-catenin. **B,** Representative images of E13.5 murine AVC immunostained for β-catenin (red), γ-tubulin (green) and nuclei counterstained with hoechst (blue). **D'**, arrows, valvular endothelial β-catenin. **D''**, arrows, valvular interstitial β-catenin.

Loss of Dzip1 causes increased nuclear β-catenin and Lef1

An interaction between DZIP1, CBY1 and β-catenin combined with our co-expression studies showing Cby1 is only present at the basal body, suggested that the DZIP1-CBY1 complex was functioning to sequester β-catenin. To test this hypothesis, we analyzed if loss of Dzip1 in the mitral valves would release this inhibition. As shown in **Figure 3.6A and B**, when Dzip1 is conditionally removed from endocardium and endocardial derived mesenchyme (*Dzip1$^{f/f}$; NfatC1$^{Cre\ (+)}$*) that populate the entire mitral valve, a statistically significant increase in activated, nuclear β-catenin is observed (*p=0.0002*) compared to control littermates at P0. This finding correlates with a significant increase in the β-catenin co-factor, Lef1 (*p<0.01*), which is required for its transcriptional regulatory function. Previous reports have indicated that β-catenin activities may be dependent on the presence of primary cilia[143, 148]. As Dzip1 conditional knockout and mutant mitral valves were previously shown to have reduced cilia length[128], it remained possible that this increase in β-catenin is due to loss of cilia, independent of a Dzip-Cby1 interaction. Analyses of activated β-catenin in cilia deficient (*NfatC1$^{Cre\ (+)}$; Ift88$^{f/f}$*) conditional knockout mitral valves failed to reveal a statistically significant change in activated β-catenin protein expression

(**Figure 3.7**). These data indicate that the presence of cilia in the mitral valve does not directly affect activation of the β-catenin pathway.

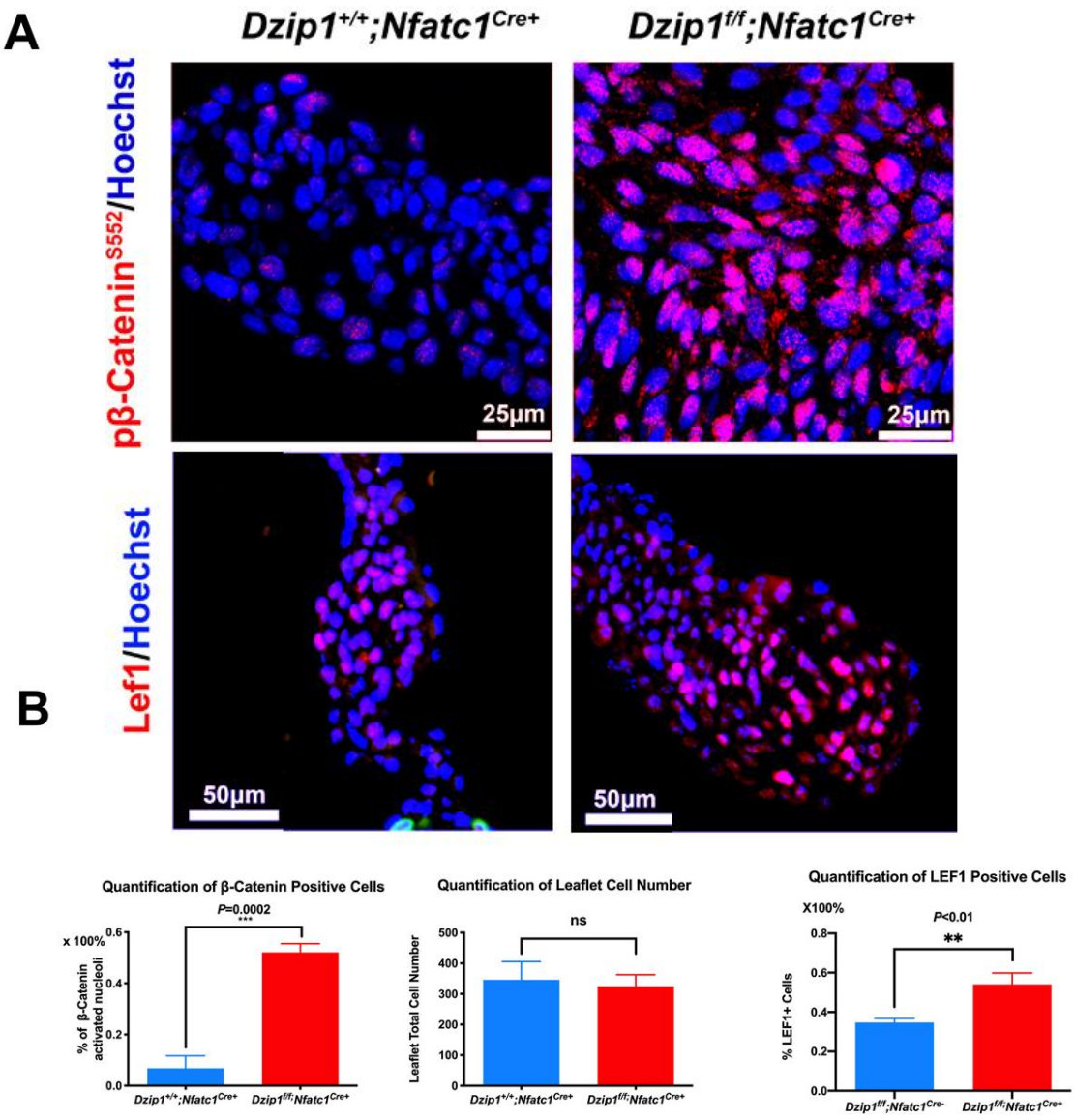

Figure 3. 6 DZIP1 MVP mutation results in increased β-catenin signaling

A, Top: P0 *Dzip1$^{f/f}$; Nfatc1^{Cre+}* murine mitral valves immunostained for pβ-catenin^{S552} (red) and nuclei counterstained with hoechst (blue) compared to littermate control; bottom: P0 murine mitral valves immunostained for Lef1 (red) and nuclei counterstained with Hoechst (blue) compared to littermate control. B: Left: quantification of pβ-cateninS552 + cell percentage; middle: quantification of anterior leaflet cell number; right: quantification of Lef1+ cell percentage. Data are means ± SD, unpaired two-tailed Student's t-test. (n=3/genotype, ***P=0.0002, **P<0.01, ns, non- significant).

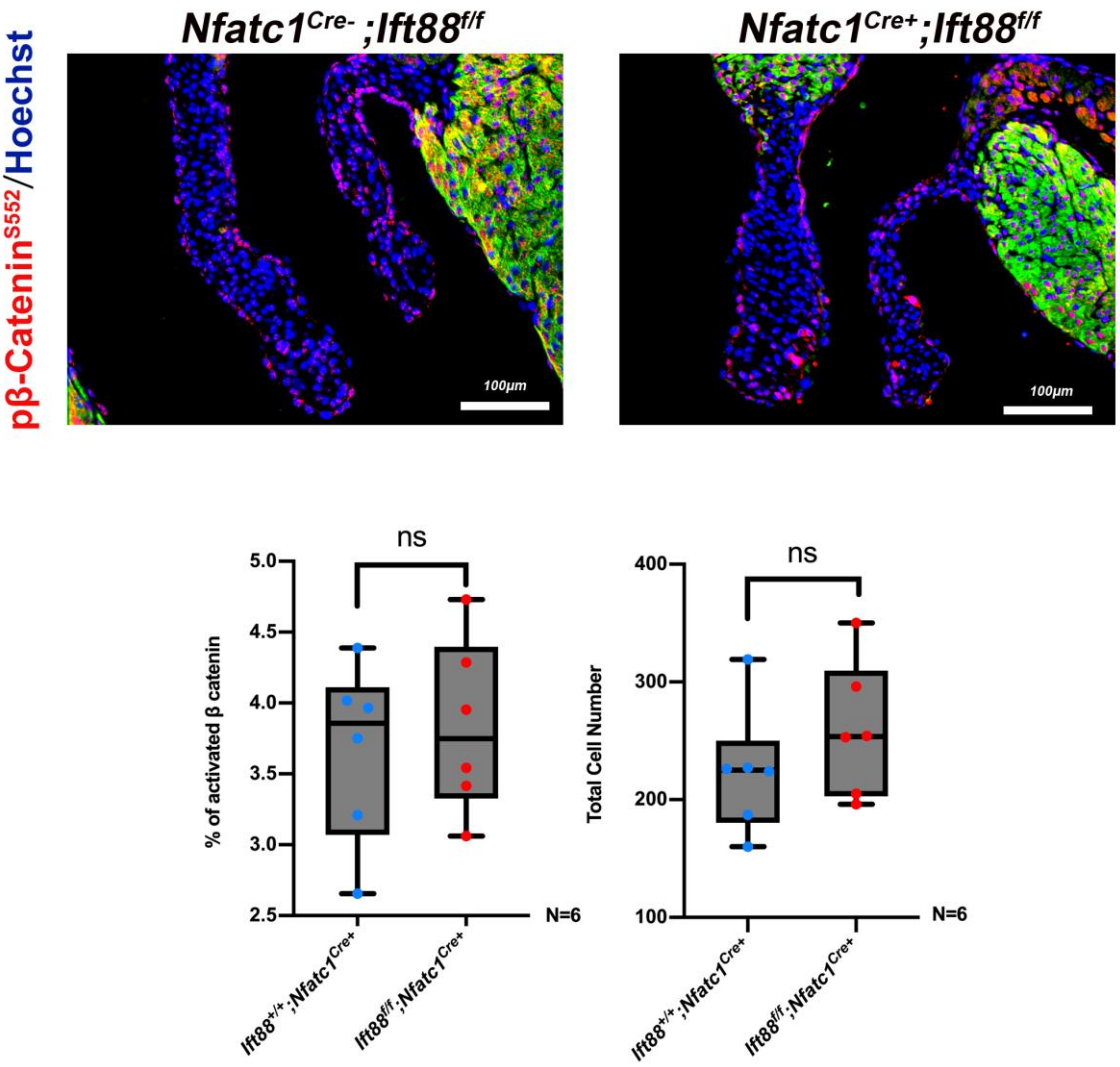

Figure 3. 7 Regulation of β-catenin is primary cilia - independent

Top panel: Representative images of *NfatC1*$^{Cre+}$*; Ift88*$^{f/f}$ P0 murine mitral valves immunostained for pβ-catenin^{S552} (red), MF20 (green) and nuclei counterstained with hoechst (blue) comparing to littermate control. Bottom panel: quantification of *NfatC1*$^{Cre+}$*; Ift88*$^{f/f}$ P0 murine anterior leaflet for pβ-catenin^{S552} $^{+}$ cell percentage and total cell number comparing to littermate control. Data are means ± SD, unpaired two-tailed Student's t-test. (n=6/genotype, ns, non-significant).

DZIP1 MVP mutation results in increased β-catenin signaling

Our previous data demonstrated that the *DZIP1*$^{S24R/+}$ mutation found in MVP patients and its corresponding mutation in mice (*Dzip1*$^{S14R/+}$) resulted in decreased protein stability and likely loss of function[128]. Thus, we tested whether this loss of Dzip1 protein would result in a similar increase in nuclear β-catenin as observed in our conditional Dzip1 knockout mice (**Figure 3.2.6**). As shown in **Figure 3.8**, we observed a significant increase in activated nuclear β-catenin and its co-factor, Lef1 in the developing mitral valves. Subcellular fractionation of MEFs isolated from E13.5 *Dzip1*$^{S14R/+}$ and wildtype littermates revealed a similar finding of increased nuclear β-catenin and reduced fraction of cytosolic β-catenin (**Figure 3.8B**). Total levels of β-catenin do not change in the MEFs nor do the total number of cells change in the valves. Coincident with this observation, cycloheximide experiments in *Dzip1*$^{S14R/+}$ MEFs and wildtype controls defined a significant reduction in Cby1 half-life when Dzip1^{S14R} was expressed. Note, that expression of Dzip1 is undetectable in our *Dzip1*$^{S14R/+}$ MEFs even in the presence of a wildtype allele (**Figure 3.9**). This is similar to what we observed for the human mutation in immortalized patient lymphoblasts and indicates that the mutant protein has a detrimental effect on either the wildtype protein or wildtype allele[128].

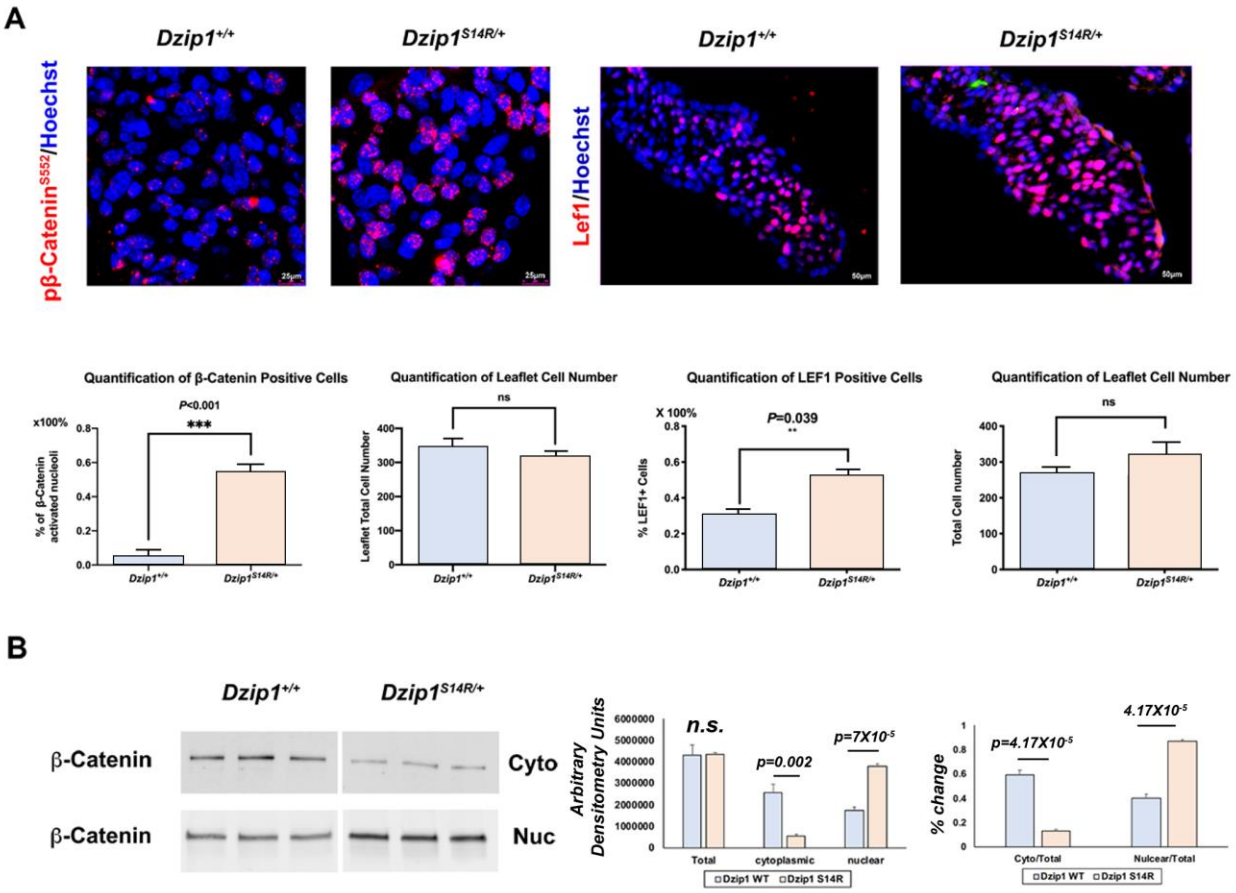

Figure 3. 8 DZIP1 MVP mutation results in increased β-catenin signaling

A, Left panel: Representative images and quantification of pβ-catenin^{S552+}(red) cells on *Dzip1*$^{S14R/+}$ mitral valves at P0 comparing to wild-type; right panel: representative images and quantification of Lef1^{+} (red) cells on *Dzip1*$^{S14R/+}$ mitral valves at P0 comparing to wild-type. Nuclei were counterstained with hoechst (blue). Data are means ± SD, unpaired two-tailed Student's t-test. (n=3/genotype, ***P<0.001, **P=0.039

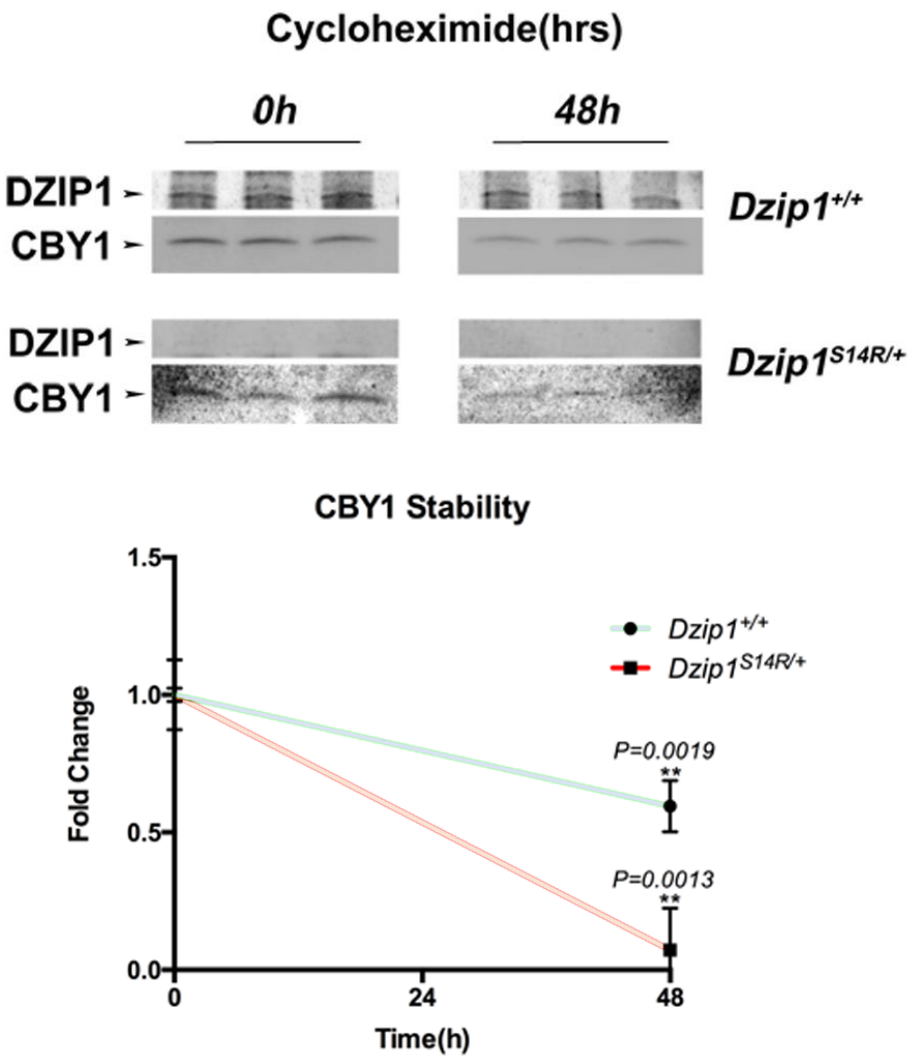

Figure 3. 9 CBY1 stability is reduced in context of DZIP1^{S14R} presence

Western blots (left) and quantification (right) of cycloheximide experiment for CBY1 in E13.5 *Dzip1*$^{S14R/+}$ MEFs compared to wild type. MEFs were treated with cycloheximide at 100ng/ml for 48 hours. Data are means ± SD, unpaired two-tailed Student's t-test (n=3/genotype).

Identification of a missense mutation affecting the CBY1 interaction domain in a family with autosomal dominant MVP

Through our whole exome sequencing project of sporadic individuals and families with non-syndromic MVP, we identified a multigenerational family with a rare variant in DZIP1, *DZIP1*$^{C585W/+}$ (**Figure 3.10**). The mutation is rare with a minor allele frequency of 0.0078 and is predicted to be damaging by SIFT and Polyphen. This particular variant has a CADD (combined annotation dependent depletion) score of 22.5, which places it in the top 1% of deleterious single-base changes possible in the entire genome and within the 95% confidence interval of gene-specific CADD scores corresponding to high-confidence pathogenic mutations for DZIP1. The mutation segregates through two generations of the family and all affected individuals harbor the mutation. None of the confirmed non-MVP individuals have the mutation. Patient II.2 had indeterminant echocardiography and the status of her mitral valve was unable to be fully assessed. We tested mutation pathogenicity by performing cycloheximide experiments on transfected HEK293 cells and observed that the DZIP1^{C585W} mutation resulted in a decrease in protein stability with a reduced half-life from 16.97 hours to 1.05 hours (**Figure 3.11A**). To test whether the mutation also had an effect on CBY1 stability a similar experiment was performed in a separate CHX assay. As shown in

Figure 3.11B, expression of DZIP1^{C585W} results in a premature loss of CBY1 expression consistent with our findings in the *Dzip1*$^{S14R/+}$ mice.

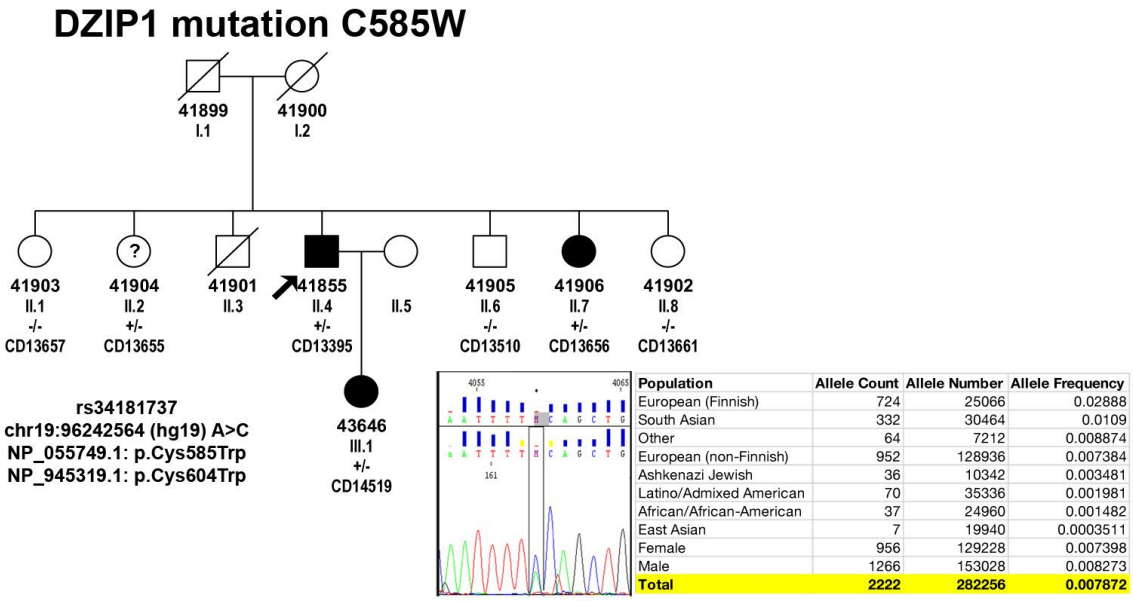

Population	Allele Count	Allele Number	Allele Frequency
European (Finnish)	724	25066	0.02888
South Asian	332	30464	0.0109
Other	64	7212	0.008874
European (non-Finnish)	952	128936	0.007384
Ashkenazi Jewish	36	10342	0.003481
Latino/Admixed American	70	35336	0.001981
African/African-American	37	24960	0.001482
East Asian	7	19940	0.0003511
Female	956	129228	0.007398
Male	1266	153028	0.008273
Total	**2222**	**282256**	**0.007872**

Figure 3. 10 Identification of a missense mutation in DZIP1 in a family with autosomal dominant MVP

Multigenerational family with inherited, autosomal dominant, non-syndromic MVP. Sanger sequencing identified a single missense mutation of DZIP1, resulting in a cysteine-to-tryptophan change. Population frequency showing the rarity of the identified DZIP1 variant in the population.

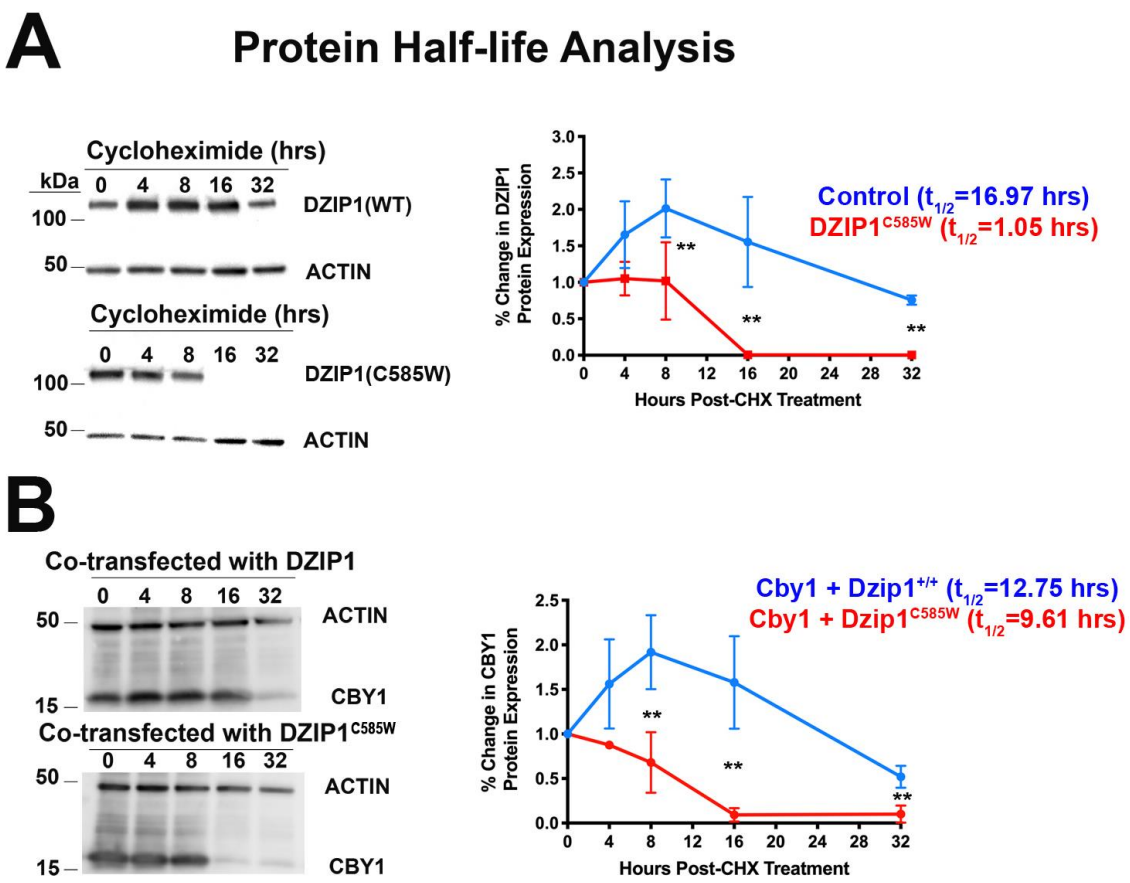

Figure 3. 11 DZIP1^{C585W} stability is reduced and CBY1 stability is reduced in the context of DZIP1^{C585W}

A, Western blots (left) and quantification (right) of cycloheximide experiment for DZIP1^{C505W} compared to DZIP1 in HEK293T whole-cell lysis. Data are means ± SD, unpaired two-tailed Student's t-test. (n=3, ***P*<0.01). **B,** Western blots (left) and quantification (right) of cycloheximide experiment for CBY1 in presence of DZIP1^{C585W} compared to presence of DZIP1 in HEK293T whole-cell lysis. Data are means ± SD, unpaired two-tailed Student's t-test. (n=3, ***P*<0.01).

MVP DZIP1^{C585W} mutation alters protein structure and binding to β-catenin and CBY1

A peptide containing the C585W mutation was synthesized and is designated P5' since its sequence is identical to that of the P5 peptide with the exception of the cysteine to tryptophan change. This peptide was tested for its ability to alter interactions with the CBY1-β-catenin complex. As shown in **Figure 3.12A**, both P5 and P5' were capable of interacting with CBY1 and β-catenin. However, in all repeated experiments (N=5), the P5' mutant peptide demonstrated greater band intensity on the Co-IP reactions, suggesting an increased affinity for CBY1 and β-Catenin. This result was confirmed in transfected HEK293 cell lines as well as primary mitral valve interstitial cells during development. This result was strikingly similar to what we observed between P5 and the P2 segment, with the P2 peptide showing enhanced binding compared to P5 (**Figure 3.2**). Protein modeling and comparative structural predictions for each of the peptides was performed using RaptorX. Secondary and tertiary models for each of the peptides revealed a similar overall structure between P2 and P5' (**Figure 3.12B**). Quantification of data obtained from structure modeling indicated that the cysteine to tryptophan (C585W) point mutation in the P5 subunit causes a drastic change in protein tertiary structure (TM Score = 0.1780) compared to wild type. This

modification renders the P5 C585W mutant more structurally similar to the P2 WT subunit (Lali: 18; RMSD: 2.28; TM Score: 0.3925) compared to the P5 WT subunit (Lali: 7; RMSD: 1.90; TM Score: 0.1780). Therefore, although the mutation causes faster degradation of the full-length protein, it is structurally more similar to the P2 region and confers increased binding to the CBY1 and β-catenin complex.

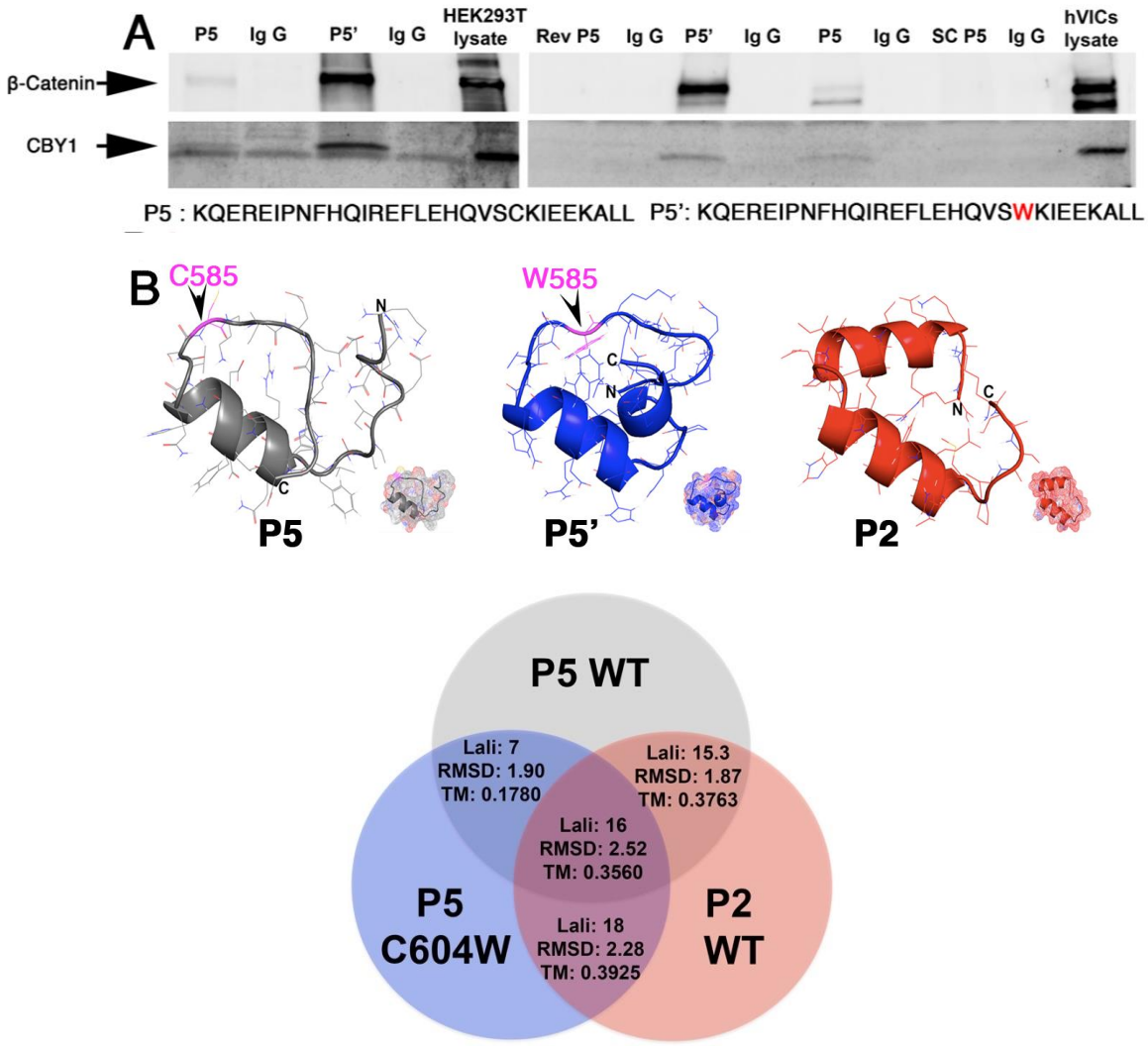

Figure 3. 12 MVP DZIP1^{C585W} mutation alters protein structure and binding to β-catenin and CBY1

A, Co-IP and IB analysis of P5 and mutant P5 (C585W) with CBY1 in HEK293T whole-cell lysis and cultured hVICs whole-cell lysis. P5', mutant P5 (C585W); Rev P5, reversed P5; SC P5, scrambled P5. Biotinylated peptides were incubated with cell lysis overnight at 4 ℃, and peptides were pulled down by streptavidin beads. **B,** 3D modeling of P5/P5'/P2 showing overall similarity between P2 and P5'. Venn diagram: quantification of modeling data indicating P5 C585W mutant is more structurally similar to the P2 WT subunit compared to the P5 WT subunit.

β-catenin transcriptional responses are regulated through Dzip1 decoy peptides

To determine whether transducing cells with these minimal interaction motifs could affect downstream β-catenin activities, we synthesized various peptides based on our Co-IP data and human DZIP1 mutation. Peptides for the P5 region as well as mutant P5 (P5') and a P5 reverse peptide were synthesized with a cell-penetrating TAT peptide sequence and a 5-FAM moiety for fluorescent visualization at the amino terminus. Peptides were also biotinylated to be able to confirm interaction with CBY1 and β-catenin. As shown in **Figure 3.13,** the 5-FAM-TAT labeled P5 was capable of interacting with both CBY1 and β-catenin in valve interstitial cells whereas the reverse peptide was not.

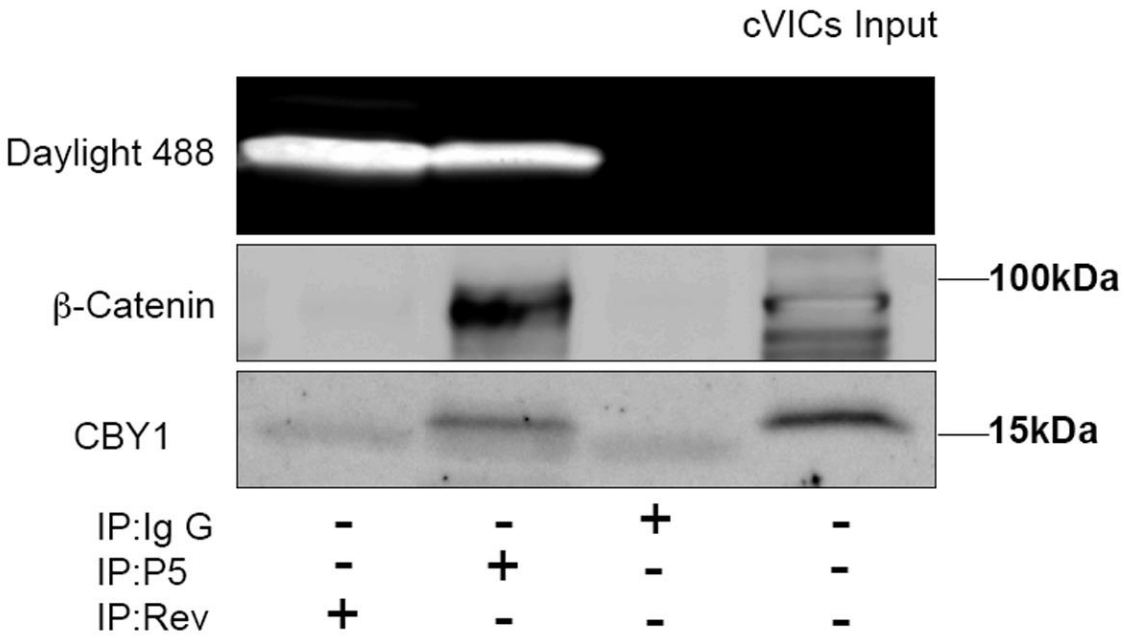

Figure 3. 13 TAT conjugated P5 forms complex with CBY1 and β-catenin in cVICs

Co-IP and IB analysis of β-catenin with TAT conjugated P5 in cVICs whole-cell lysis. TAT conjugated P5 was incubated with cVICs lysate at 4℃ overnight and was pulled down by streptavidin beads. Reverse P5 served as negative control. Rev, reverse P5. TAT conjugated peptides on the gel were imaged under daylight 488.

To test whether the peptides function to disrupt β-catenin activities within the cell, valve interstitial cells were transfected with the TOP flash β-catenin reporter plasmids. Forty-eight hours post-transfection, valve fibroblasts were stimulated with P5 (1μM, 10μM), P5' (1μM) or reverse peptide (high dose 10μM). As shown in **Figure 3.14A**, membrane permeant peptides were able to traverse the cell membrane and enter the cytoplasm. Cell viability and substrate attachment were not grossly affected with peptide administration. Localization of the peptides can be seen perinuclear and along the cell membrane. Presence of the peptides within the nucleus are not evident, suggesting potential retention of β-catenin outside of the nucleus. Luciferase readouts from the TOPflash reporter confirmed a significant reduction in β-catenin activities when treated with both the P5 and P5' mutant peptides at 1μM dose (**Figure 3.14B**). P5 treatment at 10μM dose resulted in a complete block in TOPflash luciferase activation whereas the reverse peptide had no significant effect at this higher dose. Interestingly, the mutant P5' peptide was not as robust in repressing the reporter as the wild-type, even though it showed enhanced interaction with the CBY1/β-catenin complex by biochemical approaches.

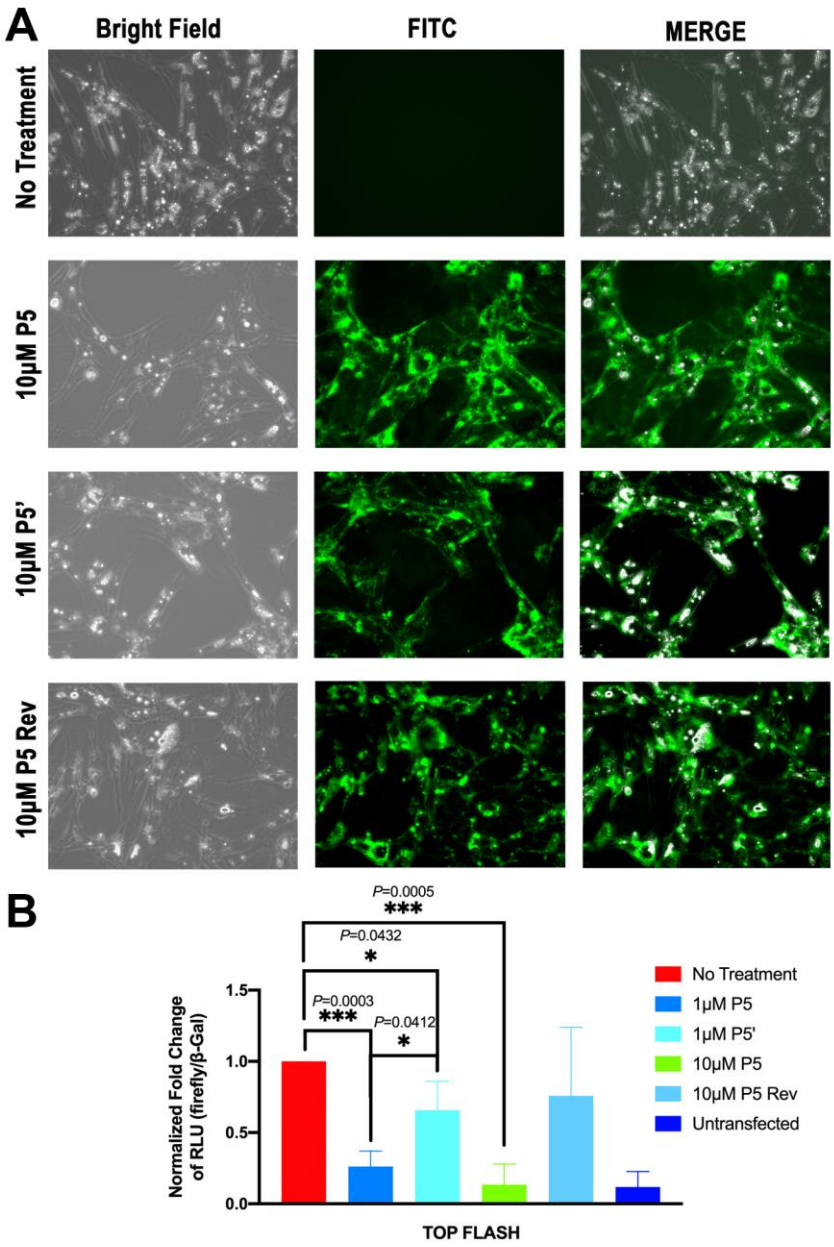

Figure 3. 14 Dzip1 decoy peptides disrupts β-catenin transcriptional responses *in vitro.*

A, Representative images of P5/P5'/P5 Rev treated chicken valvular interstitial cells (cVICs) for 24 hours at 10 μM. cVICs were transfected with TOP/FOPflash reporter construct for 48 hours before peptide treatment. P5', C585W mutant P5; P5 Rev, reverse P5. **B**, Luciferase assay of P5/P5'/Rev P5 treated cVICs. β-Gal was used as internal control. Data are means ± SD, unpaired two-tailed Student's t-test (n=3).

Enhanced MMP2 expression and altered extracellular matrix deposition in Dzip1$^{S14R/+}$ and Cby1$^{+/-}$ postnatal mitral leaflets

Enhanced Wnt/β-catenin signaling has been observed in human myxomatous valves[60, 265, 266]. Hyperactivated β-catenin can promote endothelial-to-mesenchyme transformation (EMT), endocardial proliferation, ECM remodeling and myxomatous degeneration of mitral valves[56, 57, 267]. In this study as well as our previous reports on Dzip1 mutations, we observe similar findings of increased β-catenin activities within the valves during development in a model (*Dzip1$^{S14R/+}$*) that was previously validated as having myxomatous valves and MVP[128]. For this study, we initially focused on MMP2 a known transcriptional target of β-catenin signaling that is also known to be upregulated in mitral valve disease. As shown in **Figure 3.15**, we observe increased MMP2 within the interstitium of Cby1 heterozygote (*Cby1$^{+/-}$*) mitral valves by postnatal day 0. This finding of increased MMP2 was also observed in the *Dzip1$^{S14R/+}$* model of MVP. Although our previous RNAseq data showed an increase in collagen I mRNA at this timepoint, IHC in both Cby1 and Dzip1 models show a loss of collagen protein within the valve. The reduction of collagen I, a known target of MMP2 enzyme activity was striking, especially along the atrialis of the mitral leaflets and is indicative of a potential increase in collagen fragmentation as is documented in human

myxomatous valves. Interestingly, periostin, a known β-catenin transcriptional target is also upregulated in the *Cby1*$^{+/-}$ valves, which is consistent with findings in human myxomatous valves and in hyperactive β-catenin murine models.

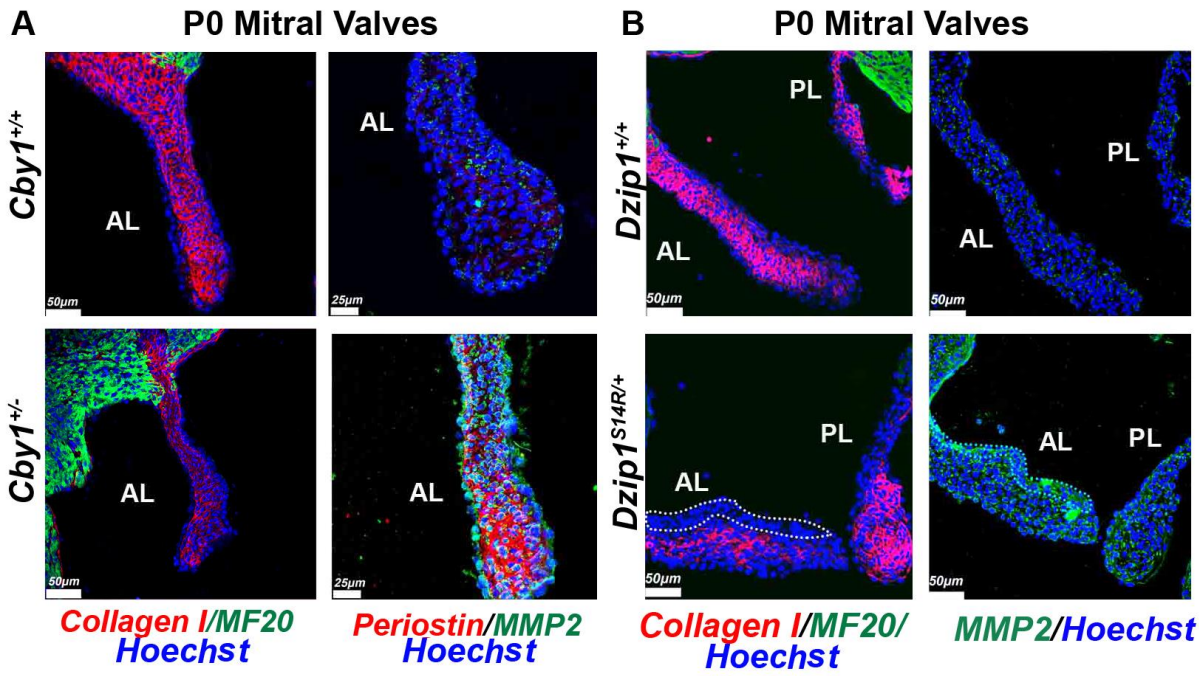

Figure 3. 15 Enhanced MMP2 expression and altered extracellular matrix deposition in *Dzip1*$^{S14R/+}$ and *Cby1*$^{+/-}$ postnatal mitral leaflets

A. Representative images of *Cby1*$^{+/-}$ P0 anterior leaflet immunostained for collagen I (red), MF20(green), periostin (red), MMP2 (green) and nuclei counterstained with hoechst (blue) comparing to wild type (N=3/genotype). **B.** Representative images of *Dzip1*$^{S14R/+}$ P0 mitral valves immunostained for collagen I (red), MF20(green), MMP2 (green) and nuclei counterstained with hoechst (blue) comparing to wild type (N=3/genotype). Dotted line highlights the MMP2 enriched area where collagen I was largely invisible.

3.3. Discussion

The genetic causes of mitral valve prolapse are only now beginning to be discovered. Once disease genes are identified, it will be important to identify the role that these genes play in disease initiation and progression. We recently identified mutations in the DZIP1 gene in multiple families with inherited non syndromic mitral valve prolapse. Through CRISPR-Cas9 genome editing, a murine model for non-syndromic MVP based on a human mutation was generated (*Dzip1*$^{S14R/+}$). Utilizing a combination of proteomic based approaches with *in vivo* and *in vitro* studies, our findings reveal a mechanism by which myxomatous degeneration may occur through altered developmental pathways that invoke both ciliogenesis and β-catenin signaling. Previous studies have indicated that primary cilia can regulate canonical Wnt/β-catenin signaling[143, 148]. This is thought to occur through localization of Wnt receptors on the axoneme of the primary cilia and/or within the ciliary clefts. However, within cilia deficient mitral valves at P0, our studies did not reveal a significant change in activated nuclear β-catenin. Thus, our findings in our Dzip1 models of increased β-catenin/Lef1 signaling highlights cilia-independent regulation of β-catenin pathways.

Our recent studies have highlighted a dynamic expression pattern between nuclear and membrane bound β-catenin[265]. Whereas nuclear β-catenin is present during early embryonic development, a shift to the membrane is observed during fetal gestation and is maintained after birth. This likely highlights the multifaceted role for this protein in both nuclear and membrane function. Mechanisms by which this nuclear vs cell membrane decision is made are not well understood, but likely critical for restricting β-catenin's transcriptional function. Our studies highlight the unique possibility that β-catenin is held at the basal body through a Dzip1-Cby1 complex. Co-IP studies confirmed the formation of this complex and identified unique protein motifs that are critical for this interaction to occur. Generation of membrane permeant peptides of the Dzip1-Cby1 interaction motif were sufficient to potently suppress β-catenin transcriptional regulation *in vitro*. However, it is unlikely that the peptides would confer sufficient structure to restrict the entire peptide-Cby1-β-catenin complex to the basal body. It is more likely that the interaction of the Dzip1-decoy peptide facilitates stabilization of a Cby1-β-catenin complex and inhibits nuclear shuttling independent of being sequestered at the basal body. This is further supported by our anecdotal evidence showing that loss of Dzip1 and/or mutations within the Dzip1-Cby1 interaction domain results in decreased protein stability

concomitant with increased nuclear β-catenin and upregulation of transcriptional activities.

Whole exome sequencing identified a multi-generational family with a rare, damaging variant in the DZIP1-CBY1 interaction motif. Peptide analyses and Co-IP studies revealed that this mutation altered the 3D structure of the protein and conferred a paradoxical increase in Cby1-β-catenin interactions. This should theoretically result in an increase in the stability of the complex and a reduction in β-catenin activity. However, this is confounded by our data showing that the Dzip1^{C585W} mutation results in a profound reduction in protein half-life and premature degradation of CBY1 protein. Thus, although the DZIP1^{C585W} mutation appears to enhance an interaction with the complex, the reduced protein expression results in an overall loss of function, consistent with our other MVP-identified mutation, *DZIP1*^{S24R} and our *Dzip1* conditional knockout mice.

How altered β-catenin signaling may lead to a myxomatous valve and mitral valve prolapse is poorly understood. Previous reports have shown that either loss or gain of β-catenin function can result in a myxomatous phenotype[54, 56, 57]. In the context of Dzip1 and Cby1, our data show that loss of either of these genes impairs ciliogenesis (ref 12 and **Figure 3.16**). RNAseq and GO analyses by us and others have shown that loss of cilia during

development results in transcriptional activation of numerous ECM genes including collagens and proteoglycans. In the context of increased collagens, one might expect to observe a fibrotic valve. Certainly, this occurs in the context of various other valve disease such as serotonin or drug-induced (e.g. fenfluramine, ergotamine) valvulopathies where the valves show stiff "stuck-on plaques" and clear evidence of fibrosis. The phenotypes of these valves are very different from a floppy myxomatous valve, which is defined as having increased proteoglycans as well as fragmented collagen and elastin. This highlights that additional signaling pathways are likely in play to explain the fragmentation of collagen and the loss of properly stratified ECM boundaries. In this context, fragmentation of collagen would permit encroachment of proteoglycan proteins that can move via interstitial fluid flow within affected regions of the valve, particularly within the fibrosa. We believe our observation of increased MMP2 in our *Dzip1* and *Cby1* deficient mitral valves is significant since MMP2 is a direct target of β-catenin/Lef1 transcriptional regulation. Major substrates for this enzyme are collagens I, III, IV, V, VII, elastin and TGF-β. Transcripts for each of these ECM genes are increased in both of our *Dzip1* and *Ift88* cilia deficient mice. However, there is an important discrepancy to note. The *Ift88* conditional knockout (*NfatC1*$^{Cre\,(+)}$*; Ift88*$^{f/f}$) mice show robust increases in collagen I transcript *and* protein at P0.

This study paired with our previous study paradoxically shows that while *Dzip1*$^{S14R/+}$ and *Dzip1* conditional knockout mice (*NfatC1*$^{Cre\,(+)}$*; Dzip1*$^{f/f}$) have increased transcripts for collagen and elastin genes, overall valvular collagen I protein levels are lower. The most likely explanation for this finding is that in a mutated *Dzip1* tissue, increased β-catenin activity leads to upregulation of MMPs and subsequent proteolysis of collagens and elastin. Our study highlights that Dzip1 mutations result in a shift in the balance of ECM synthesis and destruction through loss of cilia and/or increased β-catenin signaling. This altered ECM homeostasis eventually leads to the generation of a myxomatous phenotype that is incompatible with normal valvular function.

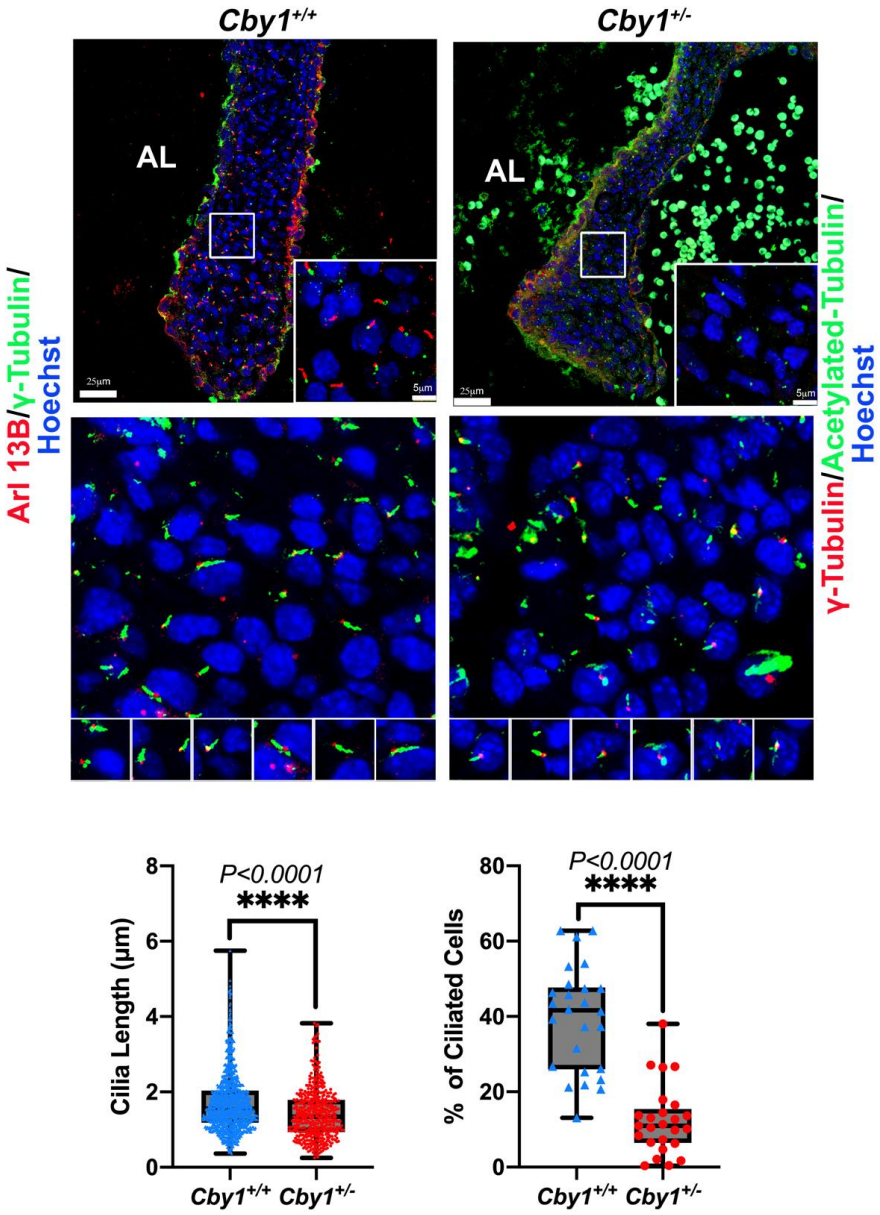

Figure 3. 16 CBY1 is necessary for ciliogenesis during valve development

Top panel, representative images of Cby1$^{+/-}$ P0 anterior leaflet immunostained for Arl13B (red), γ-tubulin (green) and nuclei counterstained with hoechst (blue) comparing to littermate control. Middle panel, representative images of Cby1$^{+/-}$ P0 anterior leaflet immunostained for acetylated-tubulin (red), γ-tubulin (red) and nuclei counterstained with hoechst (blue) comparing to littermate control. Bottom panel, quantification of primary cilia length and percentage of ciliated cells for Cby1$^{+/-}$ P0 anterior leaflet compared to littermate control.

Chapter 4 Future directions

4.1. β-catenin expression profile during valvulogenesis

In Chapter 2, we used antibody which targets endogenous level of β-catenin only when phosphorylated at Ser552. This phospho-β-catenin (Ser552) specifically locates to nucleus. As a transcription co-activator, nuclear β-catenin binds Tcf/Lef1 family member to activated downstream Wnt target genes. But we did not observe fully overlapping of Lef1 and phospho-β-catenin (Ser552) from IHC. The activities between Lef1 and β-catenin seemed to be mutually exclusive. Even though studies have shown the Lef1 independent β-catenin pathway and β-catenin independent Lef1 pathway, questions still remain unsolved that whether phospho-β-catenin (Ser552) interacts with other Tcf/Lef1 family members such as Tcf1/Tcf3/Tcf4. Additional immunostainings for those members could be done through development to determine their co-localization with phospho-β-catenin (Ser552). Except for Ser552, there are other different phospho sites on β-catenin dictating its nuclear localization, including Ser191, Tyr393, Ser 605, Ser675. The other question remained unknown is whether these phosphorylated β-catenin are present on valve tissue during development and if so, what is their association with different Tcf/Lef1 family members. Future study could use Mass Spectrometry to map out the phosphorylation sites from valve tissues at different developmental stage. Ensuing Duolink PLA

technique on valve tissue could be used to determine the interactions between β-catenin and Tcf/Lef1 family members.

Immunofluorescence stainings in Chapter 2 are descriptive data. We know little about the mechanism behind the intriguing β-catenin expression patterns. In E13.5 AV valves, activated β-catenin are restricted within the central mass of the tissue and low to non-detectable staining is observed within subendothelial cells. This demarcates at least two different cell types. No studies have been done to characterize these two cell types despite they are all interstitial fibroblasts. The drastically different activated β-catenin expression patterns between the two subsets of cells indicate the different biological events these cells may go through. This information will be critical to shed a light on the VICs biogenesis and valvulogenesis. Future studies could use single-cell RNA-seq analysis to evaluated cell heterogeneity of VICs at E13.5. Flow cytometry could be used to sort cells using specific β-catenin antibody.

Another question that is worthy for future study is why activated β-catenin starts to present on endothelial cell membranes at E13.5 AV and aortic valves. The translocation from nuclei to cell membrane is highly associated with additional phosphorylation event mediated by other kinases. To test this, we could use *Tie2-GFP* mice to isolate VECs through fluorescence activated

cell sorting (FACS). Mass Spectrometry could be used to identify new phospho sites.

4.2. Regulation of Wnt/β-catenin signaling through Dzip1

In the 3rd Chapter, we identified a novel mechanism about how β-catenin is sequestered by Dzip1-Cby1 complex in cytoplasm. A segment of Dzip1 protein (P5) is capable to substitute for Dzip1. The P5-Cby1 complex is able to sequester β-catenin in cytoplasm *in vitro*. The interesting phenomenon is that the mutant P5 (P5') seems to have higher affinity to Cby1/β-catenin than wild type P5 according to stronger Cby1 signal detected from Co-IP. This leads to the postulation that mutant P5 should sequester more β-catenin *in vitro* and the luciferase reporter read out should be lower than wild type P5. But the fact is somehow on the contrary to our expectation that P5' treated cells actually had a higher luciferase reporter read out than wild type P5. The cause is most likely due to the decreased stability of the P5'. Despite the higher affinity to β-catenin, P5' gets degraded faster. The shortened P5'half-life counteracts its inhibition on β-catenin, which leads to a higher β-catenin activity than wild type P5 *in vitro.* As mutant Dzip1 protein has a shortened half-life, the mutant peptide might have the same fate. In order to test the that, future study could use fluorescence-HPLC (High Performance Liquid Chromatography) to measure the half-lives of both peptides.

The identification of the P5 to inhibit β-catenin signaling is not only critical for valvular disease treatment, but important for cancer suppression. One of the human cancers caused by Wnt/β-catenin signaling hyperactivation is colorectal cancer (CRC). The other avenue of future direction is to test the effect of this peptide to inhibit hyperactivated Wnt/β-catenin signaling in CRC. We have detected the expression of both CBY1 and DZIP1 in Caco2 (human colorectal adenocarcinoma cells) cell lysates. Validation of CBY1-DZIP1-β-catenin complex in Caco2 could be done through Co-IP. Future studies could be done by incubating the Caco2 cells with P5 and control peptide and determine the localization of β-catenin by ICC. Western blot could be used to determine the nuclear β-catenin and cytoplasmic β-catenin expression. Anticipated results would be less nuclear β-catenin and more cytoplasmic β-catenin with P5 than control peptide.

Another segment of DZIP1 that is able to interact with CBY1 is peptide 2 (P2). A comparison between P2 and P5 could be studied in the future. We could compare the stability through fluorescence-HPLC. We could also compare the binding affinity to β-catenin and CBY1 through quantitative GST pull down. Through comparisons, we can select a more superior candidate to be potentially investigated clinically. The whole advantage of using the peptide to antagonize β-catenin signaling is that the peptide brings less side

effects. The cell penetrating peptide (CPP) is a substitute for DZIP1 in the β-catenin sequestration complex. It does not affect DZIP1's other biological functions. Trough titration experiment, we could be able to find a proper dosage to offset the hyperactivated β-catenin signaling and keep the signaling working at a normal level.

Chapter 5 Overall discussion

Wnt/β catenin signaling is one of the most important developmental signaling pathways that controls cell fate decisions and tissue patterning during early embryonic and later development. β-catenin is the key effector responsible for transduction of the signal to the nucleus and it triggers transcription of Wnt-specific gene responsible for the cell fate decision in many cells and tissue. Especially in heart valve development, β-catenin involves in the proliferation in AVC EMT and hyperactivated β-catenin leads to myxomatous ECM in mitral valve.

Even though several studies have revealed the critical roles of Wnt/signaling pathway in valvulogenesis, no information about the temporal and spatial distribution of activated β-catenin during valve development is known. Research work in Chapter 2 characterized the expression profile of activated β-catenin, which accounts for the Wnt signaling and membrane bound β-catenin, which mainly functions in maintaining cell-cell adhesion during valve development. We noticed a reduced nuclear β-catenin expression beginning at E13.5 and nuclear β-catenin started to relocate from nuclei to membrane as cardiac valves developed. This process is synchronizing cell proliferation which is also reduced with development as cardiac cells become more differentiated and mature[68]. Our study first reports the redistribution of activated β catenin from nuclei to membrane during valve development

which is contrast to what we used to think about activated β-catenin. Once Wnt ligand bind Fz receptor on cell membrane, the deconstruction of β catenin phosphorylation complex which phosphorylates residues 41,37, and 33 of β catenin prevents β-catenin from degradation, thus, activated β-catenin is capable to accumulate in cytosol and has a chance to bind Tcf/Lef1 to recruit complexes that promote transcriptional activation[56]. The activated β-catenin analyzed here in our study is phosphorylated at Ser552 by Akt which has been shown to have enhanced β-catenin/Tcf reporter activation[268-270]. However, many other residues in membrane cadherins could enhance the binding with β-catenin, as well. The local cell-signaling events, kinases and in vivo phosphorylation of cadherins, β-catenin and Tcf/Lef1 could make this redistribution significantly diverse during development. The data indicate that after E11.5, a subset of subendocardial cells start to go through a different biological process creating a biased affinity of β-catenin to membrane vs. nuclei.

Another important discovery is that within the developing mitral and aortic valves, nuclear β-catenin is profoundly downregulated. The activated nuclear β-catenin is not detectable in adult tissue. This gives rise to the question that since Wnt/β-catenin signaling is only activated during a developmental and early neonatal window, how is adult myxomatous

phenotype is associated with dysregulated Wnt/β-catenin signaling? The activated nuclear β-catenin was most robust at E11.5 and start to be downregulated as early as E13.5. This time window is very critical for EMT. When this downregulation mechanism is not working and β catenin signaling is not constrained post-EMT, a variety of downstream target genes would be activated. This process can have lasting consequences throughout a lifetime. One of the most studied target gene is MMP2, which digest collagen and versican. The ECM components which are continuously digested by MMPs would not be proper to support valve tissue. The fragile valve might not be a problem early in life, but as heart develops and blood volume in cardiac circulation increases, the sheer force and continuous heartbeat would finally overwhelm the valve structure and leads to prolapse.

Above all, multiple functional β catenin present on cell membrane and nuclei is developmentally regulated. Their temporospatial expression pattern indicate their distinct roles in cell-cell adhesion, transcriptional activity, ECM deposition during different gestational timepoint. Later studies are needed to clarify the mechanisms involving those cellular events and take into consideration of both nuclear and membrane β catenin to cardiac development and disease.

The research work in Chapter 3 starts with a genetic mutation in *DZIP1* that out lab previously identified within non-syndromic MVP families. Previous study of our lab has validated the correlation between $DZIP1^{S14R}$ and myxomatous phenotype. The mechanism of how *DZIP1* regulates valvulogenesis remains unknow. Through proteomics approach, we identified and confirmed a molecular interaction between DZIP1 and CBY1 and their spatiotemporal co-localization on mitral valve tissues. CBY1 is a well-established ciliary gene which functions in cilia formation[257-261]. On *Cby1* deficient valve tissues, we observed shortened and reduced number of primary cilia which supports those studies. Even though our study firstly validated the connection between DZIP1 and CBY1, some previous studies have actually indicated clues of this interaction by showing that both Cby1 and Dzip1 interact with Fam92 to facilitate ciliogenesis[258, 271]. Along with our previous study on the ciliogenetic function of Dzip1[128], all these evidences strengthen the cooperative role of *Dzip1* and *Cby1* in ciliogenesis.

Jean-André Lapart et al. showed that *Drosophila* Dzip1 is required to recruit or stabilize Cby1 at centrioles, but does not depend on Cby1 for its targeting to centrioles[271]. This conclusion gives rise to a hint that the higher functional hierarchy of DZIP1maintains this collaboration between DZIP1 and CBY1 for ciliogenesis. The following protein stability analysis

corroborated that CBY1 became less stable in the context of either $DZIP1^{C604W}$ or $DZIP1^{S14R}$ meanwhile both $DZIP1^{S14R}$ and $DZIP1^{C604W}$ have impaired protein stability.

Cby1 is also a well-known β-catenin antagonist which is recognized to compete with Tcf/Lef1 to bind β-catenin and re-locate β-catenin outside nucleus into cytoplasm[154, 262, 263]. The molecular interaction between DZIP1 and CBY1 is reminiscent of the possibility that DZIP1 could interact with β-catenin through CBY1. This assumption was validated by the Co-IP experiment. Together with the significantly increased nuclear β-catenin from Dzip1 deficient mitral valve, these data strongly suggested that Dzip1 plays a vital role in restricting β-catenin signaling through Cby1. The decreased protein stability of CBY1 under conditions of DZIP1 mutant shed a light for the mechanism involved in how DZIP1 regulates β-catenin.

From the data collected we propose the following working model (**Figure 4.1**). In VICs, DZIP1, CBY1 and β-catenin form a complex which locates to basal body of a primary cilium. The complex sequesters β-catenin in cytoplasm. This leads to the shut off of the β-catenin signaling. The ECM homeostasis is balanced as there would be no extra MMPs induction. When DZP1 has a mutation, its protein stability is impaired which leads to the degradation of CBY1. From that, DZIP1-CBY1-β-catenin complex would be

disrupted. β-catenin will be set free and enter nucleus to start downstream MMPs transcription. This contributes to ECM digestion. Over time, the valve tissue become thickened and mechanically incompetent.

In the future this work has the potential to influence therapies for myxomatous valvular diseases. The peptides used in this work showed striking effect on β-catenin signaling inhibition. Therapies using Nano particles which filled with the peptides are appealing for this function. Using antibody targeted against VICs, these peptides could possibly turn off the hyperactivated β-catenin signaling in VICs before they produce too much MMPs to digest collagens.

Many questions remain to be answered and more work is needed to further elucidate the molecular mechanisms involved in valve disease, however, considerable progress has been made towards increasing our knowledge about it. The identification of a complex formed by DZIP1-CBY1-β-catenin to regulate Wnt signaling during valvulogenesis is innovative and opens up the potential for further research to refine our knowledge about the genetic and molecular landscape of valve development.

.

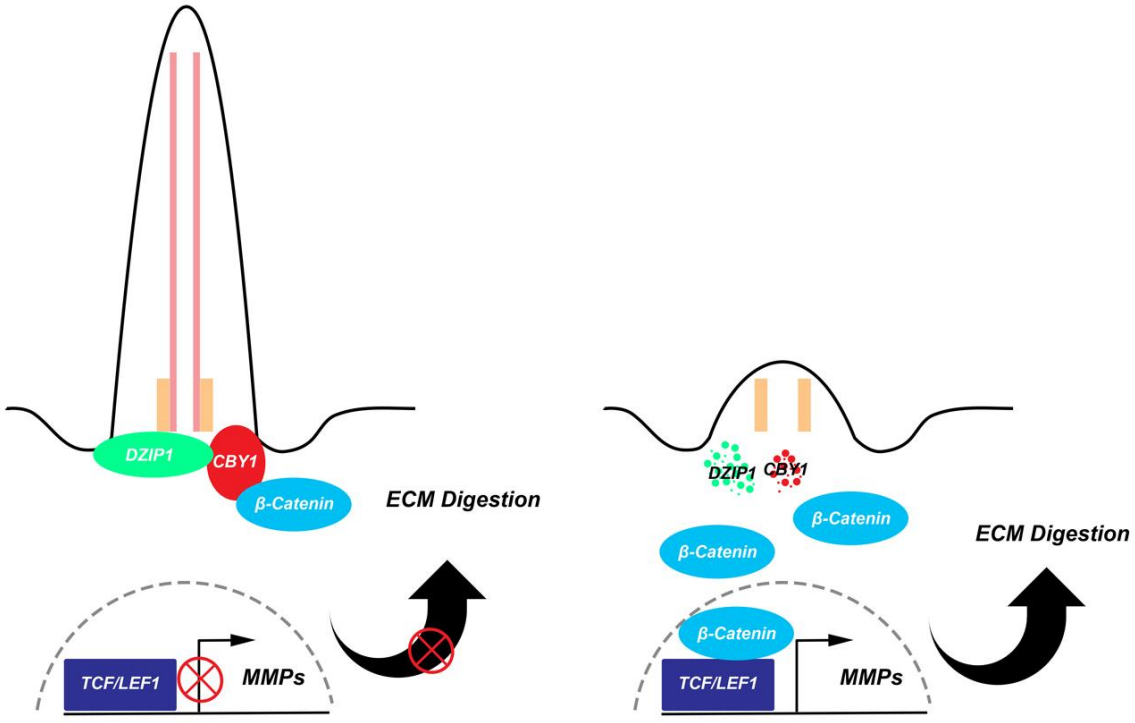

Figure 4. 1 Graphic Abstract

DZIP1, CBY1 and β-catenin form a complex which locates to basal body. This complex sequesters β-catenin in cytoplasm and β-catenin signaling is being withheld. When Dzip1 has a mutation, its protein stability is impaired and is not able to stabilize DZIP1-CBY1-β-catenin complex. β-catenin will be set free and enter nucleus to start downstream MMPs transcription which contributes to ECM digestion

Chapter 6 Materials and methods

Mouse husbandry and genotyping.

Dzip1 conditional mice and *Dzip1* knock in mice were genotyped and generated as previously described[128, 272]. *Cby1* mice were a kind gift from Dr. Ken-Ichi Takemaru. C57Bl6 mice were purchased from Charles river. Animals were kept in a 12-hour light-dark cycle with food and water *ad libitum*. Genotyping was performed by Transnetyx, Inc or inhouse with the KAPA Mouse Genotyping Kit (Kapabiosystems, #KK7301).

Immunohistochemistry (IHC) and fluorescence imaging.

Immunohistochemical and fluorescence stains were performed on 5 μm, paraffin-embedded sections from embryonic timepoints (E11.5, E13.5), fetal gestation (E17.5), neonatal (P0), and adult (6-month). Human mitral valve samples were processed and sectioned as previously described[181]. Sections were subjected to antigen unmasking (H-3300; Vector Laboratories, Burlingame, CA) and treated for 1 hour at room temperature with a blocking buffer of PBS (Sigma, St. Louis, MO) containing 1% BSA (Sigma, B4287-25G). Primary antibodies used were: mouse gamma tubulin (sigma, T6557,dilution 1:100) rabbit acetylated tubulin (cell signaling, 5335S,dilution 1:100), rabbit Arl13B(Protein tech, 17711-1-AP, dilution 1:500), activated β-catenin (Cell signaling, #9566S, 1:100), total β-catenin (cell signaling, #9581S, 1:100), MF20 (Developmental Studies Hybridoma Bank, 1:50),

PCAM-1 (Dianova, #DIA-310, 1:50), hyaluronan binding protein (HABP) (Calbiochem #385911, 1:100) and LEF1 (cell signaling, #2230S, 1:100). To determine the activated β-catenin distribution during valvulogenesis, we stained for β-catenin^{pS552}. Both Akt and PKA were shown to phosphorylate β-catenin at Ser552[268, 273]. Phosphorylation at Ser552 induces β-catenin accumulation in the nucleus and increases its transcriptional activity [268-270]. Specificity of these antibodies were validated as recognizing the appropriate epitopes in various model systems, including knockout animals and cell lines[181, 270, 274-277]. Primary antibodies were placed in blocking buffer overnight at 4°C. Following primary antibody incubations, specimens were washed five times in PBS and incubated at room temperature with Alexa Fluor goat α-rabbit 568 and goat α-mouse 488 (Invitrogen, Eugene, OR) diluted 1:100 in PBS. Nuclei were stained with Hoechst dye (1:10,000; Invitrogen) in PBS for 5 min prior to the final washes in PBS. All samples were cover-slipped using Dabco mounting medium (Sigma). Images of immunostained sections were captured with Zeiss Axioimager M2 and Leica TCS SP5 AOBS Confocal Microscope System (Leica Microsystems, Inc., 410 Eagleview Boulevard, Suite 107, Exton, PA 19341). Z-stacks were set by finding the highest and lowest depth with visible fluorescence and using the

system optimized setting to determine steps. Z-stacks were then compiled to form maximum projection images[129].N>3/timepoint or genotypes.

Yeast 2 Hybrid Screen

Y2H screens were performed by Hybrigenics Services (Paris, France; www.hybrigenics-services.com). The coding sequence of the full-length Homo sapiens DZIP1 (isoform 2) was PCR-amplified and cloned in frame with the LexA DNA binding domain (DBD) into plasmid pB27 as a C-terminal fusion to Gal4 (Gal4-bait fusion). The DZIP1-DBD bait protein was used to screen a human embryonic and adult cardiac library. A total of 274 prey fragments of the positive clones were amplified by PCR and sequenced at their 5’ and 3’ junctions.

Interaction confidence scoring

Predicted Biological Score (PBS) was attributed to each interaction as previously described[278]. The PBS score represents the probability of an interaction being non-specific which is primarily based on the comparison between the number of independent prey fragments found for an interaction and the chance of finding them at random (background noise). The value in the scores A to D varies between 0 and 1 (A < 1e-10 < B < 1e-5 < C < 1e-2.5 < D < 1). Several thresholds were arbitrarily defined in order to rank the results in the following scores:

A: Very high confidence in the interaction.

B: High confidence in the interaction.

C: Good confidence in the interaction.

D: Moderate confidence in the interaction.

E: Interactions involving highly connected (or relatively highly connected) prey domains, warning of non-specific interaction.

F: Experimentally proven technical artifacts.

Generation of Dzip1 expression constructs and TAT-fusion peptides

Control human DZIP1-Myc-DDK plasmid was purchased from Origene (clone ID: 198968). Truncated DZIP1 plasmids were sub-cloned with a HA tag sequence at the C terminus using pTARGET™ Mammalian Expression Vector System (Promega, Cat No: A1410). The Dzip1 mutation was incorporated through a QuickChange II XL Site-Directed Mutagenesis Kit (Agilent Technologies) based on the manufacturer's recommendations and had a HA-epitope tag at the C terminus. CBY1 plasmid with a HA-epitope tag at C terminus was purchased from Sino Biological (clone ID: BC016139). CBY1 plasmid with a Flag-epitope flag at the C terminus was a kind gift from Dr.Ken-Ichi Takemaru and described previously[258].All clones were sequenced through Genewiz before use. TAT-fusion peptides were synthesized by Genescript with biotin at C terminus and FAM at N terminus.

Cell culture

Human valvular cells were isolated and cultured in DMEM with 15% fetal calf serum and antibiotics (P/S, fungizone) as described previously[181]. Chicken valvular interstitial cells (cVICs) were isolated from anterior leaflet of chicken embryos at HH40 as described before[279]. cVICs were maintained in Medium 199 (M199, Invitrogen) containing 5% of chicken serum (bioworld),0.1% ITS (gibco,41400-045) and 1% antibiotics (P/S, fungizone). *Dzip1*$^{S14R/+}$ or wild type mouse embryonic fibroblast(MEFs) were derived according to the protocol published before[280] and were cultured in DMEM with 10% FBS and antibiotics (P/S, fungizone). For all experiments, these valvular interstitial cells were utilized prior to passage 5. Hek293T cells were maintained in DMEM with 10% fetal bovine serum and antibiotics (P/S, fungizone).

Primary cilia measurement

For measuring the cilia length in the *Cby1* control (*Cby1*$^{+/+}$) versus *Cby1*$^{+/-}$, values were plotted every 0.5 μm to assess cilia length distribution differences between the two genotypes at P0. We chose 3 slides from each animal, and imaged three pictures at different parts on anterior leaflets (tip, middle, root). 3 or 4/genotype were included. Cilia length measurements were performed using Z-stack images of anterior leaflet stained with acetylated

alpha tubulin/arl13b, gamma tubulin and counterstained with Hoechst. Z-stack images were then imported into Imaris software and measurements were taken from the base to the tip of the axoneme. All cilia in the field of view were measured. For control mitral leaflets, a total of n=1266 cilia lengths quantified. For Cby1+/-mitral leaflets a total of n=497 cilia lengths quantified[128]. Cell numbers from each image were counted blindly by two people. n=26 images were counted from wild type and n=25 images were counted from *Cby1*$^{+/-}$.

Co-IP and Western blotting

Hek 293T cells were seeded at 5X10^5 /well on 6-well plates one day before transfection. Cells were co-transfected with DZIP1 and CBY1 plasmids using FuGENE HD transfection Reagent (Promega, Cat No: E2311) for 72 hours and were lysed using ice-cold lysis buffer (25mM Tris HCL, 150mM Nacl, 1% NP-40,5% glycerol) with Halt protease and phosphatase Inhibitor cocktail(100x) being added before (Thermo Scientific, Cat NO:78440, dilution 1:500) followed by incubating on ice for 30 minutes with intermittent vortex. Preclearing of the cell lysates were done by adding 2.5 ul of IgG with the same species as primary antibody and 25ul of Pierce Protein A/G Agarose beads (Thermo Scientific, Cat NO:20421) into cell lysates containing 400ug protein and rotating for 2 hours at 4℃. 5ul of primary

antibody or IgG together with 50ul of Pierce Protein A/G Agarose beads were incubated with cell lysates at 4 ℃ overnight. Beads were collected and washed with 1ml of ice-cold lysis buffer for 5 times before SDS-PAGE. For peptide Co-IP, HEK293T or human valvular interstitial cell lysates were incubated with Pierce Streptavidin Magnetic Beads (Pierce, Cat NO:88816) and biotinylated peptide at 4 ℃ overnight. Collect and wash magnetic beads according manufacture's manual before SDS-PAGE. The primary antibodies used for Co-IP assays and Western blotting were as follows: mouse Flag M2 (Sigma,dilution 1:1,000), rabbit HA (Sigma,Cat NO:SAB4300603, dilution 1:1,000).rabbit CBY1(Protein tech, Cat NO: 12239-1-AP, dilution 1:1,000), rabbit β catenin(cell signaling, Cat NO: 9581, dilution 1:1,000). Horseradish peroxidase (HRP)-conjugated secondary antibodies were purchased from Sigma (dilution 1:10,000).

Computational Studies:

RaptorX Structure Alignment was used to align the protein structures of interest: P5 wild type (WT), P5 C585W mutant, P2 WT[281, 282]. RaptorX employs a statistical learning method to calculate the compatibility between a target sequence and a template structure [283]. Protein structures were prepared using PEP-FOLD 3: a publicly available software capable of de novo peptide tertiary structure prediction from amino acid sequences [284-286].

Protein structures were exported as PDB files and submitted for analysis by the RaptorX Structure Alignment Server. RaptorX calculates the structural similarity of two or more proteins by comparing the length of the core (Lali), root mean squared deviation (RMSD), and template modeling score (TM score). For multiple structure alignment (MSA), Lali is the length of core, which consists of all the fully aligned columns [281, 282]. The RMSD is calculated only on the core residues. The TM score is the measure of similarity between two or more protein structures with different tertiary structures. The TM Score ranges from 0-1.0: If TM score >0.6, there is a 90% chance that two proteins share a similar fold. When TM score <0.4, there is a 90% chance that two proteins have different folds.

Peptide treatment and reporter assay in cVICs

cVICs were seeded at $5X10^5$ /well on 6-well plates. The next day, cells were transfected with 1.6μg TopFlash (Addgene plasmid # 12456) or FopFlash (Addgene plasmid # 12457) and 0.4 μg b-galactosidase-encoding construct. Transfections were performed using FuGENE HD transfection Reagent (Promega, Cat No: E2311) and cells were incubated at 37°C for 24 hours. TAT-fusion peptide was added at 10 μM or 1 μM 24 hours post transfection. Cells were harvested the next day after two times of 1XPBS wash

and firefly luciferase activities were evaluated using the Luciferase Assay System (Promega, E1500).

Protein stability analysis

HEK293T cells were seeded at $5x10^5$ /well on 6-well plate. On the next day, cells were co-transfected with wild type DZIP1-Flag or DZIP1^{C604W}-Flag and CBY1-HA constructs using FuGENE HD transfection Reagent (Promega, Cat No: E2311). Cycloheximide were added 48 hours post transfection at concentration of 100ng/ml. Cells were lysed with RIPA buffer at 0/4/8/16/32 hours after cycloheximide treatment. *Dzip1*$^{S14/+}$ and wild type MEFs were seeded at $2X10^5$/well on 6-well plate and treated with cycloheximide at concentration of 100ng/ml the next day. Cell lysates were harvested using RIPA buffer at 0- and 48-hours post cycloheximide treatment. Immunoblotting was performed as described previously[181]. Primary antibody used for western blotting were as follows: mouse Flag M2 (Sigma), rabbit HA (Sigma, Cat NO: SAB4300603), rabbit CBY1(Protein tech, Cat NO: 12239-1-AP), rabbit DZIP1 (Protein tech, Cat NO: 13779-1-AP), mouse actin (Millipore, Cat No: MAB1501). HRP-conjugated secondary antibodies were purchased from Sigma.

Nuclear and Cytoplasmic extraction

Dzip1$^{S14R/+}$ and wild type MEFs from E13.5 embryos were plated at $2x10^5$ /well on 6-well plate. On the next day, cells were digested with trypsin and washed with 1x PBS twice and fragmentation was done following the instruction of NE-PER Nuclear and Cytoplasmic Extraction Reagents (Thermo, Cat NO:78835). Nuclear and cytoplasmic extractions were collected for Western Blotting. β-Catenin was normalized by total protein indicated by Ponceau S.

Human studies

All studies involving human research were approved by the Institutional Review Board Institut du Thorax, Nantes, France and all participants provided written informed consent.

Familial genetics and WES

Exome sequencing was performed on the proband (II.4). Exome capture was carried out using the SureSelect Human All Exon System using the manufacturer's protocol version 1.0 (Agilent Inc.) that is compatible with Illumina paired-end sequencing. Exome-enriched genomes were multiplexed by flow cell for 101-bp paired-end read sequencing according to the protocol for the HiSeq 2000 sequencer (version 1.7.0; Illumina) to allow a minimum coverage of 30Å~. Reads were aligned to the human reference genome (UCSC NCBI36/hg19) using the Burrows- Wheeler Aligner (version 0.5.9).

Quality control to determine sample and genotyping quality and to potentially remove poor SNPs and/or samples was performed as we have previously published[181]. Follow up Sanger sequencing was performed on the rest of the family to confirm phenotype-genotype correlation of the identified DZIP1 SNP.

Reference

1. Combs MD, Yutzey KE: **Heart valve development: regulatory networks in development and disease**. *Circ Res* 2009, **105**(5):408-421.
2. Anderson RH, Ho SY, Becker AE: **Anatomy of the human atrioventricular junctions revisited**. *Anat Rec* 2000, **260**(1):81-91.
3. Hinton RB, Jr., Lincoln J, Deutsch GH, Osinska H, Manning PB, Benson DW, Yutzey KE: **Extracellular matrix remodeling and organization in developing and diseased aortic valves**. *Circ Res* 2006, **98**(11):1431-1438.
4. Anderson RH: **Clinical anatomy of the aortic root**. *Heart* 2000, **84**(6):670-673.
5. Yacoub MH, Kilner PJ, Birks EJ, Misfeld M: **The aortic outflow and root: a tale of dynamism and crosstalk**. *Ann Thorac Surg* 1999, **68**(3 Suppl):S37-43.
6. Schoen FJ: **Evolving concepts of cardiac valve dynamics: the continuum of development, functional structure, pathobiology, and tissue engineering**. *Circulation* 2008, **118**(18):1864-1880.
7. Hinton RB, Yutzey KE: **Heart Valve Structure and Function in Development and Disease**. *Annual Review of Physiology* 2011, **73**(1):29-46.
8. Wight TN, Heinegård DK, Hascall VC: **Proteoglycans**. In: *Cell Biology of Extracellular Matrix: Second Edition.* Edited by Hay ED. Boston, MA: Springer US; 1991: 45-78.
9. Grande-Allen KJ, Griffin BP, Ratliff NB, Cosgrove DM, Vesely I: **Glycosaminoglycan profiles of myxomatous mitral leaflets and chordae parallel the severity of mechanical alterations**. *J Am Coll Cardiol* 2003, **42**(2):271-277.
10. Rabkin-Aikawa E, Mayer JE, Jr., Schoen FJ: **Heart valve regeneration**. *Adv Biochem Eng Biotechnol* 2005, **94**:141-179.
11. Rabkin-Aikawa E, Mayer JE, Jr., Schoen FJ: **e**. *Adv Biochem Eng Biotechnol* 2005, **94**:141-179.
12. Kunzelman KS, Cochran RP, Murphree SS, Ring WS, Verrier ED, Eberhart RC: **Differential collagen distribution in the mitral valve and its influence on biomechanical behaviour**. *J Heart Valve Dis* 1993, **2**(2):236-244.
13. Stephens EH, Chu C-K, Grande-Allen KJ: **Valve proteoglycan content and glycosaminoglycan fine structure are unique to microstructure, mechanical load and age: Relevance to an age-specific tissue-engineered heart valve**. *Acta Biomaterialia* 2008, **4**(5):1148-1160.

14. Lincoln J, Alfieri CM, Yutzey KE: **BMP and FGF regulatory pathways control cell lineage diversification of heart valve precursor cells**. *Developmental Biology* 2006, **292**(2):290-302.
15. Luna-Zurita L, Prados B, Grego-Bessa J, Luxán G, del Monte G, Benguría A, Adams RH, Pérez-Pomares JM, de la Pompa JL: **Integration of a Notch-dependent mesenchymal gene program and Bmp2-driven cell invasiveness regulates murine cardiac valve formation**. *J Clin Invest* 2010, **120**(10):3493-3507.
16. Niessen K, Fu Y, Chang L, Hoodless PA, McFadden D, Karsan A: **Slug is a direct Notch target required for initiation of cardiac cushion cellularization**. *J Cell Biol* 2008, **182**(2):315-325.
17. Dor Y, Camenisch TD, Itin A, Fishman GI, McDonald JA, Carmeliet P, Keshet E: **A novel role for VEGF in endocardial cushion formation and its potential contribution to congenital heart defects**. *Development* 2001, **128**(9):1531-1538.
18. von Gise A, Pu WT: **Endocardial and epicardial epithelial to mesenchymal transitions in heart development and disease**. *Circ Res* 2012, **110**(12):1628-1645.
19. Liu AC, Joag VR, Gotlieb AI: **The Emerging Role of Valve Interstitial Cell Phenotypes in Regulating Heart Valve Pathobiology**. *The American Journal of Pathology* 2007, **171**(5):1407-1418.
20. Blevins TL, Peterson SB, Lee EL, Bailey AM, Frederick JD, Huynh TN, Gupta V, Grande-Allen KJ: **Mitral Valvular Interstitial Cells Demonstrate Regional, Adhesional, and Synthetic Heterogeneity**. *Cells Tissues Organs* 2008, **187**(2):113-122.
21. Barth PJ, Köster H, Moosdorf R: **CD34+ fibrocytes in normal mitral valves and myxomatous mitral valve degeneration**. *Pathol Res Pract* 2005, **201**(4):301-304.
22. Lester W, Rosenthal A, Granton B, Gotlieb AI: **Porcine mitral valve interstitial cells in culture**. *Lab Invest* 1988, **59**(5):710-719.
23. Armstrong EJ, Bischoff J: **Heart valve development: endothelial cell signaling and differentiation**. *Circ Res* 2004, **95**(5):459-470.
24. Runyan RB, Markwald RR: **Invasion of mesenchyme into three-dimensional collagen gels: a regional and temporal analysis of interaction in embryonic heart tissue**. *Dev Biol* 1983, **95**(1):108-114.
25. Krug EL, Runyan RB, Markwald RR: **Protein extracts from early embryonic hearts initiate cardiac endothelial cytodifferentiation**. *Dev Biol* 1985, **112**(2):414-426.

26. Markwald RR, Fitzharris TP, Manasek FJ: **Structural development of endocardial cushions**. *Am J Anat* 1977, **148**(1):85-119.
27. Markwald RR, Smith WN: **Distribution of mucosubstances in the developing rat heart**. *J Histochem Cytochem* 1972, **20**(11):896-907.
28. Person AD, Klewer SE, Runyan RB: **Cell biology of cardiac cushion development**. *Int Rev Cytol* 2005, **243**:287-335.
29. Markwald RR, Fitzharris TP, Bolender DL, Bernanke DH: **Sturctural analysis of cell:matrix association during the morphogenesis of atrioventricular cushion tissue**. *Dev Biol* 1979, **69**(2):634-654.
30. Bolender DL, Markwald RR: **Epithelial-mesenchymal transformation in chick atrioventricular cushion morphogenesis**. *Scan Electron Microsc* 1979(3):313-321.
31. Eisenberg LM, Markwald RR: **Molecular regulation of atrioventricular valvuloseptal morphogenesis**. *Circ Res* 1995, **77**(1):1-6.
32. de Vlaming A, Sauls K, Hajdu Z, Visconti RP, Mehesz AN, Levine RA, Slaugenhaupt SA, Hagege A, Chester AH, Markwald RR *et al*: **Atrioventricular valve development: new perspectives on an old theme**. *Differentiation; research in biological diversity* 2012, **84**(1):103-116.
33. Person AD, Klewer SE, Runyan RB: **Cell Biology of Cardiac Cushion Development**. In: *International Review of Cytology*. vol. 243: Academic Press; 2005: 287-335.
34. Wessels A, Sedmera D: **Developmental anatomy of the heart: a tale of mice and man**. *Physiol Genomics* 2003, **15**(3):165-176.
35. de Lange FJ, Moorman AF, Anderson RH, Manner J, Soufan AT, de Gier-de Vries C, Schneider MD, Webb S, van den Hoff MJ, Christoffels VM: **Lineage and morphogenetic analysis of the cardiac valves**. *Circ Res* 2004, **95**(6):645-654.
36. Schroeder JA, Jackson LF, Lee DC, Camenisch TD: **Form and function of developing heart valves: coordination by extracellular matrix and growth factor signaling**. *J Mol Med (Berl)* 2003, **81**(7):392-403.
37. Restivo A, Piacentini G, Placidi S, Saffirio C, Marino B: **Cardiac outflow tract: a review of some embryogenetic aspects of the conotruncal region of the heart**. *Anat Rec A Discov Mol Cell Evol Biol* 2006, **288**(9):936-943.
38. Lin CJ, Lin CY, Chen CH, Zhou B, Chang CP: **Partitioning the heart: mechanisms of cardiac septation and valve development**. *Development* 2012, **139**(18):3277-3299.
39. Moorman AF, Christoffels VM: **Cardiac chamber formation: development, genes, and evolution**. *Physiol Rev* 2003, **83**(4):1223-1267.

40. Kirby ML, Gale TF, Stewart DE: **Neural crest cells contribute to normal aorticopulmonary septation**. *Science* 1983, **220**(4601):1059-1061.
41. Oyama MA, Elliott C, Loughran KA, Kossar AP, Castillero E, Levy RJ, Ferrari G: **Comparative pathology of human and canine myxomatous mitral valve degeneration: 5HT and TGF-beta mechanisms**. *Cardiovasc Pathol* 2020, **46**:107196.
42. Hurlstone AF, Haramis AP, Wienholds E, Begthel H, Korving J, Van Eeden F, Cuppen E, Zivkovic D, Plasterk RH, Clevers H: **The Wnt/beta-catenin pathway regulates cardiac valve formation**. *Nature* 2003, **425**(6958):633-637.
43. Conway SJ, Doetschman T, Azhar M: **The inter-relationship of periostin, TGF beta, and BMP in heart valve development and valvular heart diseases**. *ScientificWorldJournal* 2011, **11**:1509-1524.
44. Ahuja N, Ostwald P, Bark D, Garrity D: **Biomechanical Cues Direct Valvulogenesis**. *J Cardiovasc Dev Dis* 2020, **7**(2).
45. Cadigan KM, Nusse R: **Wnt signaling: a common theme in animal development**. *Genes Dev* 1997, **11**(24):3286-3305.
46. Zou Y, Salinas P: **Introduction: Wnt signaling mechanisms in development and disease**. *Dev Neurobiol* 2014, **74**(8):757-758.
47. Wodarz A, Nusse R: **Mechanisms of Wnt signaling in development**. *Annu Rev Cell Dev Biol* 1998, **14**:59-88.
48. Wang Y, Li YP, Paulson C, Shao JZ, Zhang X, Wu M, Chen W: **Wnt and the Wnt signaling pathway in bone development and disease**. *Front Biosci (Landmark Ed)* 2014, **19**:379-407.
49. Pinto D, Clevers H: **Wnt, stem cells and cancer in the intestine**. *Biol Cell* 2005, **97**(3):185-196.
50. Lowry WE, Blanpain C, Nowak JA, Guasch G, Lewis L, Fuchs E: **Defining the impact of beta-catenin/Tcf transactivation on epithelial stem cells**. *Genes Dev* 2005, **19**(13):1596-1611.
51. Reya T, Duncan AW, Ailles L, Domen J, Scherer DC, Willert K, Hintz L, Nusse R, Weissman IL: **A role for Wnt signalling in self-renewal of haematopoietic stem cells**. *Nature* 2003, **423**(6938):409-414.
52. Person AD, Garriock RJ, Krieg PA, Runyan RB, Klewer SE: **Frzb modulates Wnt-9a-mediated beta-catenin signaling during avian atrioventricular cardiac cushion development**. *Dev Biol* 2005, **278**(1):35-48.
53. van Amerongen R, Nusse R: **Towards an integrated view of Wnt signaling in development**. *Development (Cambridge, England)* 2009, **136**(19):3205-3214.

54. Liebner S, Cattelino A, Gallini R, Rudini N, Iurlaro M, Piccolo S, Dejana E: **Beta-catenin is required for endothelial-mesenchymal transformation during heart cushion development in the mouse**. *The Journal of cell biology* 2004, **166**(3):359-367.
55. Gottardi CJ, Gumbiner BM: **Distinct molecular forms of β-catenin are targeted to adhesive or transcriptional complexes**. *Journal of Cell Biology* 2004, **167**(2):339-349.
56. Bosada FM, Devasthali V, Jones KA, Stankunas K: **Wnt/beta-catenin signaling enables developmental transitions during valvulogenesis**. *Development* 2016, **143**(6):1041-1054.
57. Hulin A, Moore V, James JM, Yutzey KE: **Loss of Axin2 results in impaired heart valve maturation and subsequent myxomatous valve disease**. *Cardiovasc Res* 2017, **113**(1):40-51.
58. Kim KA, Wagle M, Tran K, Zhan X, Dixon MA, Liu S, Gros D, Korver W, Yonkovich S, Tomasevic N *et al*: **R-Spondin family members regulate the Wnt pathway by a common mechanism**. *Mol Biol Cell* 2008, **19**(6):2588-2596.
59. Qiang YW, Barlogie B, Rudikoff S, Shaughnessy JD, Jr.: **Dkk1-induced inhibition of Wnt signaling in osteoblast differentiation is an underlying mechanism of bone loss in multiple myeloma**. *Bone* 2008, **42**(4):669-680.
60. Thalji NM, Hagler MA, Zhang H, Casaclang-Verzosa G, Nair AA, Suri RM, Miller JD: **Nonbiased Molecular Screening Identifies Novel Molecular Regulators of Fibrogenic and Proliferative Signaling in Myxomatous Mitral Valve Disease**. *Circ Cardiovasc Genet* 2015, **8**(3):516-528.
61. Akhmetshina A, Palumbo K, Dees C, Bergmann C, Venalis P, Zerr P, Horn A, Kireva T, Beyer C, Zwerina J *et al*: **Activation of canonical Wnt signalling is required for TGF-beta-mediated fibrosis**. *Nat Commun* 2012, **3**:735.
62. Wang Y: **Wnt/Planar cell polarity signaling: a new paradigm for cancer therapy**. *Mol Cancer Ther* 2009, **8**(8):2103-2109.
63. Henderson DJ, Conway SJ, Greene ND, Gerrelli D, Murdoch JN, Anderson RH, Copp AJ: **Cardiovascular defects associated with abnormalities in midline development in the Loop-tail mouse mutant**. *Circ Res* 2001, **89**(1):6-12.
64. Hamblet NS, Lijam N, Ruiz-Lozano P, Wang J, Yang Y, Luo Z, Mei L, Chien KR, Sussman DJ, Wynshaw-Boris A: **Dishevelled 2 is essential for**

cardiac outflow tract development, somite segmentation and neural tube closure. *Development* 2002, **129**(24):5827-5838.
65. Wu G, Ge J, Huang X, Hua Y, Mu D: **Planar cell polarity signaling pathway in congenital heart diseases**. *J Biomed Biotechnol* 2011, **2011**:589414.
66. Chakraborty S, Cheek J, Sakthivel B, Aronow BJ, Yutzey KE: **Shared gene expression profiles in developing heart valves and osteoblast progenitor cells**. *Physiol Genomics* 2008, **35**(1):75-85.
67. Shelton EL, Yutzey KE: **Tbx20 regulation of endocardial cushion cell proliferation and extracellular matrix gene expression**. *Dev Biol* 2007, **302**(2):376-388.
68. Shelton EL, Yutzey KE: **Twist1 function in endocardial cushion cell proliferation, migration, and differentiation during heart valve development**. *Dev Biol* 2008, **317**(1):282-295.
69. Klewer SE, Krob SL, Kolker SJ, Kitten GT: **Expression of type VI collagen in the developing mouse heart**. *Dev Dyn* 1998, **211**(3):248-255.
70. Aikawa E, Whittaker P, Farber M, Mendelson K, Padera RF, Aikawa M, Schoen FJ: **Human semilunar cardiac valve remodeling by activated cells from fetus to adult: implications for postnatal adaptation, pathology, and tissue engineering**. *Circulation* 2006, **113**(10):1344-1352.
71. Chakraborty S, Combs MD, Yutzey KE: **Transcriptional regulation of heart valve progenitor cells**. *Pediatr Cardiol* 2010, **31**(3):414-421.
72. Hurle JM, Kitten GT, Sakai LY, Volpin D, Solursh M: **Elastic extracellular matrix of the embryonic chick heart: an immunohistological study using laser confocal microscopy**. *Dev Dyn* 1994, **200**(4):321-332.
73. Lincoln J, Alfieri CM, Yutzey KE: **BMP and FGF regulatory pathways control cell lineage diversification of heart valve precursor cells**. *Dev Biol* 2006, **292**(2):292-302.
74. Montero JA, Giron B, Arrechedera H, Cheng YC, Scotting P, Chimal-Monroy J, Garcia-Porrero JA, Hurle JM: **Expression of Sox8, Sox9 and Sox10 in the developing valves and autonomic nerves of the embryonic heart**. *Mech Dev* 2002, **118**(1-2):199-202.
75. Schoen FJ, Gotlieb AI: **Heart valve health, disease, replacement, and repair: a 25-year cardiovascular pathology perspective**. *Cardiovasc Pathol* 2016, **25**(4):341-352.
76. Barth PJ, Koster H, Moosdorf R: **CD34+ fibrocytes in normal mitral valves and myxomatous mitral valve degeneration**. *Pathol Res Pract* 2005, **201**(4):301-304.

77. Dreger SA, Taylor PM, Allen SP, Yacoub MH: **Profile and localization of matrix metalloproteinases (MMPs) and their tissue inhibitors (TIMPs) in human heart valves**. *J Heart Valve Dis* 2002, **11**(6):875-880; discussion 880.
78. Rabkin E, Aikawa M, Stone JR, Fukumoto Y, Libby P, Schoen FJ: **Activated interstitial myofibroblasts express catabolic enzymes and mediate matrix remodeling in myxomatous heart valves**. *Circulation* 2001, **104**(21):2525-2532.
79. Anvarian Z, Mykytyn K, Mukhopadhyay S, Pedersen LB, Christensen ST: **Cellular signalling by primary cilia in development, organ function and disease**. *Nature reviews Nephrology* 2019, **15**(4):199-219.
80. May-Simera HL, Kelley MW: **Cilia, Wnt signaling, and the cytoskeleton**. *Cilia* 2012, **1**(1):7.
81. Goetz SC, Anderson KV: **The primary cilium: a signalling centre during vertebrate development**. *Nat Rev Genet* 2010, **11**(5):331-344.
82. Lidow MS, Menco BP: **Observations on axonemes and membranes of olfactory and respiratory cilia in frogs and rats using tannic acid-supplemented fixation and photographic rotation**. *J Ultrastruct Res* 1984, **86**(1):18-30.
83. Pigino G, Ishikawa T: **Axonemal radial spokes: 3D structure, function and assembly**. *Bioarchitecture* 2012, **2**(2):50-58.
84. Satir P, Christensen ST: **Overview of structure and function of mammalian cilia**. *Annu Rev Physiol* 2007, **69**:377-400.
85. Pedersen LB, Veland IR, Schroder JM, Christensen ST: **Assembly of primary cilia**. *Dev Dyn* 2008, **237**(8):1993-2006.
86. Blacque OE, Li C, Inglis PN, Esmail MA, Ou G, Mah AK, Baillie DL, Scholey JM, Leroux MR: **The WD repeat-containing protein IFTA-1 is required for retrograde intraflagellar transport**. *Molecular biology of the cell* 2006, **17**(12):5053-5062.
87. Cole DG: **The intraflagellar transport machinery of Chlamydomonas reinhardtii**. *Traffic* 2003, **4**(7):435-442.
88. Iomini C, Babaev-Khaimov V, Sassaroli M, Piperno G: **Protein particles in Chlamydomonas flagella undergo a transport cycle consisting of four phases**. *J Cell Biol* 2001, **153**(1):13-24.
89. Tran PV, Haycraft CJ, Besschetnova TY, Turbe-Doan A, Stottmann RW, Herron BJ, Chesebro AL, Qiu H, Scherz PJ, Shah JV *et al*: **THM1 negatively modulates mouse sonic hedgehog signal transduction and affects retrograde intraflagellar transport in cilia**. *Nat Genet* 2008, **40**(4):403-410.

90. Marshall WF: **Chapter 1 Basal Bodies: Platforms for Building Cilia**. In: *Current Topics in Developmental Biology*. vol. 85: Academic Press; 2008: 1-22.
91. Nakazawa Y, Hiraki M, Kamiya R, Hirono M: **SAS-6 is a cartwheel protein that establishes the 9-fold symmetry of the centriole**. *Curr Biol* 2007, **17**(24):2169-2174.
92. Hiraki M, Nakazawa Y, Kamiya R, Hirono M: **Bld10p constitutes the cartwheel-spoke tip and stabilizes the 9-fold symmetry of the centriole**. *Curr Biol* 2007, **17**(20):1778-1783.
93. Ringo DL: **Flagellar motion and fine structure of the flagellar apparatus in Chlamydomonas**. *J Cell Biol* 1967, **33**(3):543-571.
94. Marshall WF: **What is the function of centrioles?** *J Cell Biochem* 2007, **100**(4):916-922.
95. Deane JA, Cole DG, Seeley ES, Diener DR, Rosenbaum JL: **Localization of intraflagellar transport protein IFT52 identifies basal body transitional fibers as the docking site for IFT particles**. *Curr Biol* 2001, **11**(20):1586-1590.
96. O'Toole ET, Giddings TH, Jr., Dutcher SK: **Understanding microtubule organizing centers by comparing mutant and wild-type structures with electron tomography**. *Methods Cell Biol* 2007, **79**:125-143.
97. Gilula NB, Satir P: **The ciliary necklace. A ciliary membrane specialization**. *J Cell Biol* 1972, **53**(2):494-509.
98. Williams CL, Li C, Kida K, Inglis PN, Mohan S, Semenec L, Bialas NJ, Stupay RM, Chen N, Blacque OE *et al*: **MKS and NPHP modules cooperate to establish basal body/transition zone membrane associations and ciliary gate function during ciliogenesis**. *J Cell Biol* 2011, **192**(6):1023-1041.
99. Craige B, Tsao CC, Diener DR, Hou Y, Lechtreck KF, Rosenbaum JL, Witman GB: **CEP290 tethers flagellar transition zone microtubules to the membrane and regulates flagellar protein content**. *J Cell Biol* 2010, **190**(5):927-940.
100. Hu Q, Milenkovic L, Jin H, Scott MP, Nachury MV, Spiliotis ET, Nelson WJ: **A septin diffusion barrier at the base of the primary cilium maintains ciliary membrane protein distribution**. *Science* 2010, **329**(5990):436-439.
101. Graser S, Stierhof YD, Lavoie SB, Gassner OS, Lamla S, Le Clech M, Nigg EA: **Cep164, a novel centriole appendage protein required for primary cilium formation**. *J Cell Biol* 2007, **179**(2):321-330.

102. Ishikawa H, Kubo A, Tsukita S, Tsukita S: **Odf2-deficient mother centrioles lack distal/subdistal appendages and the ability to generate primary cilia**. *Nat Cell Biol* 2005, **7**(5):517-524.
103. Nonaka S, Tanaka Y, Okada Y, Takeda S, Harada A, Kanai Y, Kido M, Hirokawa N: **Randomization of left-right asymmetry due to loss of nodal cilia generating leftward flow of extraembryonic fluid in mice lacking KIF3B motor protein**. *Cell* 1998, **95**(6):829-837.
104. Whitsett JA: **Airway Epithelial Differentiation and Mucociliary Clearance**. *Ann Am Thorac Soc* 2018, **15**(Suppl 3):S143-S148.
105. Ibanez-Tallon I, Pagenstecher A, Fliegauf M, Olbrich H, Kispert A, Ketelsen UP, North A, Heintz N, Omran H: **Dysfunction of axonemal dynein heavy chain Mdnah5 inhibits ependymal flow and reveals a novel mechanism for hydrocephalus formation**. *Hum Mol Genet* 2004, **13**(18):2133-2141.
106. Nishimura Y, Kasahara K, Shiromizu T, Watanabe M, Inagaki M: **Primary Cilia as Signaling Hubs in Health and Disease**. *Adv Sci (Weinh)* 2019, **6**(1):1801138.
107. Boukhalfa A, Miceli C, Ávalos Y, Morel E, Dupont N: **Interplay between primary cilia, ubiquitin-proteasome system and autophagy**. *Biochimie* 2019, **166**:286-292.
108. Cassioli C, Baldari CT: **A Ciliary View of the Immunological Synapse**. *Cells* 2019, **8**(8).
109. Gigante ED, Caspary T: **Signaling in the primary cilium through the lens of the Hedgehog pathway**. *Wiley Interdiscip Rev Dev Biol* 2020, **9**(6):e377.
110. Hor CH, Goh EL: **Small GTPases in hedgehog signalling: emerging insights into the disease mechanisms of Rab23-mediated and Arl13b-mediated ciliopathies**. *Curr Opin Genet Dev* 2019, **56**:61-68.
111. Lodh S: **Primary Cilium, An Unsung Hero in Maintaining Functional β-cell Population**. *Yale J Biol Med* 2019, **92**(3):471-480.
112. Ma M: **Cilia and polycystic kidney disease**. *Semin Cell Dev Biol* 2020.
113. Ma N, Zhou J: **Functions of Endothelial Cilia in the Regulation of Vascular Barriers**. *Front Cell Dev Biol* 2020, **8**:626.
114. McConnachie DJ, Stow JL, Mallett AJ: **Ciliopathies and the Kidney: A Review**. *Am J Kidney Dis* 2020.
115. Peixoto E, Richard S, Pant K, Biswas A, Gradilone SA: **The primary cilium: Its role as a tumor suppressor organelle**. *Biochem Pharmacol* 2020, **175**:113906.

116. R RF, Fukui H, Chow R, Vilfan A, Vermot J: **The cilium as a force sensor-myth versus reality**. *J Cell Sci* 2019, **132**(14).
117. Saternos H, Ley S, AbouAlaiwi W: **Primary Cilia and Calcium Signaling Interactions**. *Int J Mol Sci* 2020, **21**(19).
118. Satir P, Satir BH: **The conserved ancestral signaling pathway from cilium to nucleus**. *J Cell Sci* 2019, **132**(15).
119. Suciu SK, Caspary T: **Cilia, neural development and disease**. *Semin Cell Dev Biol* 2020.
120. Tao F, Jiang T, Tao H, Cao H, Xiang W: **Primary cilia: Versatile regulator in cartilage development**. *Cell Prolif* 2020, **53**(3):e12765.
121. Teves ME, Strauss JF, 3rd, Sapao P, Shi B, Varga J: **The Primary Cilium: Emerging Role as a Key Player in Fibrosis**. *Curr Rheumatol Rep* 2019, **21**(6):29.
122. Thomas S, Boutaud L, Reilly ML, Benmerah A: **Cilia in hereditary cerebral anomalies**. *Biol Cell* 2019, **111**(9):217-231.
123. Verschuren EHJ, Castenmiller C, Peters DJM, Arjona FJ, Bindels RJM, Hoenderop JGJ: **Sensing of tubular flow and renal electrolyte transport**. *Nat Rev Nephrol* 2020, **16**(6):337-351.
124. Rash JE, Shay JW, Biesele JJ: **Cilia in cardiac differentiation**. *J Ultrastruct Res* 1969, **29**(5):470-484.
125. Myklebust R, Engedal H, Saetersdal TS, Ulstein M: **Primary 9 + 0 cilia in the embryonic and the adult human heart**. *Anat Embryol (Berl)* 1977, **151**(2):127-139.
126. Slough J, Cooney L, Brueckner M: **Monocilia in the embryonic mouse heart suggest a direct role for cilia in cardiac morphogenesis**. *Developmental dynamics : an official publication of the American Association of Anatomists* 2008, **237**(9):2304-2314.
127. Willaredt MA, Gorgas K, Gardner HA, Tucker KL: **Multiple essential roles for primary cilia in heart development**. *Cilia* 2012, **1**(1):23.
128. Toomer KA, Yu M, Fulmer D, Guo L, Moore KS, Moore R, Drayton KD, Glover J, Peterson N, Ramos-Ortiz S *et al*: **Primary cilia defects causing mitral valve prolapse**. *Science translational medicine* 2019, **11**(493).
129. Toomer KA, Fulmer D, Guo L, Drohan A, Peterson N, Swanson P, Brooks B, Mukherjee R, Body S, Lipschutz JH *et al*: **A role for primary cilia in aortic valve development and disease**. *Dev Dyn* 2017, **246**(8):625-634.
130. Iomini C, Tejada K, Mo W, Vaananen H, Piperno G: **Primary cilia of human endothelial cells disassemble under laminar shear stress**. *The Journal of cell biology* 2004, **164**(6):811-817.

131. Van der Heiden K, Groenendijk BC, Hierck BP, Hogers B, Koerten HK, Mommaas AM, Gittenberger-de Groot AC, Poelmann RE: **Monocilia on chicken embryonic endocardium in low shear stress areas**. *Developmental dynamics : an official publication of the American Association of Anatomists* 2006, **235**(1):19-28.
132. Groenendijk BC, Hierck BP, Gittenberger-De Groot AC, Poelmann RE: **Development-related changes in the expression of shear stress responsive genes KLF-2, ET-1, and NOS-3 in the developing cardiovascular system of chicken embryos**. *Developmental dynamics : an official publication of the American Association of Anatomists* 2004, **230**(1):57-68.
133. Egorova AD, van der Heiden K, Poelmann RE, Hierck BP: **Primary cilia as biomechanical sensors in regulating endothelial function**. *Differentiation; research in biological diversity* 2012, **83**(2):S56-61.
134. Davies PF, Barbee KA, Volin MV, Robotewskyj A, Chen J, Joseph L, Griem ML, Wernick MN, Jacobs E, Polacek DC *et al*: **Spatial relationships in early signaling events of flow-mediated endothelial mechanotransduction**. *Annu Rev Physiol* 1997, **59**:527-549.
135. Niggemann B, Muller A, Nolte A, Schnoy N, Wahn U: **Abnormal length of cilia--a cause of primary ciliary dyskinesia--a case report**. *Eur J Pediatr* 1992, **151**(1):73-75.
136. Yuan S, Li J, Diener DR, Choma MA, Rosenbaum JL, Sun Z: **Target-of-rapamycin complex 1 (Torc1) signaling modulates cilia size and function through protein synthesis regulation**. *Proceedings of the National Academy of Sciences of the United States of America* 2012, **109**(6):2021-2026.
137. Broekhuis JR, Leong WY, Jansen G: **Regulation of cilium length and intraflagellar transport**. *Int Rev Cell Mol Biol* 2013, **303**:101-138.
138. Clement CA, Kristensen SG, Mollgard K, Pazour GJ, Yoder BK, Larsen LA, Christensen ST: **The primary cilium coordinates early cardiogenesis and hedgehog signaling in cardiomyocyte differentiation**. *Journal of cell science* 2009, **122**(Pt 17):3070-3082.
139. Otto EA, Schermer B, Obara T, O'Toole JF, Hiller KS, Mueller AM, Ruf RG, Hoefele J, Beekmann F, Landau D *et al*: **Mutations in INVS encoding inversin cause nephronophthisis type 2, linking renal cystic disease to the function of primary cilia and left-right axis determination**. *Nat Genet* 2003, **34**(4):413-420.
140. Simons M, Gloy J, Ganner A, Bullerkotte A, Bashkurov M, Kronig C, Schermer B, Benzing T, Cabello OA, Jenny A *et al*: **Inversin, the gene**

product mutated in nephronophthisis type II, functions as a molecular switch between Wnt signaling pathways. *Nat Genet* 2005, **37**(5):537-543.
141. Watanabe D, Saijoh Y, Nonaka S, Sasaki G, Ikawa Y, Yokoyama T, Hamada H: **The left-right determinant Inversin is a component of node monocilia and other 9+0 cilia**. *Development* 2003, **130**(9):1725-1734.
142. Ferrante MI, Zullo A, Barra A, Bimonte S, Messaddeq N, Studer M, Dolle P, Franco B: **Oral-facial-digital type I protein is required for primary cilia formation and left-right axis specification**. *Nat Genet* 2006, **38**(1):112-117.
143. Corbit KC, Shyer AE, Dowdle WE, Gaulden J, Singla V, Chen MH, Chuang PT, Reiter JF: **Kif3a constrains beta-catenin-dependent Wnt signalling through dual ciliary and non-ciliary mechanisms**. *Nat Cell Biol* 2008, **10**(1):70-76.
144. Lancaster MA, Louie CM, Silhavy JL, Sintasath L, Decambre M, Nigam SK, Willert K, Gleeson JG: **Impaired Wnt-beta-catenin signaling disrupts adult renal homeostasis and leads to cystic kidney ciliopathy**. *Nat Med* 2009, **15**(9):1046-1054.
145. Ferland RJ, Eyaid W, Collura RV, Tully LD, Hill RS, Al-Nouri D, Al-Rumayyan A, Topcu M, Gascon G, Bodell A *et al*: **Abnormal cerebellar development and axonal decussation due to mutations in AHI1 in Joubert syndrome**. *Nat Genet* 2004, **36**(9):1008-1013.
146. Huang P, Schier AF: **Dampened Hedgehog signaling but normal Wnt signaling in zebrafish without cilia**. *Development* 2009, **136**(18):3089-3098.
147. Ocbina PJ, Tuson M, Anderson KV: **Primary cilia are not required for normal canonical Wnt signaling in the mouse embryo**. *PLoS One* 2009, **4**(8):e6839.
148. Wallingford JB, Mitchell B: **Strange as it may seem: the many links between Wnt signaling, planar cell polarity, and cilia**. *Genes Dev* 2011, **25**(3):201-213.
149. Henderson DJ, Phillips HM, Chaudhry B: **Vang-like 2 and noncanonical Wnt signaling in outflow tract development**. *Trends Cardiovasc Med* 2006, **16**(2):38-45.
150. Follit JA, San Agustin JT, Xu F, Jonassen JA, Samtani R, Lo CW, Pazour GJ: **The Golgin GMAP210/TRIP11 anchors IFT20 to the Golgi complex**. *PLoS Genet* 2008, **4**(12):e1000315.
151. Mitchell B, Stubbs JL, Huisman F, Taborek P, Yu C, Kintner C: **The PCP pathway instructs the planar orientation of ciliated cells in the Xenopus larval skin**. *Curr Biol* 2009, **19**(11):924-929.

152. Antic D, Stubbs JL, Suyama K, Kintner C, Scott MP, Axelrod JD: **Planar cell polarity enables posterior localization of nodal cilia and left-right axis determination during mouse and Xenopus embryogenesis**. *PLoS One* 2010, **5**(2):e8999.
153. Borovina A, Superina S, Voskas D, Ciruna B: **Vangl2 directs the posterior tilting and asymmetric localization of motile primary cilia**. *Nat Cell Biol* 2010, **12**(4):407-412.
154. Takemaru K, Yamaguchi S, Lee YS, Zhang Y, Carthew RW, Moon RT: **Chibby, a nuclear beta-catenin-associated antagonist of the Wnt/Wingless pathway**. *Nature* 2003, **422**(6934):905-909.
155. Van Mieghem NM, Piazza N, Anderson RH, Tzikas A, Nieman K, De Laat LE, McGhie JS, Geleijnse ML, Feldman T, Serruys PW *et al*: **Anatomy of the mitral valvular complex and its implications for transcatheter interventions for mitral regurgitation**. *J Am Coll Cardiol* 2010, **56**(8):617-626.
156. Kalyanasundaram A, Qureshi A, Nassef LA, Shirani J: **Functional anatomy of normal mitral valve-left ventricular complex by real-time, three-dimensional echocardiography**. *J Heart Valve Dis* 2010, **19**(1):28-34.
157. Anwar AM, Soliman OI, ten Cate FJ, Nemes A, McGhie JS, Krenning BJ, van Geuns RJ, Galema TW, Geleijnse ML: **True mitral annulus diameter is underestimated by two-dimensional echocardiography as evidenced by real-time three-dimensional echocardiography and magnetic resonance imaging**. *Int J Cardiovasc Imaging* 2007, **23**(5):541-547.
158. Muresian H: **The clinical anatomy of the mitral valve**. *Clin Anat* 2009, **22**(1):85-98.
159. Webb RH, Grant C, Harnden A: **Acute rheumatic fever**. *BMJ* 2015, **351**:h3443.
160. Iung B: **Mitral stenosis still a concern in heart valve diseases**. *Arch Cardiovasc Dis* 2008, **101**(10):597-599.
161. Seguela PE, Houyel L, Acar P: **Congenital malformations of the mitral valve**. *Arch Cardiovasc Dis* 2011, **104**(8-9):465-479.
162. Neto FL, Marques LC, Aiello VD: **Myxomatous degeneration of the mitral valve**. *Autops Case Rep* 2018, **8**(4):e2018058.
163. Harb SC, Griffin BP: **Mitral Valve Disease: a Comprehensive Review**. *Curr Cardiol Rep* 2017, **19**(8):73.
164. Enriquez-Sarano M, Akins CW, Vahanian A: **Mitral regurgitation**. *Lancet* 2009, **373**(9672):1382-1394.

165. Kolibash AJ, Jr., Kilman JW, Bush CA, Ryan JM, Fontana ME, Wooley CF: **Evidence for progression from mild to severe mitral regurgitation in mitral valve prolapse**. *Am J Cardiol* 1986, **58**(9):762-767.
166. Freed LA, Levy D, Levine RA, Larson MG, Evans JC, Fuller DL, Lehman B, Benjamin EJ: **Prevalence and clinical outcome of mitral-valve prolapse**. *N Engl J Med* 1999, **341**(1):1-7.
167. Baddour LM, Bisno AL: **Mitral valve prolapse: multifactorial etiologies and variable prognosis**. *Am Heart J* 1986, **112**(6):1359-1362.
168. Dietz HC, Cutting GR, Pyeritz RE, Maslen CL, Sakai LY, Corson GM, Puffenberger EG, Hamosh A, Nanthakumar EJ, Curristin SM *et al*: **Marfan syndrome caused by a recurrent de novo missense mutation in the fibrillin gene**. *Nature* 1991, **352**(6333):337-339.
169. Collod G, Chu ML, Sasaki T, Coulon M, Timpl R, Renkart L, Weissenbach J, Jondeau G, Bourdarias JP, Junien C *et al*: **Fibulin-2: genetic mapping and exclusion as a candidate gene in Marfan syndrome type 2**. *Eur J Hum Genet* 1996, **4**(5):292-295.
170. Maslen CL, Corson GM, Maddox BK, Glanville RW, Sakai LY: **Partial sequence of a candidate gene for the Marfan syndrome**. *Nature* 1991, **352**(6333):334-337.
171. Teixeira LV, Lezirovitz K, Pereira LV, Perez AB: **Candidate gene linkage analysis indicates genetic heterogeneity in Marfan syndrome**. *Braz J Med Biol Res* 2011, **44**(8):793-800.
172. Neptune ER, Frischmeyer PA, Arking DE, Myers L, Bunton TE, Gayraud B, Ramirez F, Sakai LY, Dietz HC: **Dysregulation of TGF-beta activation contributes to pathogenesis in Marfan syndrome**. *Nat Genet* 2003, **33**(3):407-411.
173. Ng CM, Cheng A, Myers LA, Martinez-Murillo F, Jie C, Bedja D, Gabrielson KL, Hausladen JM, Mecham RP, Judge DP *et al*: **TGF-beta-dependent pathogenesis of mitral valve prolapse in a mouse model of Marfan syndrome**. *J Clin Invest* 2004, **114**(11):1586-1592.
174. LaHaye S, Lincoln J, Garg V: **Genetics of valvular heart disease**. *Curr Cardiol Rep* 2014, **16**(6):487.
175. Kyndt F, Gueffet JP, Probst V, Jaafar P, Legendre A, Le Bouffant F, Toquet C, Roy E, McGregor L, Lynch SA *et al*: **Mutations in the gene encoding filamin A as a cause for familial cardiac valvular dystrophy**. *Circulation* 2007, **115**(1):40-49.
176. Trochu JN, Kyndt F, Schott JJ, Gueffet JP, Probst V, Benichou B, Le Marec H: **Clinical characteristics of a familial inherited myxomatous**

valvular dystrophy mapped to Xq28. *J Am Coll Cardiol* 2000, **35**(7):1890-1897.
177. Kyndt F, Schott JJ, Trochu JN, Baranger F, Herbert O, Scott V, Fressinaud E, David A, Moisan JP, Bouhour JB *et al*: **Mapping of X-linked myxomatous valvular dystrophy to chromosome Xq28**. *Am J Hum Genet* 1998, **62**(3):627-632.
178. Le Tourneau T, Merot J, Rimbert A, Le Scouarnec S, Probst V, Le Marec H, Levine RA, Schott JJ: **Genetics of syndromic and non-syndromic mitral valve prolapse**. *Heart* 2018, **104**(12):978-984.
179. Le Tourneau T, Le Scouarnec S, Cueff C, Bernstein D, Aalberts JJJ, Lecointe S, Merot J, Bernstein JA, Oomen T, Dina C *et al*: **New insights into mitral valve dystrophy: a Filamin-A genotype-phenotype and outcome study**. *Eur Heart J* 2018, **39**(15):1269-1277.
180. Sauls K, de Vlaming A, Harris BS, Williams K, Wessels A, Levine RA, Slaugenhaupt SA, Goodwin RL, Pavone LM, Merot J *et al*: **Developmental basis for filamin-A-associated myxomatous mitral valve disease**. *Cardiovasc Res* 2012, **96**(1):109-119.
181. Durst R, Sauls K, Peal DS, deVlaming A, Toomer K, Leyne M, Salani M, Talkowski ME, Brand H, Perrocheau M *et al*: **Mutations in DCHS1 cause mitral valve prolapse**. *Nature* 2015, **525**(7567):109-113.
182. Bangs F, Anderson KV: **Primary Cilia and Mammalian Hedgehog Signaling**. *Cold Spring Harb Perspect Biol* 2017, **9**(5).
183. Dina C, Bouatia-Naji N, Tucker N, Delling FN, Toomer K, Durst R, Perrocheau M, Fernandez-Friera L, Solis J, investigators P *et al*: **Genetic association analyses highlight biological pathways underlying mitral valve prolapse**. *Nat Genet* 2015, **47**(10):1206-1211.
184. Drees F, Pokutta S, Yamada S, Nelson WJ, Weis WI: **Alpha-catenin is a molecular switch that binds E-cadherin-beta-catenin and regulates actin-filament assembly**. *Cell* 2005, **123**(5):903-915.
185. Barker N, Hurlstone A, Musisi H, Miles A, Bienz M, Clevers H: **The chromatin remodelling factor Brg-1 interacts with beta-catenin to promote target gene activation**. *EMBO J* 2001, **20**(17):4935-4943.
186. Bauer A, Chauvet S, Huber O, Usseglio F, Rothbacher U, Aragnol D, Kemler R, Pradel J: **Pontin52 and reptin52 function as antagonistic regulators of beta-catenin signalling activity**. *EMBO J* 2000, **19**(22):6121-6130.
187. Hecht A, Litterst CM, Huber O, Kemler R: **Functional characterization of multiple transactivating elements in beta-catenin,**

some of which interact with the TATA-binding protein in vitro. *J Biol Chem* 1999, **274**(25):18017-18025.
188. Hoffmans R, Stadeli R, Basler K: **Pygopus and legless provide essential transcriptional coactivator functions to armadillo/beta-catenin**. *Curr Biol* 2005, **15**(13):1207-1211.
189. Cox RT, Kirkpatrick C, Peifer M: **Armadillo is required for adherens junction assembly, cell polarity, and morphogenesis during Drosophila embryogenesis**. *J Cell Biol* 1996, **134**(1):133-148.
190. Xiang FL, Fang M, Yutzey KE: **Loss of beta-catenin in resident cardiac fibroblasts attenuates fibrosis induced by pressure overload in mice**. *Nat Commun* 2017, **8**(1):712.
191. Kasacka I, Piotrowska Z, Niezgoda M, Lewandowska A, Lebkowski W: **Ageing-related changes in the levels of beta-catenin, CacyBP/SIP, galectin-3 and immunoproteasome subunit LMP7 in the heart of men**. *PLoS One* 2020, **15**(3):e0229462.
192. Leng S, Pignatti E, Khetani RS, Shah MS, Xu S, Miao J, Taketo MM, Beuschlein F, Barrett PQ, Carlone DL *et al*: **beta-Catenin and FGFR2 regulate postnatal rosette-based adrenocortical morphogenesis**. *Nat Commun* 2020, **11**(1):1680.
193. Larive E, Nicolas M, Kaya G, Riggi N, Moulin AP: **beta-Catenin Expression and Activation in Conjunctival Melanoma**. *Dermatopathology (Basel)* 2019, **6**(2):50-62.
194. Coates JC: **Armadillo repeat proteins: beyond the animal kingdom**. *Trends Cell Biol* 2003, **13**(9):463-471.
195. Gottardi CJ, Gumbiner BM: **Distinct molecular forms of beta-catenin are targeted to adhesive or transcriptional complexes**. *J Cell Biol* 2004, **167**(2):339-349.
196. Doubilet PM, Benson CB, Wilkins-Haug L, Ringer S: **Fetuses subsequently born premature are smaller than gestational age-matched fetuses not born premature**. *J Ultrasound Med* 2003, **22**(4):359-363.
197. Huber AH, Nelson WJ, Weis WI: **Three-dimensional structure of the armadillo repeat region of beta-catenin**. *Cell* 1997, **90**(5):871-882.
198. Riggleman B, Wieschaus E, Schedl P: **Molecular analysis of the armadillo locus: uniformly distributed transcripts and a protein with novel internal repeats are associated with a Drosophila segment polarity gene**. *Genes Dev* 1989, **3**(1):96-113.
199. Coopman P, Djiane A: **Adherens Junction and E-Cadherin complex regulation by epithelial polarity**. *Cell Mol Life Sci* 2016, **73**(18):3535-3553.

200. Clarke DN, Miller PW, Lowe CJ, Weis WI, Nelson WJ: **Characterization of the Cadherin-Catenin Complex of the Sea Anemone Nematostella vectensis and Implications for the Evolution of Metazoan Cell-Cell Adhesion**. *Mol Biol Evol* 2016, **33**(8):2016-2029.
201. Henderson BR: **Nuclear-cytoplasmic shuttling of APC regulates beta-catenin subcellular localization and turnover**. *Nat Cell Biol* 2000, **2**(9):653-660.
202. Morgan RG, Ridsdale J, Payne M, Heesom KJ, Wilson MC, Davidson A, Greenhough A, Davies S, Williams AC, Blair A *et al*: **LEF-1 drives aberrant beta-catenin nuclear localization in myeloid leukemia cells**. *Haematologica* 2019, **104**(7):1365-1377.
203. Hubner K, Grassme KS, Rao J, Wenke NK, Zimmer CL, Korte L, Muller K, Sumanas S, Greber B, Herzog W: **Wnt signaling positively regulates endothelial cell fate specification in the Fli1a-positive progenitor population via Lef1**. *Dev Biol* 2017, **430**(1):142-155.
204. Takeichi M: **The cadherins: cell-cell adhesion molecules controlling animal morphogenesis**. *Development* 1988, **102**(4):639-655.
205. Meng W, Takeichi M: **Adherens junction: molecular architecture and regulation**. *Cold Spring Harb Perspect Biol* 2009, **1**(6):a002899.
206. Ozawa M, Baribault H, Kemler R: **The cytoplasmic domain of the cell adhesion molecule uvomorulin associates with three independent proteins structurally related in different species**. *EMBO J* 1989, **8**(6):1711-1717.
207. Chen YT, Stewart DB, Nelson WJ: **Coupling assembly of the E-cadherin/beta-catenin complex to efficient endoplasmic reticulum exit and basal-lateral membrane targeting of E-cadherin in polarized MDCK cells**. *J Cell Biol* 1999, **144**(4):687-699.
208. Huber AH, Stewart DB, Laurents DV, Nelson WJ, Weis WI: **The cadherin cytoplasmic domain is unstructured in the absence of beta-catenin. A possible mechanism for regulating cadherin turnover**. *J Biol Chem* 2001, **276**(15):12301-12309.
209. Yamada S, Pokutta S, Drees F, Weis WI, Nelson WJ: **Deconstructing the cadherin-catenin-actin complex**. *Cell* 2005, **123**(5):889-901.
210. Liu C, Li Y, Semenov M, Han C, Baeg GH, Tan Y, Zhang Z, Lin X, He X: **Control of beta-catenin phosphorylation/degradation by a dual-kinase mechanism**. *Cell* 2002, **108**(6):837-847.
211. Yost C, Torres M, Miller JR, Huang E, Kimelman D, Moon RT: **The axis-inducing activity, stability, and subcellular distribution of beta-**

catenin is regulated in Xenopus embryos by glycogen synthase kinase 3. *Genes Dev* 1996, **10**(12):1443-1454.
212. Zeng X, Tamai K, Doble B, Li S, Huang H, Habas R, Okamura H, Woodgett J, He X: **A dual-kinase mechanism for Wnt co-receptor phosphorylation and activation**. *Nature* 2005, **438**(7069):873-877.
213. Lybrand DB, Naiman M, Laumann JM, Boardman M, Petshow S, Hansen K, Scott G, Wehrli M: **Destruction complex dynamics: Wnt/beta-catenin signaling alters Axin-GSK3beta interactions in vivo**. *Development* 2019, **146**(13).
214. Pronobis MI, Rusan NM, Peifer M: **A novel GSK3-regulated APC:Axin interaction regulates Wnt signaling by driving a catalytic cycle of efficient betacatenin destruction**. *Elife* 2015, **4**:e08022.
215. Fagotto F, Gluck U, Gumbiner BM: **Nuclear localization signal-independent and importin/karyopherin-independent nuclear import of beta-catenin**. *Current biology : CB* 1998, **8**(4):181-190.
216. Krieghoff E, Behrens J, Mayr B: **Nucleo-cytoplasmic distribution of beta-catenin is regulated by retention**. *J Cell Sci* 2006, **119**(Pt 7):1453-1463.
217. Suh EK, Gumbiner BM: **Translocation of beta-catenin into the nucleus independent of interactions with FG-rich nucleoporins**. *Exp Cell Res* 2003, **290**(2):447-456.
218. Behrens J, von Kries JP, Kuhl M, Bruhn L, Wedlich D, Grosschedl R, Birchmeier W: **Functional interaction of beta-catenin with the transcription factor LEF-1**. *Nature* 1996, **382**(6592):638-642.
219. Molenaar M, van de Wetering M, Oosterwegel M, Peterson-Maduro J, Godsave S, Korinek V, Roose J, Destree O, Clevers H: **XTcf-3 transcription factor mediates beta-catenin-induced axis formation in Xenopus embryos**. *Cell* 1996, **86**(3):391-399.
220. Brunner E, Peter O, Schweizer L, Basler K: **pangolin encodes a Lef-1 homologue that acts downstream of Armadillo to transduce the Wingless signal in Drosophila**. *Nature* 1997, **385**(6619):829-833.
221. Sierra J, Yoshida T, Joazeiro CA, Jones KA: **The APC tumor suppressor counteracts beta-catenin activation and H3K4 methylation at Wnt target genes**. *Genes Dev* 2006, **20**(5):586-600.
222. Mosimann C, Hausmann G, Basler K: **Parafibromin/Hyrax activates Wnt/Wg target gene transcription by direct association with beta-catenin/Armadillo**. *Cell* 2006, **125**(2):327-341.
223. Chinnadurai G: **CtBP, an unconventional transcriptional corepressor in development and oncogenesis**. *Mol Cell* 2002, **9**(2):213-224.

224. Daniels DL, Weis WI: **Beta-catenin directly displaces Groucho/TLE repressors from Tcf/Lef in Wnt-mediated transcription activation**. *Nat Struct Mol Biol* 2005, **12**(4):364-371.
225. Tago K, Nakamura T, Nishita M, Hyodo J, Nagai S, Murata Y, Adachi S, Ohwada S, Morishita Y, Shibuya H *et al*: **Inhibition of Wnt signaling by ICAT, a novel beta-catenin-interacting protein**. *Genes Dev* 2000, **14**(14):1741-1749.
226. Fang M, Alfieri CM, Hulin A, Conway SJ, Yutzey KE: **Loss of beta-catenin promotes chondrogenic differentiation of aortic valve interstitial cells**. *Arterioscler Thromb Vasc Biol* 2014, **34**(12):2601-2608.
227. Castano J, Raurell I, Piedra JA, Miravet S, Dunach M, Garcia de Herreros A: **Beta-catenin N- and C-terminal tails modulate the coordinated binding of adherens junction proteins to beta-catenin**. *J Biol Chem* 2002, **277**(35):31541-31550.
228. Papagerakis P, Pannone G, Shabana AH, Depondt J, Santoro A, Ghirtis K, Berdal A, Papagerakis S: **Aberrant beta-catenin and LEF1 expression may predict the clinical outcome for patients with oropharyngeal cancer**. *International journal of immunopathology and pharmacology* 2012, **25**(1):135-146.
229. Jin YH, Kim H, Ki H, Yang I, Yang N, Lee KY, Kim N, Park HS, Kim K: **Beta-catenin modulates the level and transcriptional activity of Notch1/NICD through its direct interaction**. *Biochimica et biophysica acta* 2009, **1793**(2):290-299.
230. Tian H, Lv P, Ma K, Zhou C, Gao X: **Beta-catenin/LEF1 activated enamelin expression in ameloblast-like cells**. *Biochemical and biophysical research communications* 2010, **398**(3):519-524.
231. Porfiri E, Rubinfeld B, Albert I, Hovanes K, Waterman M, Polakis P: **Induction of a beta-catenin-LEF-1 complex by wnt-1 and transforming mutants of beta-catenin**. *Oncogene* 1997, **15**(23):2833-2839.
232. Wisniewska MB, Misztal K, Michowski W, Szczot M, Purta E, Lesniak W, Klejman ME, Dabrowski M, Filipkowski RK, Nagalski A *et al*: **LEF1/beta-catenin complex regulates transcription of the Cav3.1 calcium channel gene (Cacna1g) in thalamic neurons of the adult brain**. *The Journal of neuroscience : the official journal of the Society for Neuroscience* 2010, **30**(14):4957-4969.
233. Aloysius A, DasGupta R, Dhawan J: **The transcription factor Lef1 switches partners from beta-catenin to Smad3 during muscle stem cell quiescence**. *Science signaling* 2018, **11**(540).

234. Huber AH, Weis WI: **The structure of the beta-catenin/E-cadherin complex and the molecular basis of diverse ligand recognition by beta-catenin**. *Cell* 2001, **105**(3):391-402.
235. Lickert H, Bauer A, Kemler R, Stappert J: **Casein kinase II phosphorylation of E-cadherin increases E-cadherin/beta-catenin interaction and strengthens cell-cell adhesion**. *J Biol Chem* 2000, **275**(7):5090-5095.
236. Wang S, Jones KA: **CK2 controls the recruitment of Wnt regulators to target genes in vivo**. *Curr Biol* 2006, **16**(22):2239-2244.
237. Daugherty RL, Gottardi CJ: **Phospho-regulation of Beta-catenin adhesion and signaling functions**. *Physiology (Bethesda)* 2007, **22**:303-309.
238. Maitre JL, Heisenberg CP: **Three functions of cadherins in cell adhesion**. *Curr Biol* 2013, **23**(14):R626-633.
239. Le Bras GF, Taubenslag KJ, Andl CD: **The regulation of cell-cell adhesion during epithelial-mesenchymal transition, motility and tumor progression**. *Cell Adh Migr* 2012, **6**(4):365-373.
240. Kim W, Kim M, Jho EH: **Wnt/beta-catenin signalling: from plasma membrane to nucleus**. *Biochem J* 2013, **450**(1):9-21.
241. Sung DC, Bowen CJ, Vaidya KA, Zhou J, Chapurin N, Recknagel A, Zhou B, Chen J, Kotlikoff M, Butcher JT: **Cadherin-11 Overexpression Induces Extracellular Matrix Remodeling and Calcification in Mature Aortic Valves**. *Arterioscler Thromb Vasc Biol* 2016, **36**(8):1627-1637.
242. Bowen CJ, Zhou J, Sung DC, Butcher JT: **Cadherin-11 coordinates cellular migration and extracellular matrix remodeling during aortic valve maturation**. *Dev Biol* 2015, **407**(1):145-157.
243. Zhou J, Bowen C, Lu G, Knapp Iii C, Recknagel A, Norris RA, Butcher JT: **Cadherin-11 expression patterns in heart valves associate with key functions during embryonic cushion formation, valve maturation and calcification**. *Cells Tissues Organs* 2013, **198**(4):300-310.
244. Basso C, Perazzolo Marra M, Rizzo S, De Lazzari M, Giorgi B, Cipriani A, Frigo AC, Rigato I, Migliore F, Pilichou K *et al*: **Arrhythmic Mitral Valve Prolapse and Sudden Cardiac Death**. *Circulation* 2015, **132**(7):556-566.
245. Boudoulas KD, Pitsis AA, Boudoulas H: **Floppy Mitral Valve (FMV) - Mitral Valve Prolapse (MVP) - Mitral Valvular Regurgitation and FMV/MVP Syndrome**. *Hellenic J Cardiol* 2016, **57**(2):73-85.
246. Nalliah CJ, Mahajan R, Elliott AD, Haqqani H, Lau DH, Vohra JK, Morton JB, Semsarian C, Marwick T, Kalman JM *et al*: **Mitral valve**

prolapse and sudden cardiac death: a systematic review and meta-analysis. *Heart* 2019, **105**(2):144-151.
247. Delling FN, Vasan RS: **Epidemiology and pathophysiology of mitral valve prolapse: new insights into disease progression, genetics, and molecular basis**. *Circulation* 2014, **129**(21):2158-2170.
248. Gasser S, Reichenspurner H, Girdauskas E: **Genomic analysis in patients with myxomatous mitral valve prolapse: current state of knowledge**. *BMC Cardiovasc Disord* 2018, **18**(1):41.
249. Basso C, Perazzolo Marra M, Rizzo S, De Lazzari M, Giorgi B, Cipriani A, Frigo AC, Rigato I, Migliore F, Pilichou K *et al*: **Arrhythmic Mitral Valve Prolapse and Sudden Cardiac Death**
Mitral valve prolapse and sudden cardiac death: a systematic review and meta-analysis
Moderate Chronic Ischemic Mitral Regurgitation
Floppy Mitral Valve (FMV) - Mitral Valve Prolapse (MVP) - Mitral Valvular Regurgitation and FMV/MVP Syndrome. *Circulation* 2015, **132**(7):556-566.
250. Pagnozzi LA, Butcher JT: **Mechanotransduction Mechanisms in Mitral Valve Physiology and Disease Pathogenesis**. *Front Cardiovasc Med* 2017, **4**.
251. Kathem SH, Mohieldin AM, Nauli SM: **The Roles of Primary cilia in Polycystic Kidney Disease**. *AIMS Mol Sci* 2014, **1**(1):27-46.
252. Kuo IY, Chapman AB: **Polycystins, ADPKD, and Cardiovascular Disease**. *Kidney Int Rep* 2020, **5**(4):396-406.
253. Toomer KA, Fulmer D, Guo L, Drohan A, Peterson N, Swanson P, Brooks B, Mukherjee R, Body S, Lipschutz J *et al*: **A Role for Primary Cilia in Aortic Valve Development and Disease**. *Dev Dyn* 2017, **246**(8):625-634.
254. Zhang B, Zhang T, Wang G, Wang G, Chi W, Jiang Q, Zhang C: **GSK3β-Dzip1-Rab8 cascade regulates ciliogenesis after mitosis**. *PLoS Biol* 2015, **13**(4):e1002129.
255. Wang C, Low WC, Liu A, Wang B: **Centrosomal protein DZIP1 regulates Hedgehog signaling by promoting cytoplasmic retention of transcription factor GLI3 and affecting ciliogenesis**. *J Biol Chem* 2013, **288**(41):29518-29529.
256. Tay SY, Yu X, Wong KN, Panse P, Ng CP, Roy S, Kim HR, Richardson J, van Eeden F, Ingham PW: **The iguana/DZIP1 protein is a novel component of the ciliogenic pathway essential for axonemal biogenesis**

Gli2a protein localization reveals a role for Iguana/DZIP1 in primary ciliogenesis and a dependence of Hedgehog signal transduction on primary cilia in the zebrafish. *Dev Dyn* 2010, **239**(2):527-534.
257. Lee YL, Sante J, Comerci CJ, Cyge B, Menezes LF, Li FQ, Germino GG, Moerner WE, Takemaru K, Stearns T: **Cby1 promotes Ahi1 recruitment to a ring-shaped domain at the centriole-cilium interface and facilitates proper cilium formation and function**. *Mol Biol Cell* 2014, **25**(19):2919-2933.
258. Li FQ, Chen X, Fisher C, Siller SS, Zelikman K, Kuriyama R, Takemaru KI: **BAR Domain-Containing FAM92 Proteins Interact with Chibby1 To Facilitate Ciliogenesis**. *Mol Cell Biol* 2016, **36**(21):2668-2680.
259. Shi J, Zhao Y, Galati D, Winey M, Klymkowsky MW: **Chibby functions in Xenopus ciliary assembly, embryonic development, and the regulation of gene expression**. *Dev Biol* 2014, **395**(2):287-298.
260. Siller SS, Sharma H, Li S, Yang J, Zhang Y, Holtzman MJ, Winuthayanon W, Colognato H, Holdener BC, Li FQ *et al*: **Conditional knockout mice for the distal appendage protein CEP164 reveal its essential roles in airway multiciliated cell differentiation**. *PLoS Genet* 2017, **13**(12):e1007128.
261. Steere N, Chae V, Burke M, Li FQ, Takemaru K, Kuriyama R: **A Wnt/beta-catenin pathway antagonist Chibby binds Cenexin at the distal end of mother centrioles and functions in primary cilia formation**. *PLoS One* 2012, **7**(7):e41077.
262. Li FQ, Mofunanya A, Fischer V, Hall J, Takemaru K: **Nuclear-cytoplasmic shuttling of Chibby controls beta-catenin signaling**. *Mol Biol Cell* 2010, **21**(2):311-322.
263. Li FQ, Mofunanya A, Harris K, Takemaru K: **Chibby cooperates with 14-3-3 to regulate beta-catenin subcellular distribution and signaling activity**. *J Cell Biol* 2008, **181**(7):1141-1154.
264. Li FQ, Chiriboga L, Black MA, Takemaru KI, Raffaniello RD: **Chibby is a weak regulator of beta-catenin activity in gastric epithelium**. *J Cell Physiol* 2019, **234**(2):1871-1879.
265. Guo L, Glover J, Risner A, Wang C, Fulmer D, Moore K, Gensemer C, Rumph MK, Moore R, Beck T *et al*: **Dynamic Expression Profiles of beta-Catenin during Murine Cardiac Valve Development**. *J Cardiovasc Dev Dis* 2020, **7**(3).
266. Chopra S, Al-Sammarraie N, Lai Y, Azhar M: **Increased canonical WNT/beta-catenin signalling and myxomatous valve disease**. *Cardiovasc Res* 2017, **113**(1):6-9.

267. Foulquier S, Daskalopoulos EP, Lluri G, Hermans KCM, Deb A, Blankesteijn WM: **WNT Signaling in Cardiac and Vascular Disease**. *Pharmacol Rev* 2018, **70**(1):68-141.
268. Fang D, Hawke D, Zheng Y, Xia Y, Meisenhelder J, Nika H, Mills GB, Kobayashi R, Hunter T, Lu Z: **Phosphorylation of beta-catenin by AKT promotes beta-catenin transcriptional activity**. *J Biol Chem* 2007, **282**(15):11221-11229.
269. He XC, Yin T, Grindley JC, Tian Q, Sato T, Tao WA, Dirisina R, Porter-Westpfahl KS, Hembree M, Johnson T *et al*: **PTEN-deficient intestinal stem cells initiate intestinal polyposis**. *Nat Genet* 2007, **39**(2):189-198.
270. Goretsky T, Bradford EM, Ye Q, Lamping OF, Vanagunas T, Moyer MP, Keller PC, Sinh P, Llovet JM, Gao T *et al*: **Beta-catenin cleavage enhances transcriptional activation**. *Sci Rep* 2018, **8**(1):671.
271. Lapart JA, Gottardo M, Cortier E, Duteyrat JL, Augiere C, Mange A, Jerber J, Solassol J, Gopalakrishnan J, Thomas J *et al*: **Dzip1 and Fam92 form a ciliary transition zone complex with cell type specific roles in Drosophila**. *Elife* 2019, **8**.
272. Haycraft CJ, Zhang Q, Song B, Jackson WS, Detloff PJ, Serra R, Yoder BK: **Intraflagellar transport is essential for endochondral bone formation**. *Development* 2007, **134**(2):307-316.
273. Taurin S, Sandbo N, Qin Y, Browning D, Dulin NO: **Phosphorylation of beta-catenin by cyclic AMP-dependent protein kinase**. *J Biol Chem* 2006, **281**(15):9971-9976.
274. Sande-Melon M, Marques IJ, Galardi-Castilla M, Langa X, Perez-Lopez M, Botos MA, Sanchez-Iranzo H, Guzman-Martinez G, Ferreira Francisco DM, Pavlinic D *et al*: **Adult sox10(+) Cardiomyocytes Contribute to Myocardial Regeneration in the Zebrafish**. *Cell Rep* 2019, **29**(4):1041-1054 e1045.
275. Salazar VS, Zarkadis N, Huang L, Watkins M, Kading J, Bonar S, Norris J, Mbalaviele G, Civitelli R: **Postnatal ablation of osteoblast Smad4 enhances proliferative responses to canonical Wnt signaling through interactions with beta-catenin**. *J Cell Sci* 2013, **126**(Pt 24):5598-5609.
276. Fu R, Han CF, Ni T, Di L, Liu LJ, Lv WC, Bi YR, Jiang N, He Y, Li HM *et al*: **A ZEB1/p53 signaling axis in stromal fibroblasts promotes mammary epithelial tumours**. *Nat Commun* 2019, **10**(1):3210.
277. Park H, Yamamoto H, Mohn L, Ambuhl L, Kanai K, Schmidt I, Kim KP, Fraccaroli A, Feil S, Junge HJ *et al*: **Integrin-linked kinase controls**

retinal angiogenesis and is linked to Wnt signaling and exudative vitreoretinopathy. *Nat Commun* 2019, **10**(1):5243.
278. Rain JC, Selig L, De Reuse H, Battaglia V, Reverdy C, Simon S, Lenzen G, Petel F, Wojcik J, Schachter V *et al*: **The protein-protein interaction map of Helicobacter pylori**. *Nature* 2001, **409**(6817):211-215.
279. Ghatak S, Misra S, Norris RA, Moreno-Rodriguez RA, Hoffman S, Levine RA, Hascall VC, Markwald RR: **Periostin induces intracellular cross-talk between kinases and hyaluronan in atrioventricular valvulogenesis**. *J Biol Chem* 2014, **289**(12):8545-8561.
280. Durkin ME, Qian X, Popescu NC, Lowy DR: **Isolation of Mouse Embryo Fibroblasts**. *Bio Protoc* 2013, **3**(18):e908.
281. Wang S, Ma J, Peng J, Xu J: **Protein structure alignment beyond spatial proximity**. *Sci Rep* 2013, **3**:1448.
282. Wang S, Peng J, Xu J: **Alignment of distantly related protein structures: algorithm, bound and implications to homology modeling**. *Bioinformatics* 2011, **27**(18):2537-2545.
283. Peng J, Xu J: **RaptorX: exploiting structure information for protein alignment by statistical inference**. *Proteins* 2011, **79 Suppl 10**:161-171.
284. Lamiable A, Thevenet P, Rey J, Vavrusa M, Derreumaux P, Tuffery P: **PEP-FOLD3: faster de novo structure prediction for linear peptides in solution and in complex**. *Nucleic Acids Res* 2016, **44**(W1):W449-454.
285. Shen Y, Maupetit J, Derreumaux P, Tuffery P: **Improved PEP-FOLD Approach for Peptide and Miniprotein Structure Prediction**. *J Chem Theory Comput* 2014, **10**(10):4745-4758.
286. Thevenet P, Shen Y, Maupetit J, Guyon F, Derreumaux P, Tuffery P: **PEP-FOLD: an updated de novo structure prediction server for both linear and disulfide bonded cyclic peptides**. *Nucleic Acids Res* 2012, **40**(Web Server issue):W288-293.